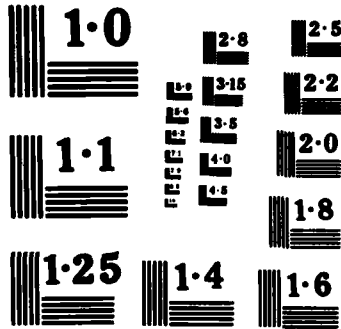


AD-A158 267 MBE GROWTH OF CdTe AND Hg SUB 1-X Cd SUB X Te FILMS AND 1/1  
MULTILAYER STRUCT. (U) WESTINGHOUSE RESEARCH AND  
DEVELOPMENT CENTER PITTSBURGH PA R F FARROW ET AL.  
UNCLASSIFIED 16 APR 85 85-9F3-EPCAD-R2 ARO-20202. 4-EL F/G 20/2 NL

END  
FIMED  
DSC



NATIONAL BUREAU OF STANDARDS  
MICROCOPY RESOLUTION TEST CHART

DTIC FILE COPY

AD-A158 267

MBE GROWTH OF CdTe AND  $\text{Hg}_{1-x}\text{Cd}_x\text{Te}$   
FILMS AND MULTILAYER STRUCTURES

ARO 20202-4-EL

(2)

R. F. C. Farrow, A. J. Noreika, W. J. Takei,  
S. Wood, J. Gregg, Jr., T. A. Temofonte,  
F. A. Shirland, and W. J. Choyke

Final Report for the Period  
January 1, 1983 to December 31, 1984

ARO Project Number P20202-EL  
Contract Number DAAG 29-83-C-0008

April 16, 1985

DTIC  
ELECTED  
AUG 26 1985  
S D  
A B

DISTRIBUTION STATEMENT A  
Approved for public release  
Distribution Unlimited

Westinghouse R&D Center  
1310 Beulah Road  
Pittsburgh, Pennsylvania 15235

85 8 23 009

MBE GROWTH OF CdTe AND  $Hg_{1-x}Cd_xTe$   
FILMS AND MULTILAYER STRUCTURES

R. F. C. Farrow, A. J. Noreika, W. J. Takei,  
S. Wood, J. Gregg, Jr., T. A. Temofonte,  
F. A. Shirland, and W. J. Choyke

Final Report for the Period  
January 1, 1983 to December 31, 1984

ARO Project Number P20202-EL  
Contract Number DAAG 29-83-C-0008

April 16, 1985

DTIC  
ELECTE  
AUG 26 1985  
S D  
B

DISTRIBUTION STATEMENT A  
Approved for public release  
Distribution Unlimited



Westinghouse R&D Center  
1310 Beulah Road  
Pittsburgh, Pennsylvania 15235

REPORT DOCUMENTATION PAGE		READ INSTRUCTIONS BEFORE COMPLETING FORM	
1. REPORT NUMBER <b>ARO 20202.4-EL</b>	2. GOVT ACCESSION NO. N/A	RECIPIENT'S CATALOG NUMBER <b>4158267</b>	N/A
4. TITLE (and Subtitle) MBE GROWTH OF CdTe AND Hg <sub>1-x</sub> Cd <sub>x</sub> Te FILMS AND MULTILAYER STRUCTURES		5. TYPE OF REPORT & PERIOD COVERED Final Report 1-1-83 to 12-31-84	
7. AUTHOR(s) R.F.C. Farrow, A. J. Noreika, W. J. Takei, S. Wood, J. Gregg, Jr., T. A. Temofonte, F. A. Shirland, and W. J. Choyke		6. PERFORMING ORG. REPORT NUMBER 85-9F3-EPCAD-R2	
9. PERFORMING ORGANIZATION NAME AND ADDRESS Westinghouse R&D Center 1310 Beulah Road Pittsburgh, PA 15235		10. PROGRAM ELEMENT, PROJECT, TASK AREA & WORK UNIT NUMBERS	
11. CONTROLLING OFFICE NAME AND ADDRESS U. S. Army Research Office Post Office Box 12211 Research Triangle Park, NC 27709		12. REPORT DATE April 16, 1985	
		13. NUMBER OF PAGES 11	
14. MONITORING AGENCY NAME & ADDRESS(if different from Controlling Office)		15. SECURITY CLASS. (of this report) Unclassified	
		15a. DECLASSIFICATION/DOWNGRADING SCHEDULE	
16. DISTRIBUTION STATEMENT (of this Report) Approved for public release; distribution unlimited.			
17. DISTRIBUTION STATEMENT (of the abstract entered in Block 20, if different from Report) N/A			
18. SUPPLEMENTARY NOTES The view, opinions, and/or findings contained in this report are those of the author(s) and should not be construed as an official Department of the Army position, policy, or decision, unless so designed by other documentation.			
19. KEY WORDS (Continue on reverse side if necessary and identify by block number) thin films, molecular, beams, epitaxy, growth, MBE, alloys, improvement, structure, cadmium telluride, control, mercury cadmium telluride, doping, extrinsic, multilayers, compounds III-V, compounds II-IV.			
20. ABSTRACT (Continue on reverse side if necessary and identify by block number) The MBE growth of CdTe and Hg <sub>1-x</sub> Cd <sub>x</sub> Te films on InSb and CdTe substrates has been investigated. Growth conditions for high-perfection CdTe films, exactly lattice-matched to InSb substrates, have been identified. These films are ideal for substrates for Hg <sub>1-x</sub> Cd <sub>x</sub> Te film growth since they are free from low-angle grain boundaries and also provide electrical isolation of the Hg <sub>1-x</sub> Cd <sub>x</sub> Te film from the InSb substrate. Magnetophotoconductivity studies of abrupt n-CdTe/p-InSb heterojunctions indicate the presence of an n-type inversion layer in the InSb. This could be the basis for a new type of FET device.			
CONTINUED			

## 20. CONTINUED

Conditions for growth of  $Hg_{1-x}Cd_xTe$  films have been explored and films of suitable quality for LWIR device fabrication have been prepared. Original  
Supplied Keywords include:

CDW 1731

Accession For	
NTIS	<input checked="" type="checkbox"/>
DTIC TAB	<input type="checkbox"/>
Microfiche	<input type="checkbox"/>
Classification	
By	
Distribution/	
Availability Codes	
Dist	Avail and/or Special
A-1	



## CONTENTS

	Page
<b>LIST OF FIGURES.....</b>	<b>iii</b>
<b>ABSTRACT.....</b>	<b>vii</b>
<b>1. INTRODUCTION AND BACKGROUND.....</b>	<b>1</b>
<b>2. PROGRAM OBJECTIVES.....</b>	<b>3</b>
<b>3. MBE GROWTH AND CHARACTERIZATION OF CdTe FILMS ON InSb.....</b>	<b>4</b>
<b>3.1 Growth Conditions.....</b>	<b>4</b>
<b>3.2 Characterization of CdTe Films.....</b>	<b>8</b>
<b>3.2.1 Transmission Electron Microscopy (TEM).....</b>	<b>9</b>
<b>3.2.2 X-Ray Diffraction.....</b>	<b>11</b>
<b>3.2.3 Photoluminescence.....</b>	<b>22</b>
<b>3.2.4 Electrical Characterization of CdTe/InSb Heterostructures.....</b>	<b>24</b>
<b>3.2.5 Magnetophotoconductivity Studies of MBE-Grown CdTe/InSb Structures.....</b>	<b>34</b>
<b>3.3 Growth Kinetics and Doping Limitations of CdTe.....</b>	<b>37</b>
<b>4. MBE GROWTH AND INVESTIGATION OF <math>Hg_{1-x}Cd_xTe</math> FILMS.....</b>	<b>41</b>
<b>4.1 Growth Conditions.....</b>	<b>41</b>
<b>4.2 Characterization of <math>Hg_{1-x}Cd_xTe</math> Films.....</b>	<b>45</b>
<b>5. SUMMARY AND CONCLUSIONS.....</b>	<b>51</b>
<b>6. REFERENCES.....</b>	<b>53</b>
<b>APPENDIX A A Study of the Growth Conditions Necessary for Reproducible Preparation of High Perfection CdTe Films on InSb by MBE.....</b>	<b>55</b>
<b>APPENDIX B Microstructural Studies of CdTe and InSb Films Grown by Molecular Beam Epitaxy.....</b>	<b>57</b>

APPENDIX C A Photoluminescence Study of Molecular Beam Epitaxy-Grown CdTe Films on (001) InSb Substrates.....	64
APPENDIX D Transmission Electron Microscopy of Liquid Phase Epitaxial $Hg_{1-x}Cd_xTe$ Layers on CdTe Substrates.....	76

## LIST OF FIGURES

	Page
<b>Figure 1.</b> Photograph of Westinghouse-built MBE machine. Note Varian-style, magnetically operated sample transfer arm and horizontally mounted Varian triode ion pump ( $400 \text{ l sec}^{-1}$ ). The RHEED screen and top-mounted sample manipulator on the growth chamber are also visible.	5
<b>Figure 2.</b> Photograph of second-generation MBE machine (V.G. Semicon Ltd. Type VG80HI). This view shows the growth chamber with near-horizontal sources separated by a gate valve from the preparation chamber. The AES and XPS control consoles are visible on the right-hand side while part of the main console is visible on the left-hand side. The auxiliary Hg-handling system used for post-HgCdTe-growth Hg transfer is not shown here since it is connected only during the transfer cycle.	6
<b>Figure 3.</b> Bright-field, cross-section transmission electron micrographs of CdTe films grown on InSb (001) orientation substrates at $T_s \sim 200^\circ\text{C}$ . The improvement in film quality from (a) through (c) was due to improvements in the substrate cleaning process prior to epitaxy of CdTe; (a) exhibits a highly twinned and large dislocation density film, and (c) shows a near-perfect film with very few extended defects.	10
<b>Figure 4.</b> Bright-field, cross-section transmission electron micrographs for a good-quality CdTe film grown on a thin (0.2 $\mu\text{m}$ ) InSb buffer layer. The CdTe/InSb interface is clean, whereas the InSb/InSb interface is defined by residual surface contamination and In-rich precipitates.	12
<b>Figure 5.</b> Photograph of double-crystal X-ray diffractometer used for quantitative double-crystal rocking curve analysis of CdTe, InSb substrates, and epitaxial heterostructures. This instrument is custom designed and computer controlled.	14

- Figure 6.** Double-crystal X-ray diffraction rocking curves (DCRC) of InSb and two CdTe (001) orientation wafers recorded using CuK $\alpha$  radiation and InSb (001) reference crystal operating in (008) Bragg diffraction. Note that the linewidth for the InSb crystal is close to the intrinsic value (~9 arc sec) expected for a perfect crystal. On the other hand, the linewidths for the CdTe wafers greatly exceed the intrinsic value (~9 arc sec) due to the presence of low-angle subgrain boundaries. Diffraction maxima for individual subgrains in the beam are indicated by arrows in Figure 1(c). The great difference in linewidths for the two CdTe wafers reflects the variability in substrate quality. 15
- Figure 7.** X-ray topographs of the InSb and CdTe wafers used in the DCRC analysis. Note the near-uniform grey scale of the InSb topograph, indicative of primary extinction in a near-perfect crystal. The CdTe topographs, on the other hand, are characteristic of mosaic crystals with low-angle subgrain boundary structure, long-range strain, and lineage features. The presence of long-range strain is indicated by the fact that only part of the wafer operates in the Bragg diffraction at the setting used. The reflection topographs were recorded with CuK $\alpha$  radiation and the operating Bragg diffraction was (531). 16
- Figure 8.** Double-crystal X-ray diffraction rocking curves of CdTe substrate #1 and of a 2  $\mu\text{m}$  homoepitaxial CdTe film grown on CdTe substrate #1 by MBE at  $T_g = 220^\circ\text{C}$ . Note the significant broadening of the DCRC of the film and substrate, indicative of propagation of substrate defects into the film. 18
- Figure 9.** Double-crystal X-ray rocking curve of a 1.4  $\mu\text{m}$  thick MBE-grown CdTe film on (001) InSb substrate. The single, symmetric CdTe peak is consistent with a film which has a dislocation density of  $10^4$ - $10^5 \text{ cm}^{-2}$ , is free of low-angle boundaries, and is exactly lattice-matched to the InSb substrate in the growth plane. Lattice misfit between InSb and CdTe is accommodated by a uniform elastic strain in the film. 20

- Figure 10.** Double-crystal X-ray rocking curve of a 2.5 um thick MBE-grown CdTe film on (001) InSb substrate. The single symmetric CdTe peak is consistent with a film which has a dislocation density of  $<10^5 \text{ cm}^{-2}$ , is free of low-angle grain boundaries, and is exactly lattice-matched to the InSb substrate in the growth plane. Lattice misfit between InSb and CdTe is accommodated by a uniform elastic strain in the film. 21
- Figure 11.** Photoluminescence spectra of MBE-grown CdTe films grown at temperatures from  $T_g = 220^\circ\text{C}$  to  $160^\circ\text{C}$  and recorded at low-energy resolution to cover the range 1.4-1.6 eV. Note the decrease in the broad, deep-level peak centered at  $\sim 1.4$  eV compared with the near band-edge emission with decreasing growth temperature. 23
- Figure 12.** Capacitance ( $1/C^2$ )-voltage plot for an undoped CdTe film (sample #139) grown on (001) InSb at  $200^\circ\text{C}$ . Film grown in Westinghouse MBE machine. 26
- Figure 13.** Capacitance ( $1/C^2$ )-voltage plots for an array of Schottky barrier diodes to undoped CdTe film (sample #139) grown on (001) InSb at  $200^\circ\text{C}$ . Note the dispersion of C-V plots for different diodes, due to lateral spatial variations in the heterojunction contribution to film depletion. The near-constant slopes of the C-V plots suggest, however, that the film carrier concentration varies only slightly both laterally and through the film depth. 29
- Figure 14.** Capacitance ( $1/C^2$ )-voltage plots for (a) nominally undoped CdTe film (sample MBV49) and (b) In-doped CdTe film (sample MBV59). Both films were grown at  $234^\circ\text{C}$  on (001) InSb in the VC80HI MBE machine. The In-doped film has a lower free-electron concentration than  $8 \times 10^{14} \text{ cm}^{-3}$ . On the other hand, the nominally undoped film has a free-electron concentration  $> 10^{16} \text{ cm}^{-3}$ . This film was grown under nonideal conditions before adequate charge conditioning. 32
- Figure 15.** Photoconductive response of MBE-grown CdTe film on InSb (001) orientation substrate, sample #189 (recorded by Dr. B. D. McCombe; see text for details). 36

- Figure 16.** Transition energies as a function of magnetic field for sample #189 (recorded by Dr. B. D. McCombe; see text for details). 38
- Figure 17.** Photograph of VG80HI MBE machine with auxiliary pumping system shown in foreground. The auxiliary system incorporates a large-capacity liquid-nitrogen-cooled cryotrap for condensing Hg transferred from the VG80HI growth chamber. The auxiliary system is Hg diffusion pumped. 42
- Figure 18.** Measured beam pressure (broad line) of Hg versus temperature of Hg reservoir for Hg source on VG80HI machine. The light line indicates the equilibrium vapor pressure of Hg. 43
- Figure 19.** Cross-section transmission electron micrograph of MBE-grown  $Hg_{1-x}Cd_xTe/CdTe/InSb$  (001) substrate structure (see text for details); sample number MBV 88. 46
- Figure 20.** High spatial resolution compositional data from EDS of cross section of sample MBV 88. The regions probed by the electron beam are indicated in the micrographs. Note the positive identification of microprecipitates of elemental Te in the  $Hg_{1-x}Cd_xTe$  film. 47
- Figure 21.** Double-crystal X-ray rocking curve of a  $2.1\text{ }\mu\text{m}$  thick  $Hg_{1-x}Cd_xTe$  ( $x \approx 0.4$ ) film grown on (001) orientation CdTe substrate at  $190^\circ\text{C}$ . Growth of the  $Hg_{1-x}Cd_xTe$  film was preceded by a CdTe buffer layer  $0.1\text{ }\mu\text{m}$  thick, grown at  $T_g = 275^\circ\text{C}$ . 49
- Figure 22.** Infrared transmission spectrum for  $6.4\text{ }\mu\text{m}$  thick film of  $Hg_{1-x}Cd_xTe$  ( $x \approx 0.22$ ) grown on (001) orientation CdTe substrate at  $190^\circ\text{C}$ . 50

INVESTIGATION OF MOLECULAR BEAM EPITAXIAL GROWTH OF CdTe  
AND  $Hg_{1-x}Cd_xTe$  FILMS AND MULTILAYER STRUCTURES

R. F. C. Farrow, A. J. Noreika, W. J. Takei,  
S. Wood, J. Greggi, Jr., T. A. Temofonte,  
F. A. Shirland, and W. J. Choyke

ABSTRACT

The MBE growth of CdTe and  $Hg_{1-x}Cd_xTe$  films on InSb and CdTe substrates has been investigated. Growth conditions for high-perfection CdTe films, exactly lattice-matched to InSb substrates, have been identified. These films are ideal for substrates for  $Hg_{1-x}Cd_xTe$  film growth since they are free from low-angle grain boundaries and also provide electrical isolation of the  $Hg_{1-x}Cd_xTe$  film from the InSb substrate. Magnetophotoconductivity studies of abrupt n-CdTe/p-InSb heterojunctions indicate the presence of an n-type inversion layer in the InSb. This could be the basis for a new type of FET device. Conditions for growth of  $Hg_{1-x}Cd_xTe$  films have been explored and films of suitable quality for LWIR device fabrication have been prepared.

## 1. INTRODUCTION AND BACKGROUND

The thin-film technology of molecular beam epitaxy (MBE) and related in-situ analysis techniques have, over the past decade, led to major improvements both in our understanding and control of epitaxial growth of III-V compounds. The application of MBE techniques to the growth of II-VI compounds is expected to lead to a similar improvement and development in epitaxial growth of these compounds. Such an improvement is made all the more necessary by the growing importance of epitaxial structures of II-VI compounds and alloys, such as CdTe and  $Hg_{1-x}Cd_xTe$ , in infrared device structures.

MBE techniques permit the growth of epitaxial CdTe and  $Hg_{1-x}Cd_xTe$  films of device quality at temperatures far below those of other growth technologies. Thus, MBE has major advantages over these technologies in preparation of advanced multilayer device structures for infrared imaging. However, quite apart from these potential advantages in device fabrication, MBE techniques permit the investigation of growth and doping mechanisms of II-VI compound films in a particularly direct way. For example, primary growth species and dopant species can be identified by modulated beam mass spectrometry. Film composition can be controlled and tuned with the solidus range by adjusting beam impingement rates or growth temperature. Furthermore, the low growth temperatures permitted by MBE growth allows the use of large-area, high structural perfection lattice-matched substrates of InSb. This makes possible the first investigation of intrinsic and extrinsic doping mechanisms in high-perfection, homogeneous CdTe films free of twins and low-angle boundaries. This approach can be generalized and extended to other II-VI compounds which can be grown and lattice-matched to high-perfection III-V compound substrates by MBE; for example, ZnSe grown on GaAs.

The ability of MBE techniques to prepare abrupt CdTe-InSb interfaces raises the prospect of growth of abrupt heterojunctions in this system which have<sup>1,2</sup> unique material and electronic properties.

## 2. PROGRAM OBJECTIVES

The program objectives are threefold: firstly, to prepare high-perfection, high-purity films of CdTe and to investigate the mechanisms of film growth and doping; secondly, to prepare CdTe-InSb heterojunctions which have unique material and electronic properties that are attractive in preparing and studying the behavior of ultra-small electronic (USER) devices; and thirdly, to investigate the growth of device-quality films of  $Hg_{1-x}Cd_xTe$ .

### 3. MBE GROWTH AND CHARACTERIZATION OF CdTe FILMS ON InSb

The technique of MBE growth of CdTe from a single, congruently subliming effusion source was originally used by Farrow et al.<sup>3</sup> at RSRE, Malvern, U.K. to prepare high-perfection, lattice-matched CdTe films on (001) orientation InSb substrates. The films were characterized by X-ray diffraction but not by transmission electron microscopy. Variations in growth parameters such as growth rate, substrate temperature, and surface preparation conditions and their effect on film properties were not systematically explored at that time. These variations have been systematically studied under this contract and the films characterized by a multiplicity of techniques. A major finding is that the structural and optical quality of the films is optimized at a particular growth temperature. This suggests that the growth temperature influences the stoichiometry and point defect concentration in the films through subtle changes in growth kinetics.

#### 3.1 Growth Conditions

MBE growth of CdTe was carried out in two separate MBE systems: a small Westinghouse-built machine (Figure 1) fitted with a vacuum load lock and reflection high-energy electron diffraction (8 keV) RHEED system; and a second-generation MBE machine (Type VG80HI, see Figure 2), equipped with a cassette load-lock, RHEED, Auger electron spectroscopy (AES), and X-ray photoelectron spectroscopy facilities.

In view of the promising potential for InSb as a large-area lattice-matched substrate for MBE growth of  $Hg_{1-x}Cd_xTe$ , emphasis was placed on growth of CdTe on InSb substrates, although some preliminary studies were carried out on growth on GaAs substrates. In both the Westinghouse machine and in the V80HI machine, the CdTe effusion source



Figure 1. Photograph of Westinghouse-built MBE machine. Note Varian-style, magnetically operated sample transfer arm and horizontally mounted Varian triode ion pump ( $400 \text{ l sec}^{-1}$ ). The RHEED screen and top-mounted sample manipulator on the growth chamber are also visible.

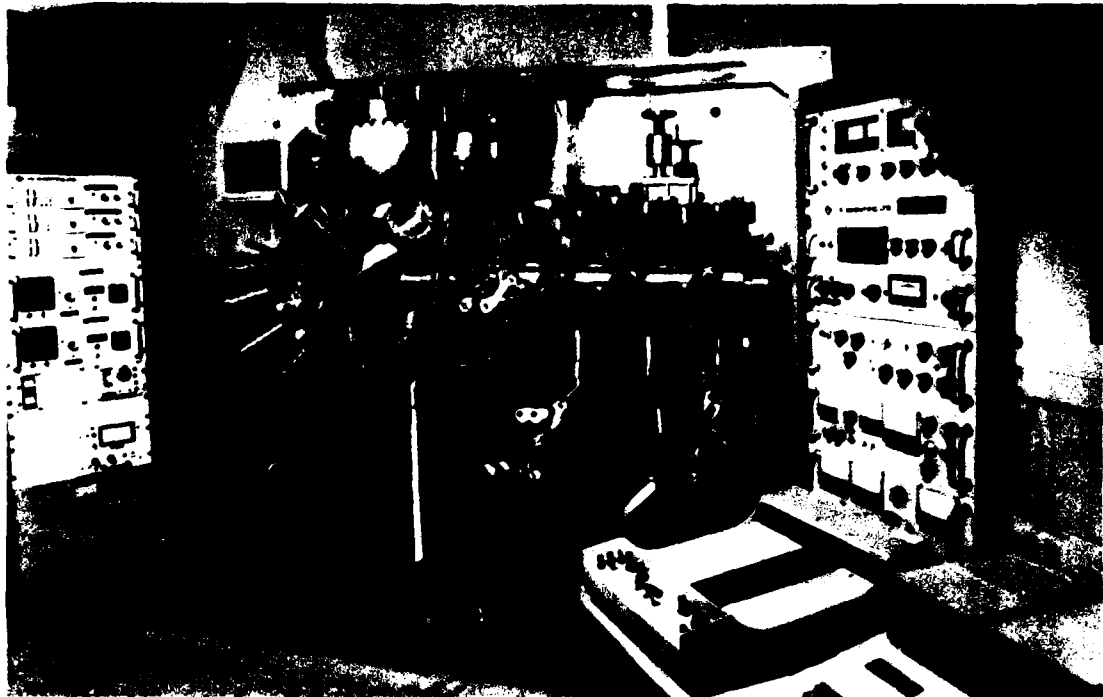


**Figure 2.** Photograph of second-generation MBE machine (V.G. Semicon Ltd. Type VG80HI). This view shows the growth chamber with near-horizontal sources separated by a gate valve from the preparation chamber. The AES and XPS control consoles are visible on the right-hand side while part of the main console is visible on the left-hand side. The auxiliary Hg-handling system used for post-HgCdTe-growth Hg transfer is not shown here since it is connected only during the transfer cycle.

was constructed of graphite with a 3 mm orifice. A 1 mm orifice was also used for a series of experiments in the Westinghouse machine.

The growth of CdTe films at low ( $\leq 200^{\circ}\text{C}$ ) substrate temperatures is necessary both to avoid interdiffusion between CdTe and InSb and between CdTe and  $\text{Hg}_{1-x}\text{Cd}_x\text{Te}$  when CdTe is grown as part of a heterostructure for device applications. At such low temperatures, growth from separate elemental sources of Cd and  $\text{Te}_2$  would lead to fluctuations in film stoichiometry and degradation in structural quality. The basic assumption behind CdTe film growth<sup>3</sup> from a single CdTe effusion source is that of a steady state of Knudsen effusion in which the beam composition is locked<sup>4</sup> to the congruently subliming composition with Cd and  $\text{Te}_2$  beam fluxes given by:

$$J_{\text{cd}} = 2J_{\text{Te}_2}$$

Consideration of the self-diffusion coefficients<sup>5</sup> of Cd and Te in crystalline CdTe shows that the approach to this steady state may take many hours at temperatures around  $500^{\circ}\text{C}$ , but is very rapid at temperatures above  $700^{\circ}\text{C}$ . We find<sup>6</sup> (see Appendix 1) that reproducible growth of very high-perfection CdTe films with double-crystal diffraction linewidths below 25 arc sec (see Section 3.2.2) is possible only if a new (crushed) CdTe charge is conditioned by heating to temperatures above  $700^{\circ}\text{C}$ . Small orifices ( $\leq 3$  mm diameter) enable this to be carried out without excessive loss of the charge.

A study of the influence of in-situ InSb substrate preparation conditions on film and interface structure has been reported by the authors elsewhere<sup>7</sup> (see Appendix B). In brief, optimum quality was obtained for argon ion bombardment at 500 eV. Higher energies and heavier ion species (e.g., Kr) caused extensive damage to the InSb surface and produced extended defects in the film. All the results reported here were for CdTe films grown on InSb substrates which were held at  $200^{\circ}\text{C}$  during the ion bombardment. This process greatly speeded up the cleaning process over the method used by the RSRE group in which

the InSb substrate was subjected to repeated cycles of room-temperature ion bombardment followed by annealing at 200°C.

$\text{Ar}^+$  ion current densities of  $\sim 0.1 \mu\text{A cm}^{-2}$  were used here and a defocussed and scanning ion beam was necessary to uniformly remove surface impurities prior to film growth. In the Westinghouse machine, the ion gun to substrate distance was  $\sim 100 \text{ mm}$  and typical cleaning times were 15 min. In the VG80HI machine, the corresponding distance was  $\sim 200 \text{ mm}$  and cleaning times were 1-2 hours. Continuous sample rotation during ion bombardment was used to uniformly clean large-area ( $\sim 2 \text{ inch diameter}$ ) InSb wafers in the VG80HI machine. During CdTe film growth, background pressures in the growth chamber were usually in the low  $10^{-9} \text{ Torr}$  range, although they were occasionally in the  $10^{-10} \text{ Torr}$  range.

### 3.2 Characterization of CdTe Films

In order to optimize CdTe film growth and to fully explore the dependence of film properties on growth parameters, a multiplicity of characterization techniques was employed. This was found to be essential since no single technique provided a complete picture of film or interface properties. Taken together, the techniques were complementary. For example, long-range structural perfection of CdTe films (and of  $\text{Hg}_{1-x}\text{Cd}_x\text{Te}$  overlayers) is of crucial importance in array technology since photovoltaic device yield is sensitive to defects such as low-angle grain boundaries. X-ray techniques such as double-crystal diffraction (see Section 3.2.2) can identify and map such defects but are insensitive to randomly distributed microprecipitates ( $\leq 100 \text{ \AA}$  across) or to point defects which may strongly influence carrier lifetimes by providing recombination centers. Transmission electron microscopy is ideally suited to detection and identification of localized and extended defects, while photoluminescence is a sensitive probe of point defect structure and impurity-related centers.

### 3.2.1 Transmission Electron Microscopy (TEM)

In the early stages of this investigation, the causes of poor structural quality of CdTe films indicated by broad ( $\geq 60$  arc sec) double-crystal rocking curves (DCRC) were unknown. Transmission electron microscopy provided the solution by pinning down the problem to one of inadequate substrate cleaning prior to epitaxy. This problem was due to nonuniform removal of substrate impurities by the ion beam. It was eliminated by sample centering in the ion beam and increasing the beam scan amplitude. Figure 3 illustrates the progressive improvement in CdTe film perfection resulting from improvements in substrate preparation. The absence of misfit dislocation networks at the InSb-CdTe interface suggests that the small ( $\Delta a/a \sim 0.05\%$ ) lattice parameter misfit is accommodated by elastic strain in the CdTe film. This point was confirmed by the X-ray diffraction investigations of the structures (see Section 3.2.2). Lattice images of the CdTe/InSb interface also confirmed this point.

TEM studies of the MBE-grown CdTe films revealed a "window" of growth conditions for film quality comparable to that illustrated in Figure 3(c). Films grown at rates of  $\geq 1.2 \mu\text{m h}^{-1}$  at  $T_s \approx 200^\circ\text{C}$  had a high density of defects, both at the interface and in the bulk of the film. Films grown at temperatures below  $150^\circ\text{C}$  were invariably polycrystalline. This indicates that breakdown of epitaxial growth at low temperatures or high growth rates is due to incomplete reaction between arising Cd and Te<sub>2</sub>. At temperatures of  $\leq 150^\circ\text{C}$ , incomplete reaction would lead to condensation of Te precipitates but desorption of Cd, which is much more volatile at this temperature. This model is supported by the recent observation<sup>9</sup> of Te precipitates in CdTe films grown from a single effusion source by MBE at temperatures of  $\sim 150^\circ\text{C}$ . It seems that faulting of the CdTe film is nucleated at the Te precipitates.

The upper temperature limit to high-perfection epitaxial growth appears<sup>8</sup> to be in the region of  $310^\circ\text{C}$ . Above this temperature,



Figure 3. Bright-field, cross-section transmission electron micrographs of CdTe films grown on InSb (001) orientation substrates at  $T_s \sim 200^\circ\text{C}$ . The improvement in film quality from (a) through (c) was due to improvements in the substrate cleaning process prior to epitaxy of CdTe; (a) exhibits a highly twinned and large dislocation density film, and (c) shows a near-perfect film with very few extended defects.

catastrophic breakdown of the film-substrate interface occurs by interdiffusion.

In concluding this section, it should be stated that XTEM techniques have provided the microstructural information necessary to optimize growth of the highest perfection films of CdTe yet reported. In addition, although the surface preparation technique of ion bombardment-annealing requires careful attention to detail for its success, it provides a reproducible way of uniformly cleaning large InSb substrates. The alternative technique of heat cleaning InSb in a background Sb<sub>4</sub> flux invariably leads<sup>6</sup> to surface nucleation of In islands which introduce structural and optical<sup>10</sup> defects into CdTe films grown onto heat-cleaned substrates. We have also demonstrated<sup>6</sup> that high-perfection CdTe films can be grown onto InSb buffer layers grown on heat-cleaned InSb substrates (see Figure 4). However, unless the InSb buffer layer growth can be carried out in a growth chamber separate from that used for Hg<sub>1-x</sub>Cd<sub>x</sub>Te film growth, this technique may not be applicable to subsequent growth of Hg<sub>1-x</sub>Cd<sub>x</sub>Te since residual Sb<sub>4</sub> in the growth chamber remaining after buffer layer growth may dope the Hg<sub>1-x</sub>Cd<sub>x</sub>Te film.

### 3.2.2 X-Ray Diffraction

While the XTEM technique described in Section 3.2.1 provides high spatial resolution microstructural data on substrate, film, and interface zones, it requires lengthy preparation times for sample foils, is essentially destructive, and cannot image large macroscopic defects such as grain boundaries and long-range strain inhomogeneities. The techniques of X-ray topography and double-crystal rocking curve analysis are ideally suited to detection and imaging of such defects and provide quantitative information on film perfection and strain anisotropy.

A custom-built double-crystal diffractometer designed by W. J. Takei and built by Blake Instruments, N.J., was commissioned by Westinghouse in 1983 and has been extensively used to characterize CdTe

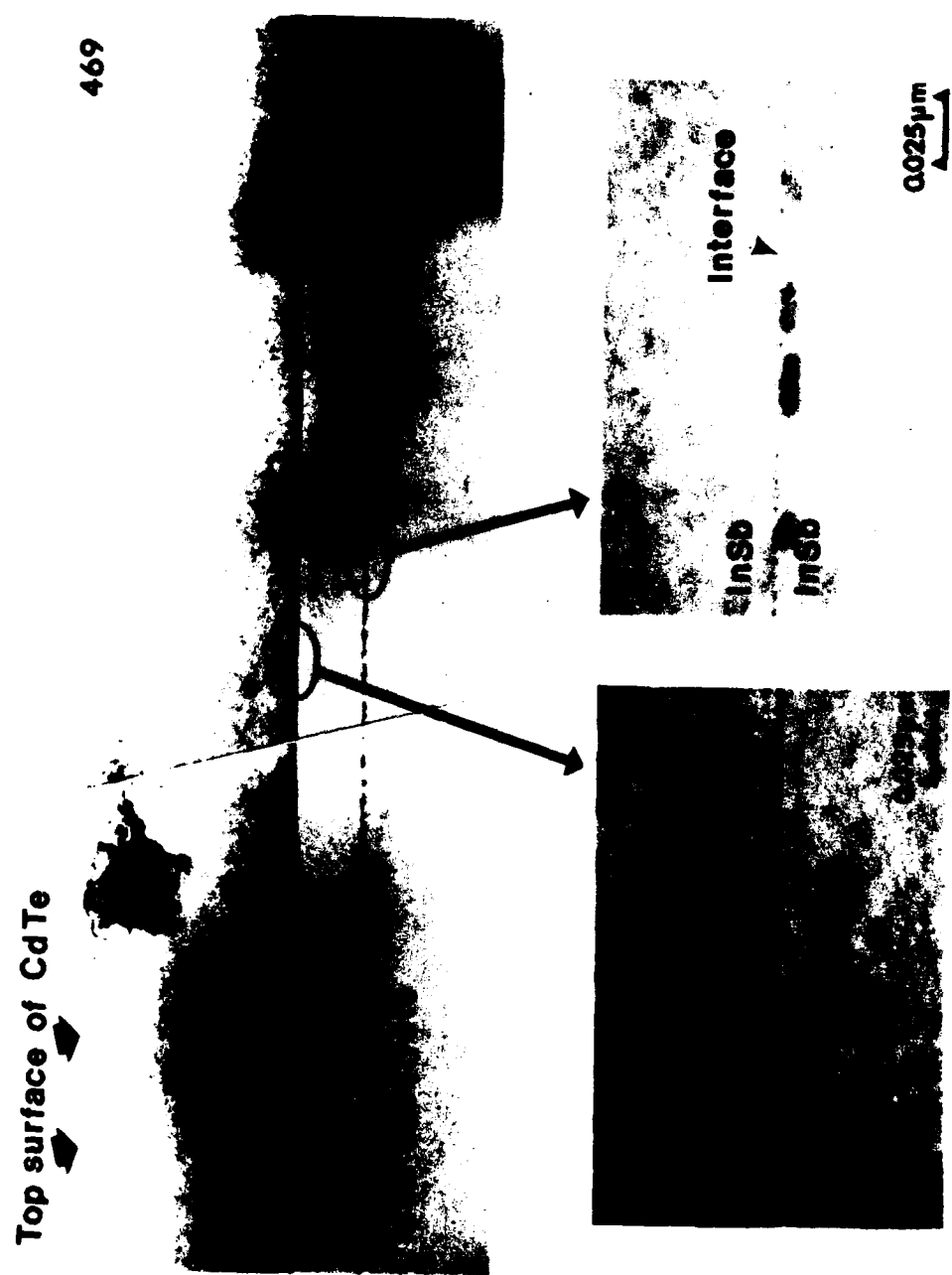


Figure 4. Bright-field, cross-section transmission electron micrographs for a good-quality CdTe film grown on a thin ( $0.2 \mu\text{m}$ ) InSb buffer layer. The CdTe/InSb interface is clean, whereas the InSb/InSb interface is defined by residual surface contamination and In-rich precipitates.

films on InSb,  $Hg_{1-x}Cd_xTe/CdTe/CdTe$ , and  $Hg_{1-x}Cd_xTe/CdTe/InSb$  multilayer structures. This diffractometer is illustrated in Figure 5. The use of this instrument was complemented by a single-crystal diffractometer, operated as a Lang camera, for X-ray topography studies of the structures.

One of the first applications of X-ray diffraction techniques in this contract was to use both double-crystal rocking curve analysis and topography to compare and contrast the structural quality of commercially available CdTe and InSb wafers. Figure 6 contrasts the double-crystal rocking curve for an InSb (001) orientation wafer with that for two representative CdTe (001) orientation wafers from a leading commercial supplier. CdTe wafer #1 is a rare example of a relatively high-perfection sample in comparison with typical wafers of which wafer #2 is an example. The rocking curve linewidth (FWHM) in double-crystal diffraction is a measure of structural perfection of a near (~5  $\mu m$  deep for (008) Bragg diffraction CuKa X-radiation) surface region of crystal illuminated by the X-ray beam. In the present case, this area is about 1 mm square. The intrinsic linewidths expected for the (008) Bragg diffraction from perfect (zero dislocation density) InSb and CdTe crystals are ~9 arc sec. While the linewidth for the InSb crystal wafer is very close to this value, the linewidths for the two CdTe crystals greatly exceed the intrinsic value because of the presence of structural defects. The nature of these defects is directly revealed in X-ray topographs (see Figure 7) of ~1 cm square regions of the samples. The general light-dark contrast is due to long-range strains in the crystals which cause only part of the wafer to be operating in the Bragg diffraction condition at a particular setting. In this respect, substrate #1 is clearly less strained than substrate #2. In addition to long-range strain, two other features are evident. Orthogonal lineage features in {110} directions form a "checkerboard" pattern. These features may be due to slip, although this assignment must be considered tentative at present. A sub-grain structure comprising grains of ~100-200  $\mu m$  in dimension separated by low-angle grain boundaries is evident

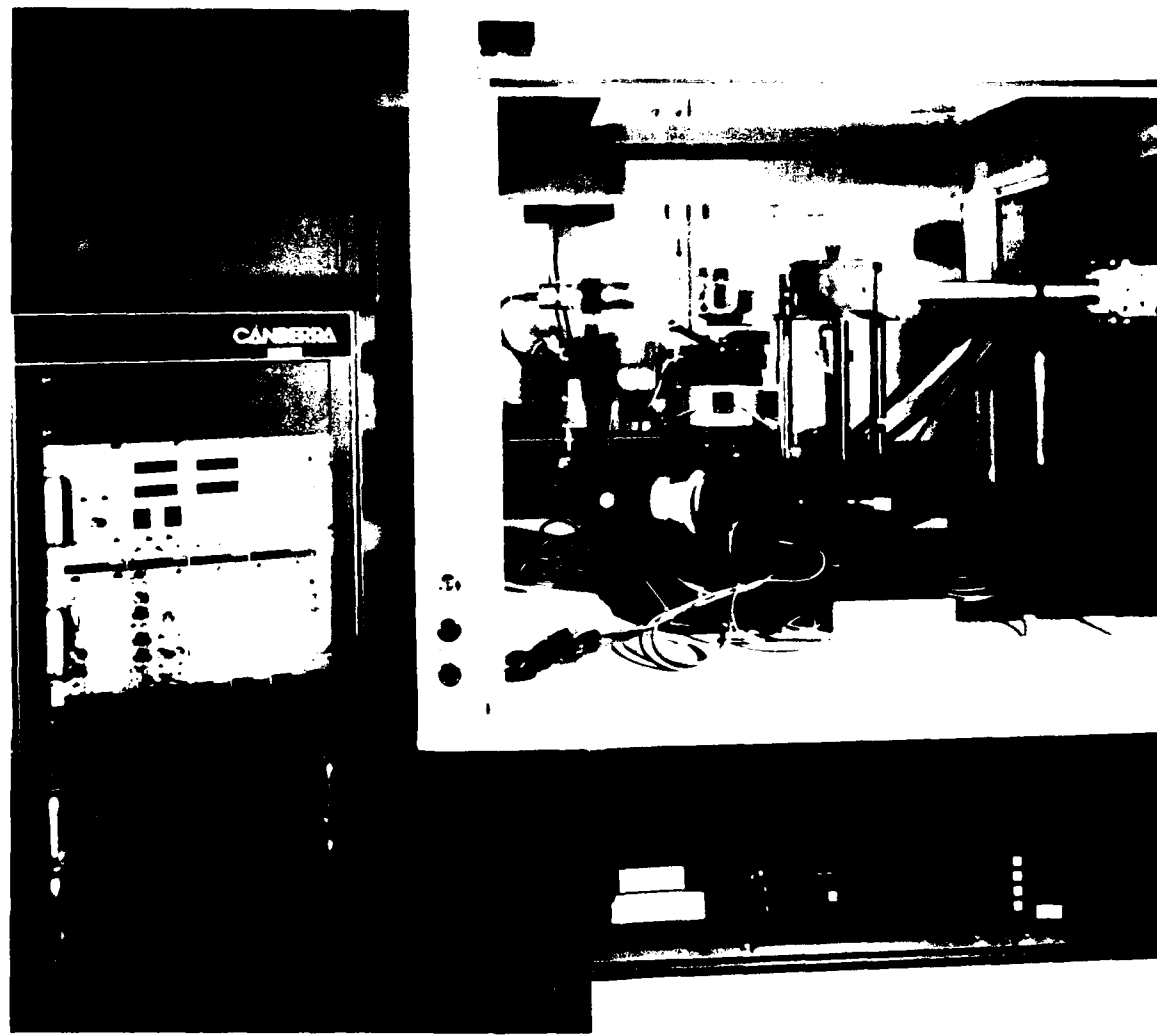


Figure 5. Photograph of double-crystal X-ray diffractometer used for quantitative double-crystal rocking curve analysis of CdTe, InSb substrates, and epitaxial heterostructures. This instrument is custom designed and computer controlled.

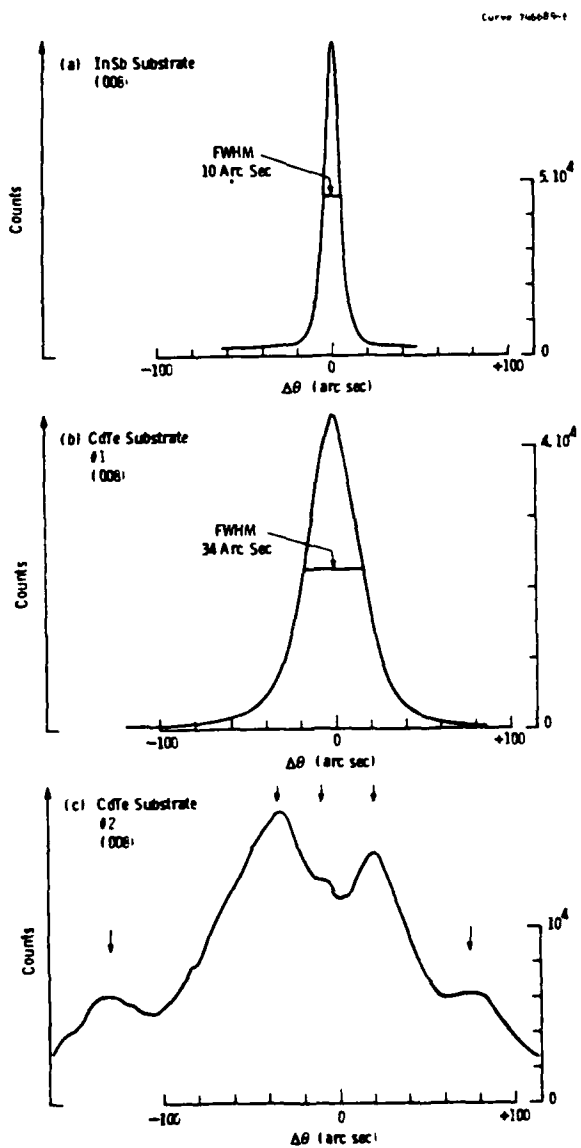


Figure 6. Double-crystal X-ray diffraction rocking curves (DCRC) of InSb and two CdTe (001) orientation wafers recorded using CuK $\alpha$  radiation and InSb (001) reference crystal operating in (008) Bragg diffraction. Note that the linewidth for the InSb crystal is close to the intrinsic value (~9 arc sec) expected for a perfect crystal. On the other hand, the linewidths for the CdTe wafers greatly exceed the intrinsic value (~9 arc sec) due to the presence of low-angle subgrain boundaries. Diffraction maxima for individual subgrains in the beam are indicated by arrows in Figure 1(c). The great difference in linewidths for the two CdTe wafers reflects the variability in substrate quality.



**InSb (001) Substrate**  
**15 mm × 13 mm**



**CdTe (001) Substrate #1**  
**11 mm × 10 mm**



**CdTe (001) Substrate #2**  
**10 mm × 9 mm**

Figure 7. X-ray topographs of the InSb and CdTe wafers used in the DCRC analysis. Note the near-uniform grey scale of the InSb topograph, indicative of primary extinction in a near-perfect crystal. The CdTe topographs, on the other hand, are characteristic of mosaic crystals with low-angle subgrain boundary structure long-range strain, and lineage features. The presence of long-range strain is indicated by the fact that only part of the wafer operates in the Bragg diffraction at the setting used. The reflection topographs were recorded with CuK $\alpha$  radiation and the operating Bragg diffraction was (531).

in both CdTe wafers. It must be stressed that the CdTe and InSb crystals were subjected to free etching prior to X-ray examination to remove polishing damage. As a result, the defect features in the X-ray topographs are believed to be intrinsic to the bulk of the wafers. All bulk CdTe wafers examined at Westinghouse R&D have exhibited low-angle sub-grain boundary structure to some extent. This situation is to be contrasted with the case of InSb wafers (see Figure 7), which invariably show featureless X-ray topographs with a generally uniform grey scale of intensity, indicative of a uniformly high structural perfection with the intensity of Bragg diffraction limited by primary extinction. This is not surprising since the InSb wafers reproducibly have <200 dislocations  $\text{cm}^{-2}$ .

The main implication of the preceding substrate analysis is that the use of CdTe substrates for growth of epitaxial  $\text{Hg}_{1-x}\text{Cd}_x\text{Te}$  films is likely to lead to defect propagation in the overayers. The propagation of low-angle sub-grain boundaries, for example, into epitaxial  $\text{Hg}_{1-x}\text{Cd}_x\text{Te}$  films would lead to rapid vertical diffusion of impurities along sub-grain boundaries with consequent failure of junctions which intersect sub-grain boundaries. Such effects are indeed known<sup>11</sup> to occur and are a yield-limiting factor in photovoltaic device array fabrication. That low-angle boundaries do indeed propagate from CdTe substrates into MBE-grown CdTe films is illustrated by the DCRC data in Figure 8. This shows a DCRC analysis of a 2  $\mu\text{m}$  thick CdTe film grown onto the substrate wafer #1. The growth conditions for single (CdTe) source growth of the film were known to be optimized from parallel studies of CdTe heteroepitaxy on InSb. The growth temperature  $T_g$  was 220°C and growth rate 0.5  $\mu\text{m h}^{-1}$ . The CdTe substrate was heat cleaned at 300–350°C and confirmed to be both clean and well ordered by parallel AES/RHEED studies. The significantly broadened linewidth for the film-substrate combination confirms the propagation of sub-grain boundaries into the film. This defect propagation and consequent film degradation is also known to occur in growth of  $\text{Hg}_{1-x}\text{Cd}_x\text{Te}$  films on CdTe substrates by MBE,<sup>12</sup> MOCVD,<sup>13</sup> and LPE<sup>14</sup> and is the main reason for the exploration

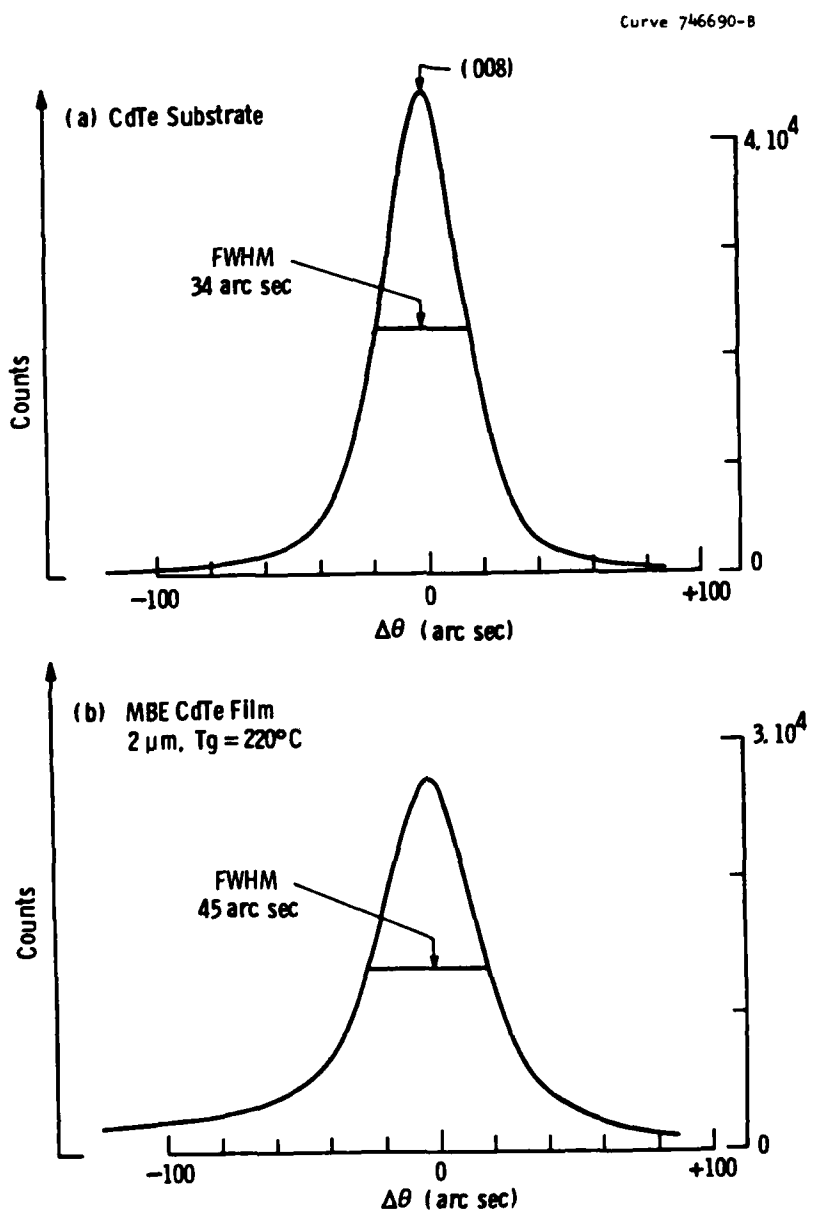


**Figure 8.** Double-crystal X-ray diffraction rocking curves of CdTe substrate #1 and of a 2  $\mu$ m homoepitaxial CdTe film grown on CdTe substrate #1 by MBE at  $T_g = 220^\circ\text{C}$ . Note the significant broadening of the DCRC of the film and substrate, indicative of propagation of substrate defects into the film.

and development of multilayer structures, based on foreign substrates, for focal plane imaging applications.

The reproducible growth of high-perfection lattice-matched CdTe films on InSb (001) substrates has been achieved by careful attention<sup>6</sup> to CdTe source conditioning and substrate preparation (see section 3.1). Figures 9 and 10 show double-crystal rocking curves for high-perfection CdTe films grown at a substrate temperature of 186°C. The CdTe film is free of low-angle grain boundaries and exhibits DCRC linewidths of 17.8 arc sec and 19.5 arc sec for film thicknesses of 1.4 μm and 2.5 μm, respectively. These linewidths are significantly broader than those expected for perfect, zero-dislocation density films (~10 arc sec). This broadening can be accounted for<sup>15</sup> by a uniform dislocation density in the range  $10^4$ - $10^5$  cm<sup>-3</sup>. The InSb linewidth is much closer to the value (~10 arc sec) for a perfect InSb crystal, suggesting<sup>15</sup> a dislocation density (~200 cm<sup>-2</sup>) consistent with the dislocation etch pit count quoted by the supplier (Metal Specialties, Inc.). The measured film strain ( $\Delta d/d$ ) for the (004) Bragg planes, i.e., in the [001] direction, for both films is

$$\Delta d/d = -\cot \theta \Delta \theta = 94 \pm 1 \times 10^{-5}$$

This value is identical to that previously measured<sup>3</sup> at RSRE for films grown at 220°C and is consistent with perfect in-place lattice matching between film (relaxed lattice parameter 6.48229 Å) and substrate.

Studies of film quality, measured by FWHM of the CdTe rocking curve, indicated no systematic dependence of quality on growth rate over the range 0.29 μm h<sup>-1</sup> to 1.27 μm h<sup>-1</sup> for a substrate temperature of 275°C. This is illustrated in Table 1.

Recent studies of film quality<sup>16</sup> as a function of growth temperature indicated a broad minimum in FWHM in the region of  $T_s \sim 185^\circ\text{C}$ . This minimum coincided with a minimum in radiative defect

Curve 747598-A

DCRC MBE CdTe/InSb (001) #207  
1.4  $\mu$ m Tg = 186°C

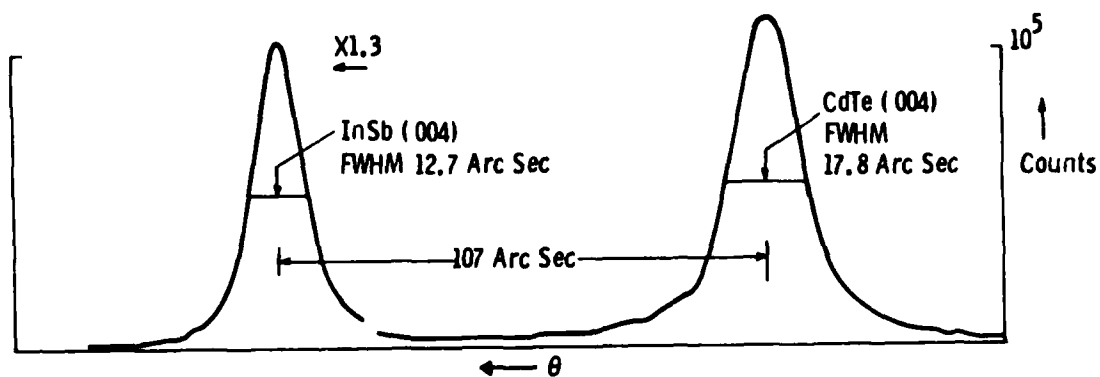


Figure 9. Double-crystal X-ray rocking curve of a 1.4  $\mu$ m thick MBE-grown CdTe film on (001) InSb substrate. The single, symmetric CdTe peak is consistent with a film which has a dislocation density of  $10^4$ - $10^5$   $\text{cm}^{-2}$ , is free of low-angle boundaries, and is exactly lattice-matched to the InSb substrate in the growth plane. Lattice misfit between InSb and CdTe is accommodated by a uniform elastic strain in the film.

Curve 747596-A

DCRC MBE CdTe/InSb (001) #215

2.5  $\mu$ m Tg = 186°C

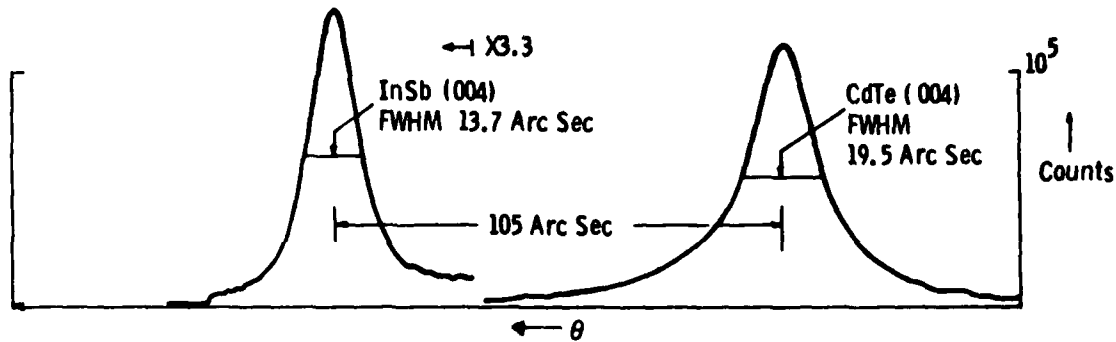


Figure 10. Double-crystal X-ray rocking curve of a 2.5 um thick MBE-grown CdTe film on (001) InSb substrate. The single symmetric CdTe peak is consistent with a film which has a dislocation density of  $<10^5 \text{ cm}^{-2}$ , is free of low-angle grain boundaries, and is exactly lattice-matched to the InSb substrate in the growth plane. Lattice misfit between InSb and CdTe is accommodated by a uniform elastic strain in the film.

TABLE 1  
CdTe FILM QUALITY VERSUS FILM GROWTH RATE ( $T_s = 275^\circ\text{C}$ )

Run Number	Source T °C	Growth Rate $\mu\text{m h}^{-1}$	Film Thickness $\mu\text{m}$	DCRC FWHM arc sec
252	645	0.29	1.30	23.1
239	655	0.37	1.48	27.8
246	665	0.44	1.16	21.2
242	670	0.54	1.08	22.4
217	675	0.52	1.22	20.1
240	675	0.62	1.09	21.7
243	675	0.61	1.22	23.2
241	680	0.66	1.16	23.3
218	685	0.70	1.40	20.6
238	695	1.03	1.55	31.2
253	705	1.27	1.27	23.7

density of the films measured by photoluminescence (see Appendix 3 and Section 3.2.3).

### 3.2.3 Photoluminescence

Photoluminescence studies of MBE-grown CdTe films on InSb were undertaken by J. Furneaux at Naval Research Laboratory during the first half of 1984 and subsequently at the University of Pittsburgh by W. J. Choyke. These studies provided information, complementary to the structural studies on film quality and, in addition, gave information on free-carrier concentration and on impurity and defect states in the films. Figure 11 shows spectra, recorded at NRL, for a series of films grown at progressively lower temperatures. The most significant feature of these spectra is the systematic decrease, with decreasing growth temperature, of the emission from the broad, donor-acceptor pair region and defect-related band around 1.46 eV. Over this growth temperature

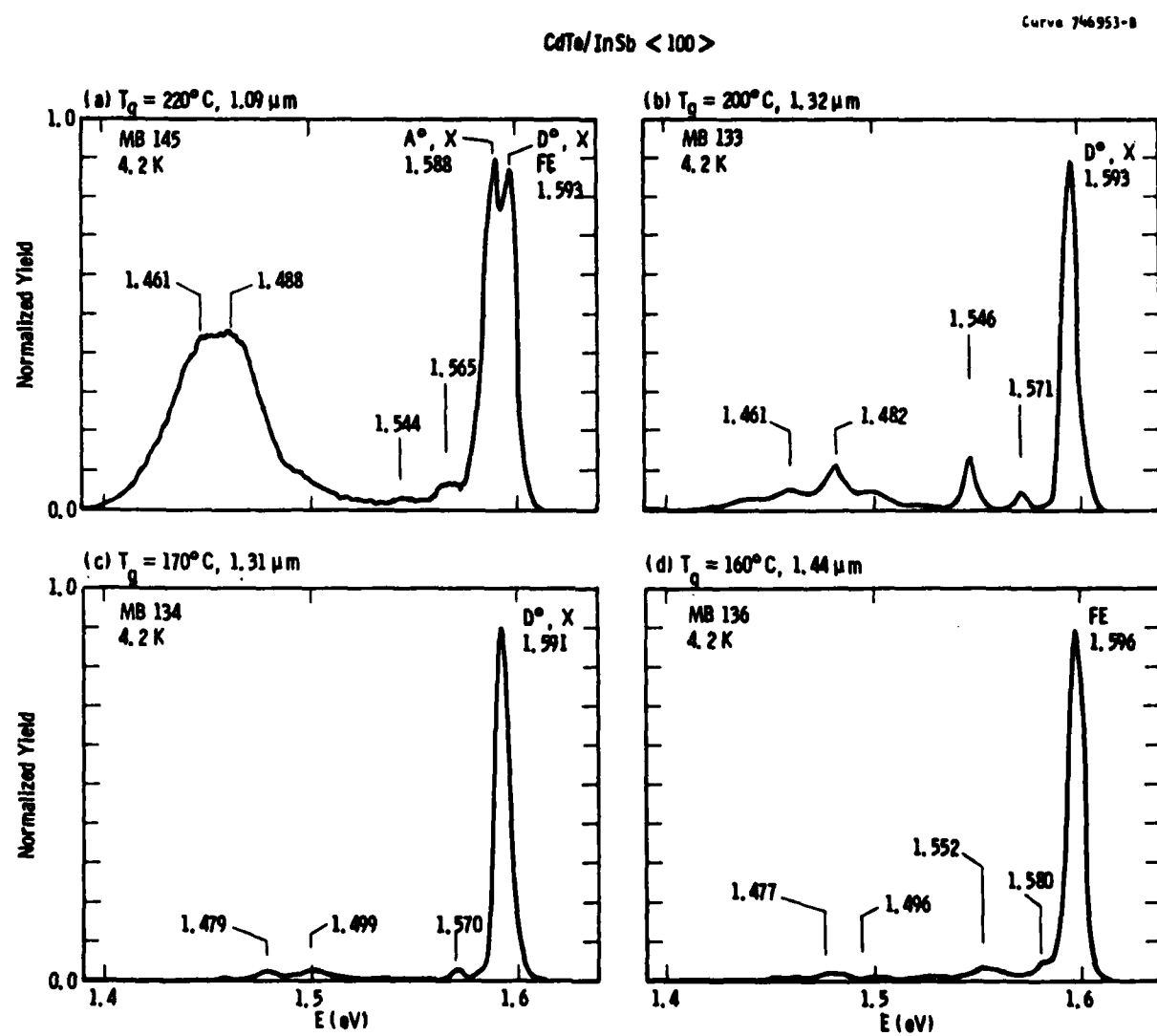


Figure 11. Photoluminescence spectra of MBE-grown CdTe films grown at temperatures from  $T_s = 220^\circ\text{C}$  to  $160^\circ\text{C}$  and recorded at low-energy resolution to cover the range  $1.4\text{--}1.6\text{ eV}$ . Note the decrease in the broad, deep-level peak centered at  $\sim 1.4\text{ eV}$  compared with the near band-edge emission with decreasing growth temperature.

range, the emission becomes increasingly dominated by the near band-edge emission. Subsequent studies<sup>16</sup> (see Appendix C) carried out at the University of Pittsburgh on a large sample population revealed that the radiative defect density,  $\rho$  (defined as the ratio of the intensity of a band at ~1.45 eV, attributed to defects, to that of the principal bound exciton peak, ~1.59 eV), followed a systematic decrease over the temperature range 285 to 185°C to a minimum value of 0.006, then increased again at even lower temperatures. The substrate temperatures in this later work were carefully calibrated using melting point standards (In, Sn, Pb) and are believed to be accurate to within  $\pm 2^\circ\text{C}$ . The temperatures quoted in the NRL data (Figure 11) are believed to be  $\sim 20^\circ\text{C}$  lower than the true temperatures. Nevertheless, both sets of photoluminescence data reveal a clear trend in radiative defect density with growth temperature: the radiative defect density increases with growth temperature over the range 185–285°C. This behavior indicates an activated process for radiative defect formation possibly related to the kinetics of film growth (see Section 3.3).

Studies of photoluminescence of CdTe films grown in the second-generation VG80HI machine show a similar behavior of radiative defect density with growth temperature to that described above. These films, however, exhibit much weaker exciton-neutral acceptor ( $\text{\AA}$ , X) transitions than for films grown in the Westinghouse machine. This is indicative of higher purity films with less acceptor impurities, and may be due to the greatly increased area of cryoshrouding around the sample holder in the VG machine.

### 3.2.4 Electrical Characterization of CdTe/InSb Heterostructures

The structural properties of MBE CdTe films have been studied extensively<sup>3,7,8,9</sup>; however, no detailed studies of the electronic properties of MBE CdTe have been reported. In particular, Hall data for such films have not been reported to the best of our knowledge. This is not surprising since a) ohmic contacts to lightly doped CdTe are not readily obtainable, b) high-temperature treatments are likely to cause

diffusion of the contacts through very thin films to the underlying substrate, and c) film depletion from the heterojunction side of the thin film (for growth on InSb substrates) is expected to give Hall data which are difficult to interpret. Also, unintentionally doped MBE CdTe films grown on bulk CdTe substrates have low net acceptor concentrations ( $N_A - N_D \sim 3 \times 10^{13} \text{ cm}^{-3}$ ) and are p-type.<sup>28</sup> MBE CdTe films grown on InSb substrates, however, have a net donor concentration in the  $10^{15}$ - $10^{16} \text{ cm}^{-3}$  range.<sup>18</sup> Since rectifying contacts to bulk CdTe have been reported<sup>20,21</sup> and since our early CdTe films were only  $\sim 1.0 \mu\text{m}$  thick, it was decided that C-V profiling techniques were best suited for electrical characterization.

### 3.2.4.1 Capacitance-Voltage Profiling

MBE films of CdTe grown on InSb (001) substrates have been electrically characterized using C-V profiling techniques. In all cases, data were taken at a temperature of 295°K and at a measurement frequency of 1 MHz.

Device fabrication involved evaporation of 2000 Å indium onto the back of the InSb substrates (high carrier concentration n-type at 295°K) and evaporation of an array of Au Schottky barriers onto the MBE CdTe front surface as shown in the insert of Figure 12.

The C-V behavior shown in Figure 12 is typical for nearly ideal data obtained with this work. Several types of less ideal data have also been obtained from which careful interpretation can still provide useful information, as discussed later in this section. From this single curve, one can deduce carrier type (from the sign of the slope), built-in potential ( $V_{bi}$ ), net carrier concentration ( $N_D - N_A$ ), and film thickness ( $w_{max}$ ) nondestructively. Note that

$$N_D - N_A = \frac{2}{q\epsilon_s} \left[ \frac{d}{dV} (C^{-2}) \right]^{-1} \quad (1)$$

where  $C$  = capacitance per unit area.  $N_D - N_A$  is constant with distance below the film surface only if  $[\frac{d}{dV}(C^{-2})]^{-1}$ , i.e., the slope of the curves in Figures 12 and 13 are constant.

C-V data obtained for an array of Schottky barrier diodes also provide information regarding the spatial variation of all these parameters over the film surface and the variation of carrier concentration with distance below the film surface. Thus, the data shown in Figure 12 characterize an n-type MBE CdTe film 1.36  $\mu\text{m}$  thick, having a carrier concentration of  $8.25 \times 10^{14} \text{ cm}^{-3}$ . Also, the value of  $N_D - N_A$  is constant from  $\sim 0.94 \mu\text{m}$  to 1.36  $\mu\text{m}$  below the CdTe surface. Attempts to use conventional thermal probing to obtain carrier type were not successful. The value of  $V_{bi}$  for this case was  $\sim 0.95 \text{ eV}$ , which is reasonable for a Au Schottky contact to lightly doped N-CdTe. The zero-bias depletion depth ( $W_0$ ) in this case was  $\sim 1.15 \mu\text{m}$ . For small values of forward bias applied to this structure, we were able to probe to within 0.94  $\mu\text{m}$  of the film surface before significant diode forward current flow prevented accurate capacitance measurements. Thus, for  $N_D - N_A \lesssim 8 \times 10^{14} \text{ cm}^{-3}$ , film thickness must exceed 0.94  $\mu\text{m}$  to permit electrical characterization unless a lower work function barrier metal were used in place of the Au contact. However, for  $N_D - N_A > 8 \times 10^{14} \text{ cm}^{-3}$ , thinner films can be characterized.

Data taken at various locations on all the sample surfaces generally gave  $N_D$  values varying by no more than 15% (50% in the worst case). In all cases, plots of  $C^{-2}$  versus  $V$  gave straight lines for the range of depletion depths accessible, indicating highly uniform film doping for all unintentionally doped films. The curvature and subsequent nearly flat C-V behavior shown in Figure 12 for reverse bias merely indicate that the films are totally depleted under these bias conditions, i.e.,  $W_{max} = d_{film}$  (film thickness independently determined using surface profilometry measurements on films deposited onto oxidized silicon). Values of film thickness ( $d_{film}$ ) were in excellent agreement with  $W_{max}$  values obtained from C-V data. In general, however, we have more

Curve 745920-A

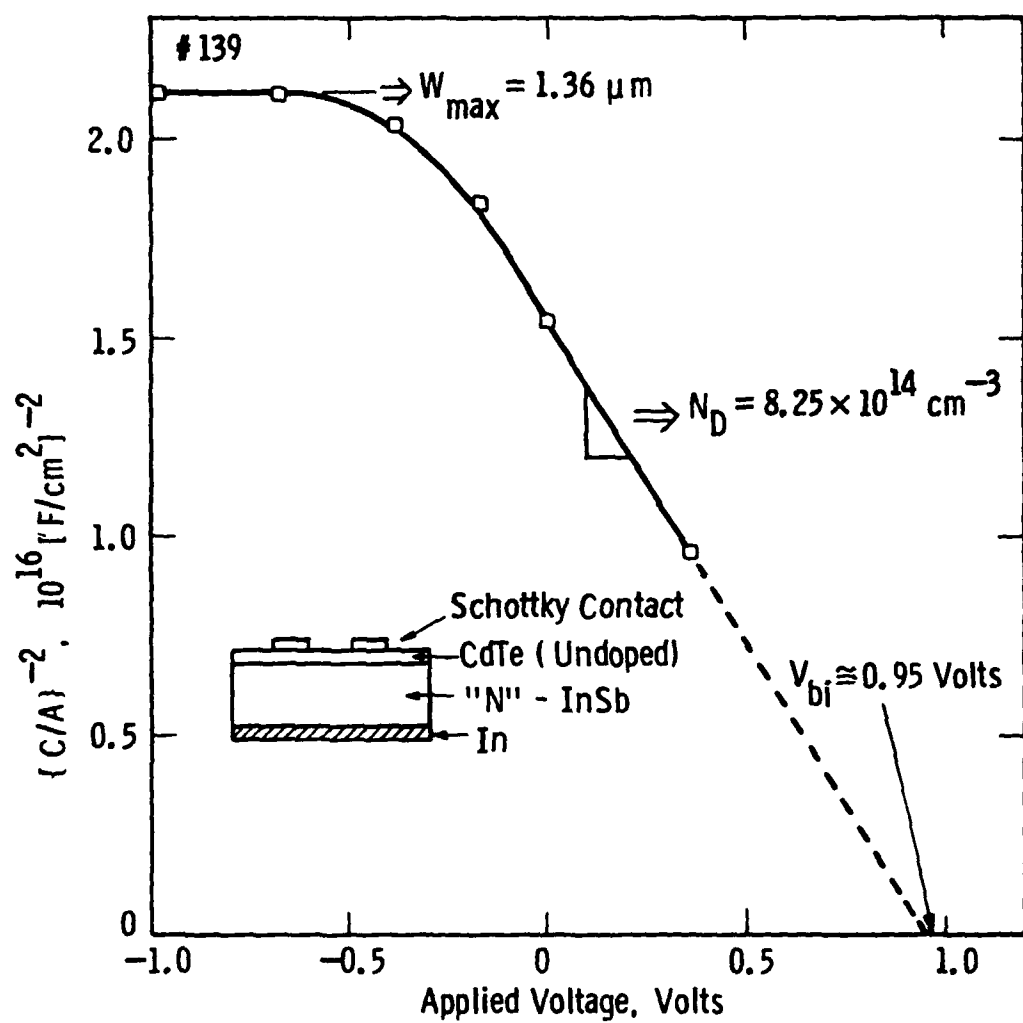


Figure 12. Capacitance ( $1/C^2$ ) - voltage plot for an undoped CdTe film (sample #139) grown on (001) InSb at 200°C. Film grown in Westinghouse MBE machine.

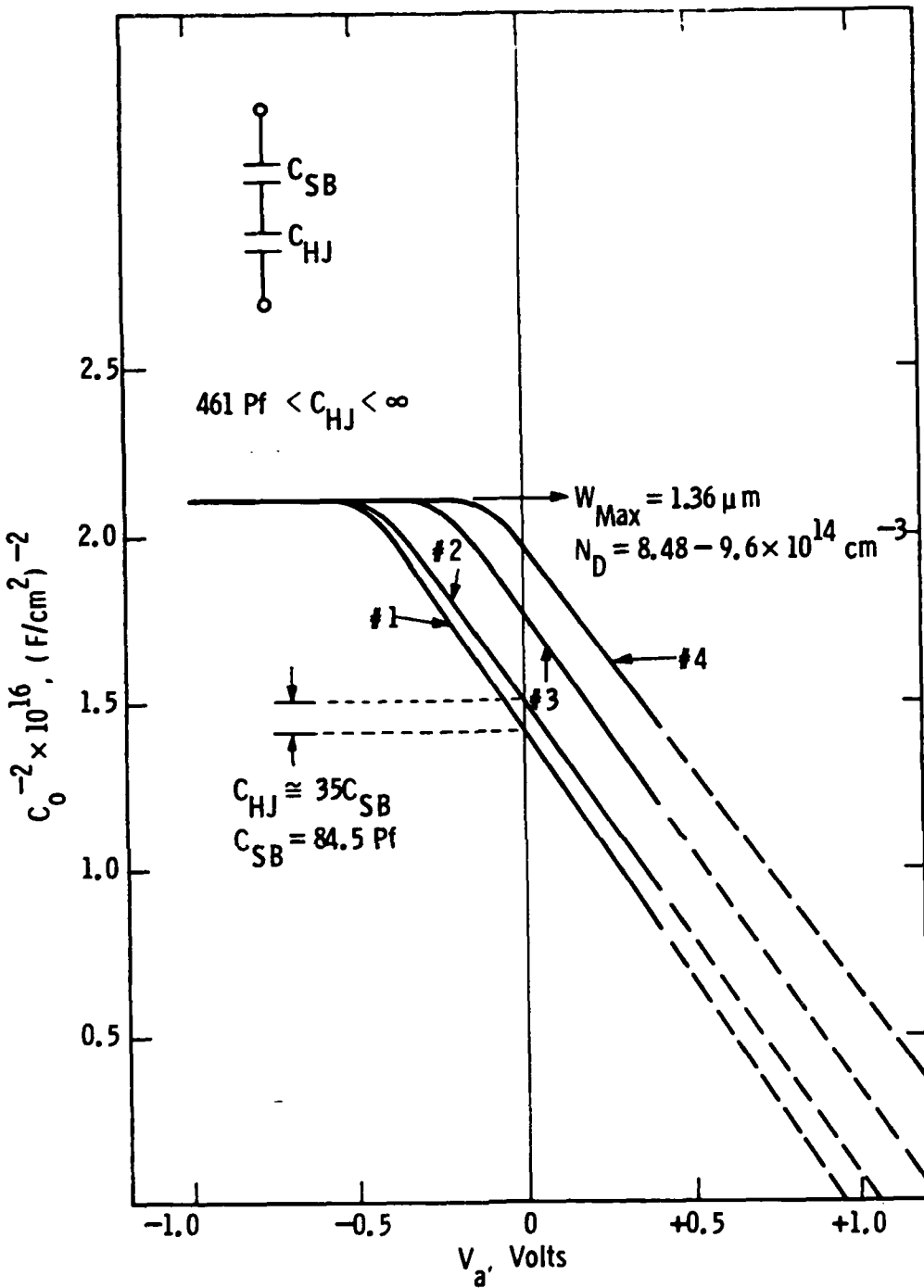


Figure 13. Capacitance ( $1/C^2$ )-voltage plots for an array of Schottky barrier diodes to undoped CdTe film (sample #139) grown on (001) InSb at 200°C. Note the dispersion of C-V plots for different diodes, due to lateral spatial variations in the heterojunction contribution to film depletion. The near-constant slopes of the C-V plots suggest, however, that the film carrier concentration varies only slightly both laterally and through the film depth.

confidence in those values obtained from C-V analysis of films grown on the substrate of interest. Also,  $W_{\max}$  is obtained from

$$W_{\max} = \frac{\epsilon_s}{C_{\min}} \quad (2)$$

where  $C_{\min}$  is the capacitance of the fully depleted film and varies as  $(N_D - N_A)^{1/2}$ . Very little change in capacitance is observed for larger values of reverse bias since the substrate doping is much larger than that of the film at 300°K. This behavior also suggests an abrupt isotype heterojunction at the CdTe/InSb interface.

This three-dimensional uniformity of net doping density obtained for our CdTe films is consistent with the overall deposition control expected for MBE films.

### 3.2.4.2 Heterojunction Interference Effects

One would intuitively expect that the presence of the CdTe/InSb heterojunction could result in behavior far more complex than that shown in Figure 12, and indeed, this is possible since the heterojunction capacitance ( $C_{HJ}$ ) is in series with the Schottky barrier capacitance ( $C_{SB}$ ). However, if the heterojunction depletion width is small compared to the Schottky depletion width, i.e.,  $C_{HJ} \gg C_{SB}$ , then the total capacitance measured will be  $C_{SB}$ . More importantly, if the  $C_{HJ}$  derives from a much larger effective area than that of the SB contact,  $C_{SB}$  will again dominate.

In a number of cases, we have observed some variation in the C-V data which we attribute to the presence of the underlying heterojunction. One case in point is shown in Figure 13. These data were obtained for various locations on the surface of the same film used to obtain the data in Figure 12. Note that devices #2, #3, and #4 are characterized simultaneously by larger values of  $W_0$  and  $V_{bi}$  than #1, while  $N_D$  varies by no more than  $\pm 7\%$  and  $W_{\max}$  (i.e., film thickness) is essentially constant. We believe that the only self-consistent explanation for this

behavior is the spatially variable influence of the underlying heterojunction, either regarding its depletion width or its effective area, both of which influence the total series capacitance measured. However, even though  $C_{HJ}$  is variable, film thickness, carrier type, and carrier concentration can be fairly accurately and nonambiguously determined.

Assuming that curve #1 of Figure 13 is characteristic of  $C_{SB}$  alone (i.e.,  $C_{HJ}/C_{SB} \rightarrow \infty$ ), then the relatively small displacement between curves #1 and #2 corresponds to  $C_{HJ}/C_{SB} = 35$ . Similarly, the larger displacement between curves #1 and #4 corresponds to  $C_{HJ}/C_{SB} = 5.5$ .\*

We have attempted to more precisely characterize the capacitance and the effective area of the heterojunction in several ways. The first approach involved attempts to make ohmic contacts to both the CdTe and the InSb to permit direct measurement of  $C_{HJ}$ . However, we were unable to make non-SB contacts to our CdTe films ( $N_D - N_A \sim 8 \times 10^{14} \text{ cm}^{-3}$ ). Sintered contacts (e.g., In) to such lightly doped thin films would be expected to readily diffuse through to the InSb substrate,<sup>22</sup> and thus sintering was not explored.

We also etched a deep (~50  $\mu\text{m}$ ) moat around the periphery of a single device so that  $A_{SB} = A_{HJ}$ . The MBE film thickness was 1.29  $\mu\text{m}$ . In this case, from the overall drop in total measured capacitance, we deduced a maximum zero-bias heterojunction depletion width of 0.45  $\mu\text{m}$  assuming that initially  $A_{HJ} = A$  film. If  $A_{HJ} < A$  film, then  $W_{HJ} < 0.45 \mu\text{m}$ . Thus,

---

\*It seems likely that the spatial variation of  $C_{HJ}$  may be due to a variation in the depletion potential at the heterojunction. This parameter is sensitive to structural quality and compositional grading at the interface. Small but significant spatial variations in the double-crystal rocking curve linewidth, for the samples used in the C-V studies, have recently been observed and linked to nonuniform ion bombardment of the InSb substrate prior to CdTe growth. This problem has been reduced in the Westinghouse machine and eliminated in the VG80HI machine by appropriate adjustment of the ion beam direction and by sample rotation during ion bombardment.

we infer that for equal areas,  $C_{HJ} > C_{SB}$  or  $W_{SB} > W_{AJ}$  at zero bias. It should be noted here that this was done for only one device on one substrate. Further work should include a larger sampling to separate heterojunction depletion width variations from heterojunction effective area effects. Also,  $W_{HJ}$  and/or  $A_{HJ}$  are expected to vary with position based on the results shown in Figure 13. Note here that due to the presence of the underlying heterojunction, the accuracy of this technique improves as the Schottky barrier contact area is reduced. Also, use of a higher density of smaller area diodes would permit higher resolution mapping of carrier type, carrier concentration, and film thickness.

In addition, the zero-bias capacitance of several SB devices was measured in a back-to-back configuration which excludes  $C_{HJ}$ . For those devices measured in this way, the back-to-back capacitance of two Schottky junctions in series was approximately half that of either junction measured with respect to the substrate. A larger data base is needed here also and should be useful for situations like that shown in Figure 13. This also allows for further verification of the uniformity of  $C_{SB}$ .

#### 3.2.4.3 Preliminary Doping Studies

These studies were carried out at an early stage in the VG80HI machine described in Section 3.1. C-V characterization of the first film we received, which was grown in the VG80HI machine, showed minimal heterojunction interference. However, the carrier concentration deduced from the data shown in Figure 14(a) was  $\sim 1.5 \times 10^{16} \text{ cm}^{-3}$ . This was the largest value of  $N_D - N_A$  for any unintentionally doped film characterized in this program and about an order of magnitude larger than the largest value measured in the old system. However, this film was grown under nonideal conditions and exhibited some twinning.

We also received one sample grown some ten runs later in which a deliberate attempt was made to increase the net donor density by incorporating indium into the beam flux at a fraction corresponding to

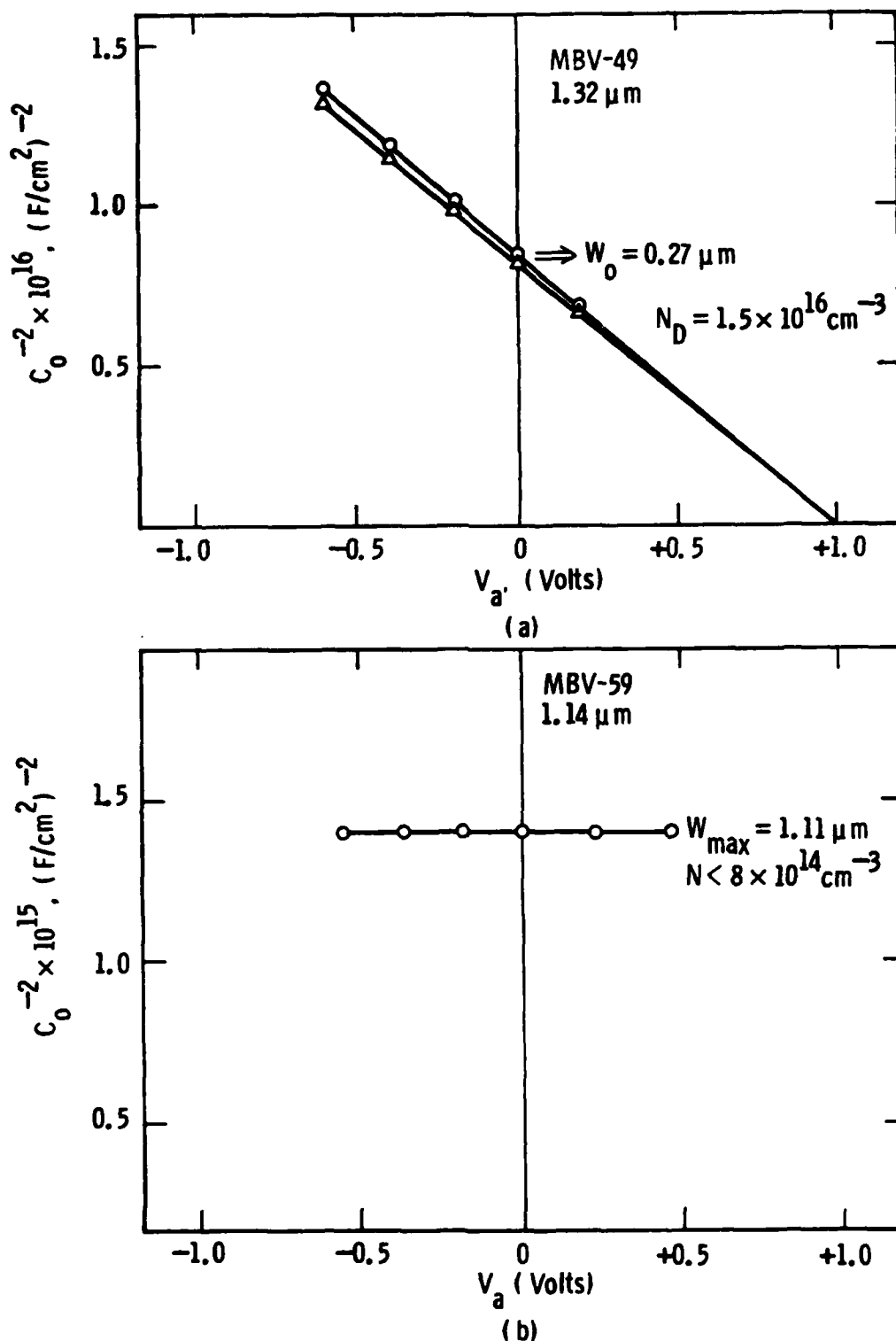


Figure 14. Capacitance ( $1/C^2$ )-voltage plots for (a) nominally undoped CdTe film (sample MBV49) and (b) In-doped CdTe film (sample MBV59). Both films were grown at  $234^\circ\text{C}$  on (001) InSb in the VC80HI MBE machine. The In-doped film has a lower free-electron concentration than  $8 \times 10^{14} \text{ cm}^{-3}$ . On the other hand, the nominally undoped film has a free-electron concentration  $> 10^{16} \text{ cm}^{-3}$ . This film was grown under nonideal conditions before adequate charge conditioning.

$10^{16} \text{ cm}^{-3}$ . Unfortunately, the film thickness ( $\sim 1.3 \mu\text{m}$ ) and net doping were such that the films were fully depleted and gave a flat C-V response as shown in Figure 14(b). Similar behavior was observed earlier in the program for thin films ( $\sim 1 \mu\text{m}$ ). We infer from  $W_0$  ( $= W_{\max}$  in this case) that the net donor doping in this case must be  $< 8 \times 10^{14} \text{ cm}^{-3}$ . Thus, we conclude that our first extrinsic doping attempt was unsuccessful.

#### 3.2.4.4 Conclusions

MBE CdTe films grown on InSb (001) substrates have been electrically characterized using C-V profiling techniques (see Table 2). Film thicknesses ranged from  $1.14 \mu\text{m}$  to  $2.8 \mu\text{m}$ . This technique has also allowed us to obtain useful electrical information on the CdTe/InSb heterojunction. All films showed n-type conduction and typically  $N_D - N_A = 3 \times 10^{14} - 1.5 \times 10^{15}$ . In all cases, capacitance values

TABLE 2  
ELECTRICAL PROPERTIES OF MBE CdTe FILMS

Film I.D.	Film Thickness ( $\mu\text{m}$ )	$W_{\max}$ ( $\mu\text{m}$ )	$W_0$ ( $\mu\text{m}$ )	Type	$(N_D - N_A) \text{cm}^{-3}$	$T_s (\text{ }^\circ\text{C})$
#135	1.29	1.27	1.27	N	$4.4 \times 10^{14}$	233
#139	1.40	1.36	1.15	N	$8.9 \times 10^{14}$	186
#141	2.80	2.78	+	N	$3 \times 10^{14}$	186
#148	1.92	1.91	+	N	$1.35 \times 10^{15}$	186
MBV 49	1.32	*	0.84	N	$1.5 \times 10^{16}$	236
MBV 59	1.14	1.11	0.27	*	$< 8 \times 10^{14}$	232

\* Insufficient data

+ Interference from heterojunction

measured for fully depleted films gave a precise and nondestructive measure of film thickness. Values of  $N_D - N_A$  were invariant over the range of depletion depths accessible, indicating highly uniform film doping for all unintentionally doped layers. Very small variations, typically  $\sim \pm 7\%$ , in  $N_D - N_A$  were observed for measurements taken at various positions on the film surface. This three-dimensional uniformity of net doping density obtained for our CdTe films is consistent with the overall deposition control expected for MBE growth.

### 3.2.5 Magnetophotoconductivity Studies of MBE-Grown CdTe/InSb Structures

Far-infrared magnetophotoconductivity studies of MBE-grown CdTe films on InSb (001) were carried out at NRL (by Dr. R. J. Wagner) on samples prepared prior to October 1983. The technique and experimental method is described in Reference 22. These studies revealed no features in the photoconductivity spectra attributable either to carrier transport in the CdTe films or to an inversion layer in the p-type InSb substrate. In the period from October 1983 to July 1984, considerable improvements were made in the structural and optical quality of the CdTe films by optimizing<sup>6</sup> InSb surface preparation, growth temperature, and conditioning of the CdTe effusion source. The high-perfection films described in Section 3.2.2 were prepared in this period. Several of these films were sent to Dr. B. D. McCombe (SUNY) for magnetophotoconductivity studies. Here, the results of a study on one of the samples, MBE 189, are presented. Additional studies on further samples are presently in progress. The growth conditions and InSb substrate parameters are summarized in Table 3.

Figure 15 shows the photoconductivity response for MBE 189 versus photon energy for several different magnetic fields (top trace to bottom trace:  $B = 0, 1.5T, 2.5T, 3.0T$ , and  $3.5T$ ). All data were taken with a Fourier Transform Interferometric Spectrometer with the sample in a light-pipe system immersed in liquid helium and cooled by helium exchange gas. The photoconductive spectrum is rich in structure. The features which can be assigned with near certainty are identified by the

light lines and labelling. The minimum which occurs at about  $144\text{ cm}^{-1}$  and which is independent of magnetic field is due to TO phonon absorption in the CdTe epilayer. The line labelled "InSb substrate" is due to acceptor impurity transitions in the substrate that contribute to the photoconductivity due to contacts being made right through the CdTe film to the InSb substrate.

TABLE 3  
GROWTH AND SUBSTRATE PARAMETERS FOR SAMPLE MBE 189

InSb Substrate: p-type, Cd-doped, (001) wafer plane

77K electrical data:

$$n_A = n_D = 5.10^{14} \text{ cm}^{-3}$$

$$u_H = 9000 \text{ cm}^2 \text{ V}^{-1} \text{ s}^{-1}$$

Supplier: Metal Specialties, Inc.

Crystal Grower: MCP Ltd. Wembley, U.K. Ingot 1SC 119

Etch pit density < 300  $\text{cm}^{-2}$

CdTe Film Growth Parameters:

CdTe Effusion Source Orifice	1 mm
CdTe Effusion Source Temperature	670°C
(Cd + 1/2 Te <sub>2</sub> ) Beam Pressure at Sample	2.1 $10^{-7}$ Torr
Growth Temperature	185°C
Growth Rate	0.5 $\mu\text{m/hr}^{-1}$
Film Thickness	1.0 $\mu\text{m}$

Film Grown on April 10, 1984

Double-Crystal X-Ray Diffraction Linewidth:

21.5 arc sec for (004), Bragg Diffraction, CuK $\alpha$  Radiation

The line labelled CdTe 1s + 3p appears to be a transition from the ground state (1s) to a higher excited state of the hydrogenic system of a donor impurity. The 1s + 3p transitions are clearly observed as

PHOTOCONDUCTIVE RESPONSE

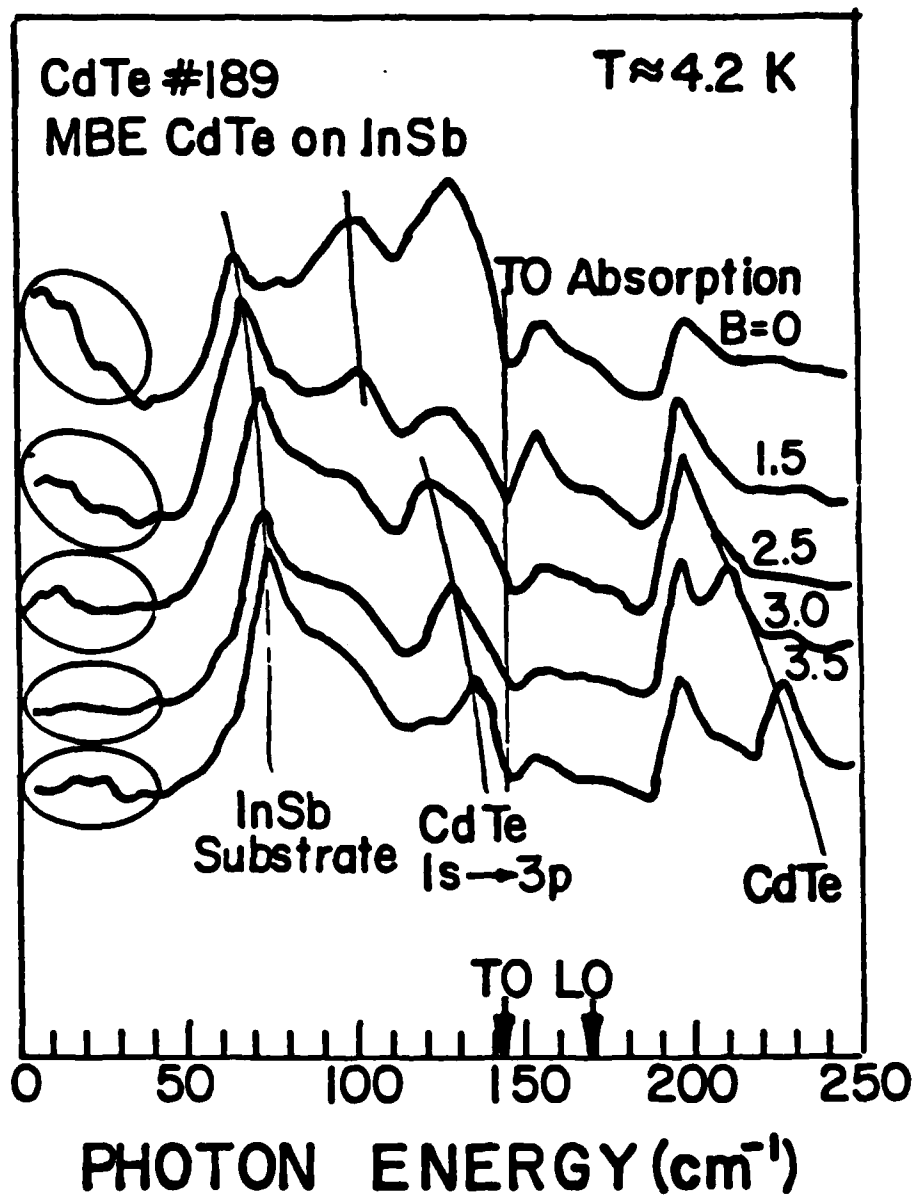


Figure 15. Photoconductive response of MBE-grown CdTe film on InSb (001) orientation substrate, sample #189 (recorded by Dr. B. D. McCombe; see text for details).

labelled. Photoresponse from the  $1s + 2p$  transitions is not observed because  $kT$  at the ambient temperature is not sufficient to ionize this excited state. The  $2p +$  continuum energy at zero magnetic field is about 3.5 meV, 10 times  $kT$  at 4.2K, and this energy increases with magnetic field.

The circled region at very low photon energies has the character of free-carrier photoresponse (intensity decreases with increasing photon energy). As the magnetic field is increased, this photoresponse decreases; it is very weak at 3T. At higher magnetic fields, it takes on the character of a resonant response. This may<sup>23</sup> be due to free electrons in an inversion layer in the InSb at the InSb-CdTe interface resulting from charge transfer from the CdTe donors to the p-type InSb (as in modulation-doped GaAs-AlGaAs heterostructures). Further investigations are in progress at SUNY to investigate this possibility.

Figure 16 shows a compilation of the major features in the photoconductive signal that can be identified with some degree of certainty. The transition energy, at which the peaks are observed, is plotted as a function of magnetic field. For comparison purposes, data from donors in bulk CdTe<sup>22</sup> (solid lines) and acceptors in bulk InSb<sup>24</sup> (dashed lines) are also shown. The data points attributed to CdTe donor transitions are shown as solid circles, while the data points attributed to acceptor transitions in the InSb substrate are shown as solid triangles. By heating the samples to about 10-15K, it should be possible to observe the  $1s + 2p$  transitions easily, and by studying them at high resolution, it should be possible to determine the chemical nature of the donor impurities.

### 3.3 Growth Kinetics and Doping Limitations of CdTe

The primary beam species in the growth of CdTe from a single congruently subliming source of CdTe are<sup>3</sup> Cd and Te<sub>2</sub> with a beam flux ratio locked (in the steady state) to:

$$J_{cd} / 2J_{Te_2} = 1$$

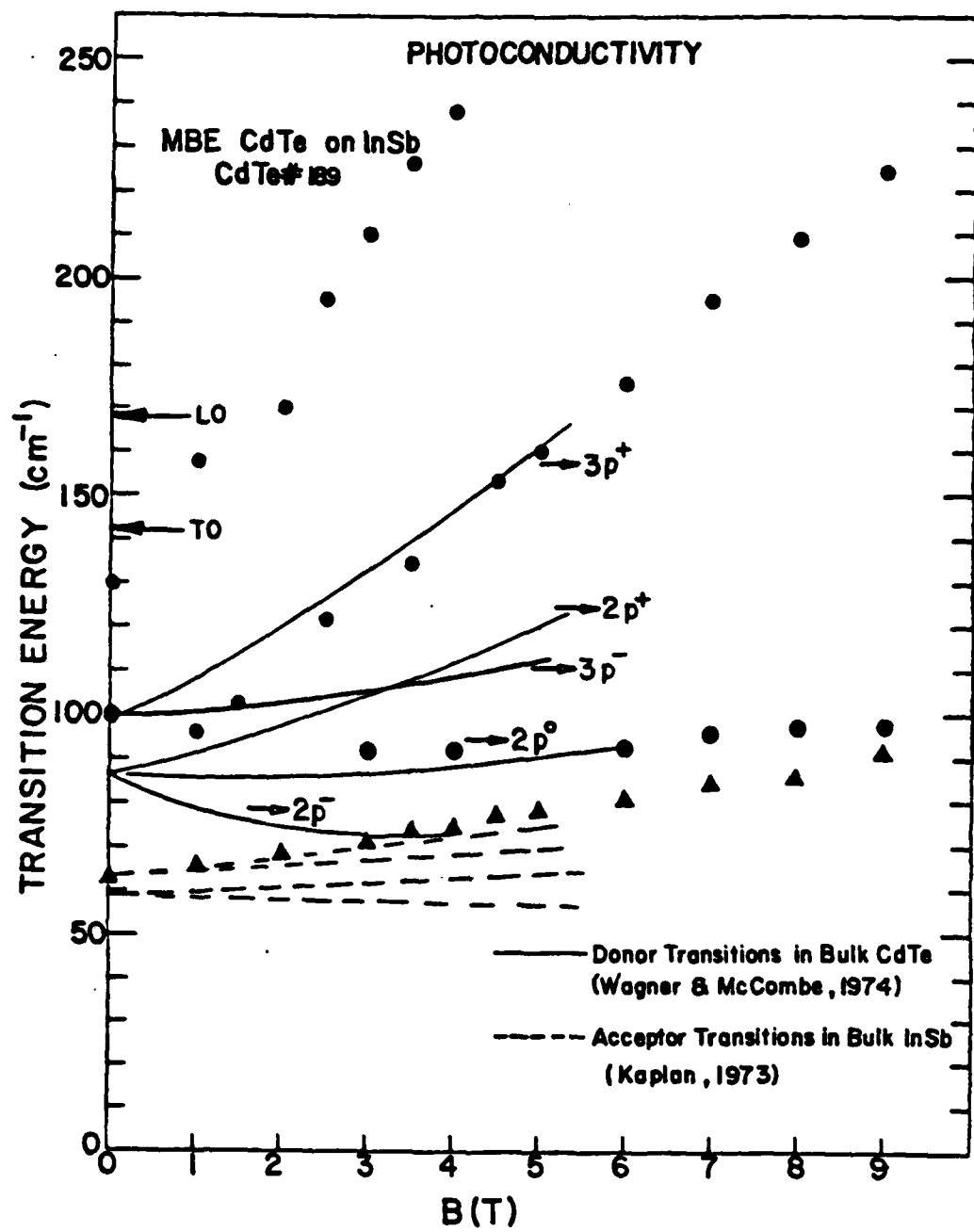


Figure 16. Transition energies as a function of magnetic field for sample #189 (recorded by Dr. B. D. McCombe; see text for details).

physisorbed precursor state before meeting up with Te from dissociated  $\text{Te}_2$ . In this case, excess Te might be incorporated into the film as isolated atoms rather than the undissociated  $\text{Te}_2$  units at lower temperatures. At even higher temperatures,  $\text{Te}_2$  desorption would compete with reaction with Cd. Both  $\text{Te}_2$  and Cd would have a short surface residence time and a fall-off in growth rate would result. In fact, we observe that the growth rate of CdTe falls off rapidly at surface temperatures above 300°C.

The photoluminescence spectra of films grown in the 185-285°C temperature range show clear evidence (see Appendix 3) for an activated process creating defect-related peaks. The radiative defect density ( $\rho$ ) increases with an Arrhenius behavior with an activation energy of ~35 kcal mole<sup>-1</sup>. At this stage, the exact nature of the defects is unclear. However, several distinct types probably exist as evidenced by the multiplicity of deep-level peaks superimposed on a broad continuum. Cd vacancies and Te interstitials are likely candidates.

As for the question of In doping of CdTe, the limited amount of data obtained (see Section 3.2.4) shows that In is not, under the limited set of conditions so far explored, incorporated as a simple substitutional impurity on a Cd site. Much more data are required to determine whether it is complexed with a defect. The quality of the CdTe films at the time of the doping studies was not optimized and in view of the strongly temperature-dependent concentration of defects, simple substitutional In may be possible only in a narrow range of growth temperatures. These studies are being actively pursued.

On the basis of a very limited amount of DCRC data, the RSRE group found<sup>3</sup> that the lattice parameter of a film grown at  $T_s = 150^\circ\text{C}$  was significantly less than a film grown at  $220^\circ\text{C}$ . On the basis of this observation, they speculated that the expansion of the CdTe lattice at  $220^\circ\text{C}$  was due to nonequivalent sticking coefficients of Cd and Te<sub>2</sub>, leading to preferential desorption of Cd at the higher growth temperature. From a much greater data base (~250 films), we find no such systematic trend in film lattice parameter with growth temperature calculated from<sup>25</sup>:

$$\left(\frac{\Delta d}{d}\right)_{\text{relax}} = \frac{1-v}{1+v} \left(\frac{\Delta d}{d}\right)_\perp$$

where v is Poisson's ratio for CdTe,  $\left(\frac{\Delta d}{d}\right)_{\text{relax}}$  is the lattice misfit between relaxed, unstrained film material and the substrate, and  $\left(\frac{\Delta d}{d}\right)_\perp$  is the strain measured for (004) Bragg planes. The measured values of  $\left(\frac{\Delta d}{d}\right)_\perp$  are remarkably constant at  $(94\pm2) \times 10^{-5}$  for all high-perfection films grown at temperatures from 170 to  $285^\circ\text{C}$  and at rates from  $0.29$ - $1.27 \mu\text{m h}^{-1}$ . This value of  $\left(\frac{\Delta d}{d}\right)_\perp$  is identical to that found by the RSRE group for the film grown at  $220^\circ\text{C}$  and indicates a film lattice parameter of  $6.48229(1) \text{ \AA}$ . We find, however, that films grown below  $170^\circ\text{C}$  and at rates above  $1.27 \mu\text{m h}^{-1}$  frequently exhibit broad rocking curves with significantly lower values of  $\left(\frac{\Delta d}{d}\right)_\perp$  than  $(94\pm2) \times 10^{-5}$ . In these cases, the films are clearly heavily faulted with a significant fraction of lattice misfit accommodated by dislocation networks. The observation<sup>9</sup> of Te precipitates in heavily faulted films grown below  $170^\circ\text{C}$  is indicative of incomplete reaction between Cd and Te<sub>2</sub> leading to condensation of Te<sub>2</sub> and desorption of Cd, the volatile species. The growth kinetics of CdTe involves a delicate balance between the competing processes of Cd desorption from a precursor state and Cd reaction with chemisorbed Te<sub>2</sub>. For example, if the surface temperature is too low for activation of Te<sub>2</sub> chemisorption, then the Cd + Te reaction cannot occur. Cd will be desorbed (above  $\sim 130^\circ\text{C}$ ) leaving crystalline Te precipitates formed by condensation of molecular Te<sub>2</sub>. In a higher surface temperature regime, Cd may be desorbed from a

#### 4. MBE GROWTH AND INVESTIGATION OF $Hg_{1-x}Cd_xTe$ FILMS

The growth of  $Hg_{1-x}Cd_xTe$  films by MBE techniques requires<sup>26</sup> a stable high-intensity flux of Hg atoms in addition to stable Cd and  $Te_2$  fluxes. It also requires a method of pumping the large gas loads of Hg vapor and transfer of large quantities (~0.5 kg) of condensed Hg from the growth chamber following growth. We have designed, commissioned, and successfully used a novel type of Hg source on the VG80HI machine for  $Hg_{1-x}Cd_xTe$  alloy film growth.

##### 4.1 Growth Conditions

The problem of removal of condensed Hg from the cryoshroud, following a long sequence of growth runs, has been solved by interfacing an auxiliary pumping system (Hg-diffusion pumped) to the VG80HI machine. For Hg removal, a six-inch-bore gate valve between the VG machine and the auxiliary system is opened and the entire growth chamber is heated to 70°C. The ion and cryopumps are sealed off from the growth chamber, the Hg vapor pressure then increases in the growth chamber, and Hg is condensed on a liquid nitrogen-cooled trap in the auxiliary pumping system. Typically, removal of 500 gm from the growth chamber takes about 48 hours.

A photograph showing the auxiliary system connected to the VG80HI machine during a Hg transfer is shown in Figure 17. The Hg source comprises a large reservoir of mercury, external to the MBE growth chamber, connected by a heated inlet tube to the growth chamber. The Hg beam flux at the substrate is controlled by the reservoir temperature which sets up the pressure gradient down the inlet tube. The temperature of the inlet tube is maintained some 20°C higher than the reservoir to prevent Hg condensation. Figure 18 shows the

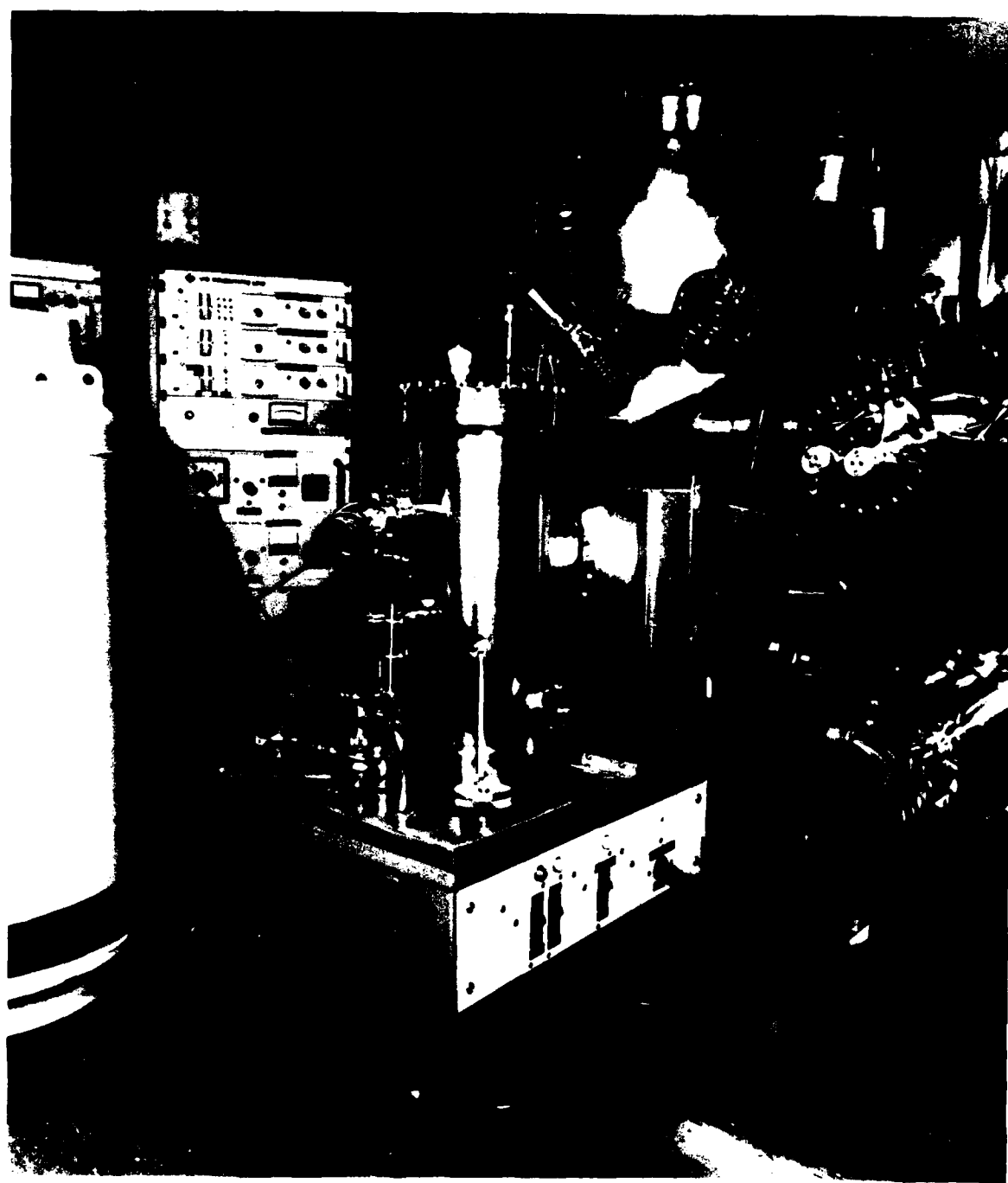


Figure 17. Photograph of VG80HI MBE machine with auxiliary pumping system shown in foreground. The auxiliary system incorporates a large-capacity liquid-nitrogen-cooled cryotrap for condensing Hg transferred from the VG80HI growth chamber. The auxiliary system is Hg diffusion pumped.

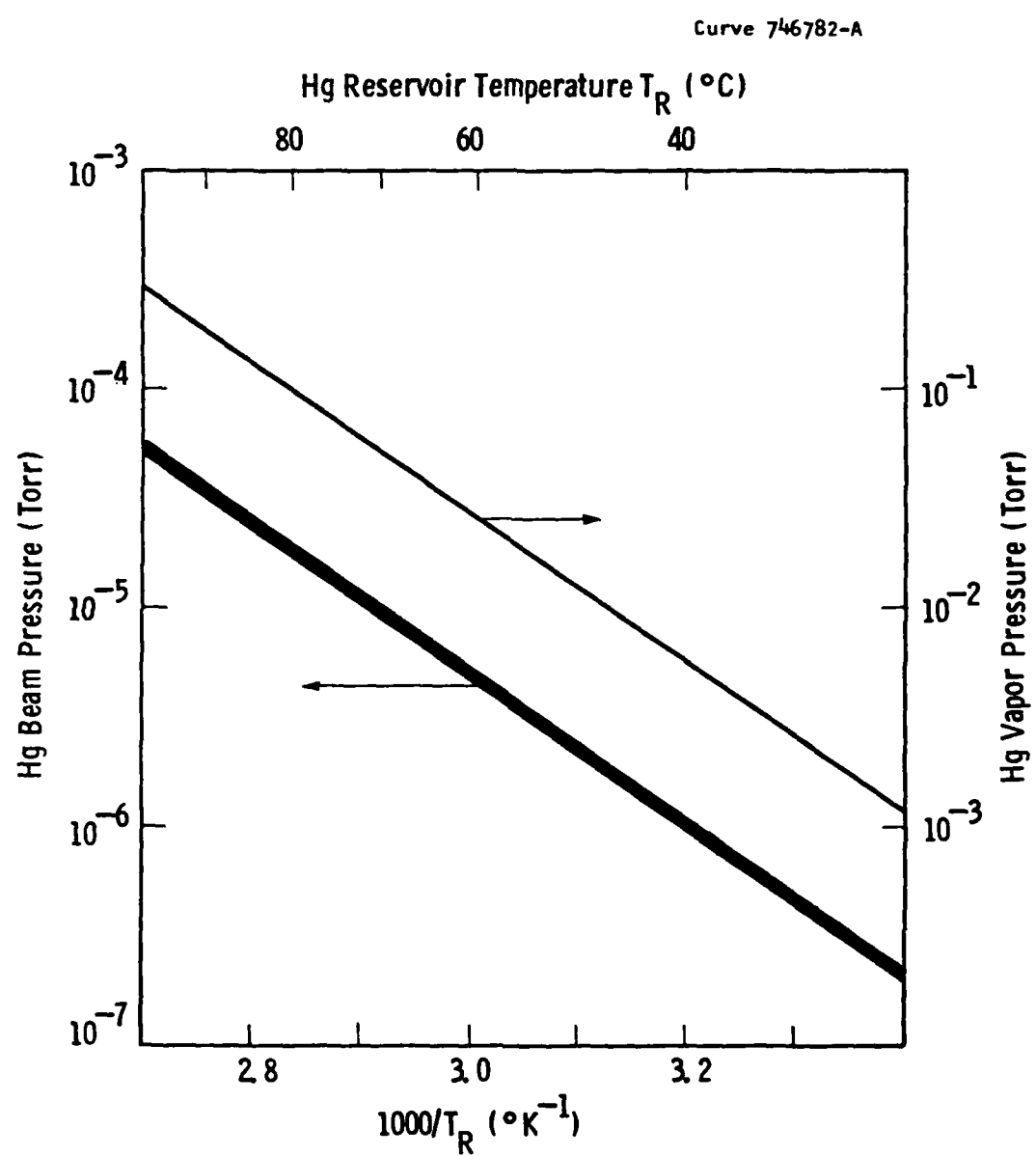


Figure 18. Measured beam pressure (broad line) of Hg versus temperature of Hg reservoir for Hg source on VG80HI machine. The light line indicates the equilibrium vapor pressure of Hg.

results of measurements of Hg-beam impingement pressure (measured using an ion gauge at the substrate position) as a function of reservoir temperature. The broad line represents the Hg beam pressure while the light line indicates the equilibrium vapor pressure of Hg. As expected, the beam pressure has the same (Arrhenius) temperature dependence as the equilibrium vapor pressure for Hg. Growth of  $Hg_{1-x}Cd_xTe$  ( $x \sim 0.2$ ) films at substrate temperatures of 180-200°C requires Hg beam pressures in the  $10^{-4}$  Torr range. These values are readily obtained by setting the reservoir temperature at 130-140°C. Automatic temperature control on the reservoir is to within  $\pm 0.2^\circ C$ . A major advantage of this type of Hg source is that the reservoir can be refilled without the need for complex vacuum interlocks or other complex transfer schemes. The flow of Hg can be cut off (using a valve in the inlet tube) instantly if required.

Growth of  $Hg_{1-x}Cd_xTe$ , using the new source, has been investigated under a variety of exploratory growth conditions. During the period of this report, growth of CdTe films has been optimized in the VG80HI machine. Exploratory  $Hg_{1-x}Cd_xTe$  films were grown onto CdTe buffer layers grown on (001) InSb substrates. Buffer layer growth was carried out at 275°C, and the  $Hg_{1-x}Cd_xTe$  films were grown at 160°C for a variety of  $[Cd]/[Te_2]$  flux ratios. Following InSb surface cleaning, the RHEED pattern exhibited the 4 x 2 In-stabilized reconstruction. During CdTe buffer layer growth, the RHEED pattern developed into a well-defined 2 x 1 reconstruction. It was found that even for very high Hg fluxes (beam equivalent pressures in the mid  $10^{-4}$  Torr range), the film quality progressively degraded with increasing film thickness. This degradation was clear from the fading of the (2 x 1) RHEED pattern and broadening of the diffraction streaks. We believe this behavior is a result of too low a substrate temperature for growth of the alloy. As in the case of CdTe growth, incomplete reaction between Cd and  $Te_2$  (and Hg and  $Te_2$ ) occurs at too low ( $\leq 160^\circ C$ ) a substrate temperature and results in Te precipitation with consequent faulting of the film. This diagnosis was confirmed by direct observation of Te precipitates in the

$Hg_{1-x}Cd_xTe$  films using cross-section TEM analysis (see Section 4.2). The use of higher substrate temperatures, in the period following termination of this contract, considerably improved film quality (see also Section 4.2).

#### 4.2 Characterization of $Hg_{1-x}Cd_xTe$ Films

Detailed structural examination of only one MBE-grown  $Hg_{1-x}Cd_xTe$  film was possible in the period of this contract. X-ray photographic studies of the film MBV 88 revealed extensive twinning. Detailed microstructural analysis of the film was carried out using cross-section transmission electron microscopy (XTEM) analysis. The method used for preparation of sample foils for XTEM of this materials system ( $CdTe-Hg_{1-x}Cd_xTe$ ) was first developed<sup>27</sup> by the Westinghouse electron microscopy group and represents a major development in the infrared materials characterization field. Appendix D describes the method of foil preparation and analysis.

Figure 19 shows a cross-section transmission electron micrograph of an MBE-grown structure comprising a CdTe buffer layer 0.44  $\mu m$  thick, grown on an (001) InSb substrate at  $T_g = 275^\circ C$ , followed by a 2.9  $\mu m$  thick film of  $Hg_{1-x}Cd_xTe$  grown at 160°C. The micrograph reveals no extended defects in the CdTe buffer layer, but it shows that, at the onset of growth of the alloy film, precipitates are formed which lead to extended defect (microtwin) propagation and to deterioration of film quality to columnar polycrystallinity. Compositional analysis of the foil by the EDS (energy-dispersive spectroscopy analysis of X-rays) technique is possible with high spatial resolution (<100 Å) and reveals the origin of the precipitates. Figure 20 shows EDS spectra from the near-surface region of the alloy film (upper spectrum), from a precipitate, and from points close to the alloy film-buffer layer interface. The precipitates are positively identified as pure Te. The alloy film-buffer layer interface is compositionally hyperabrupt, while significant variations in film composition through the film depth are

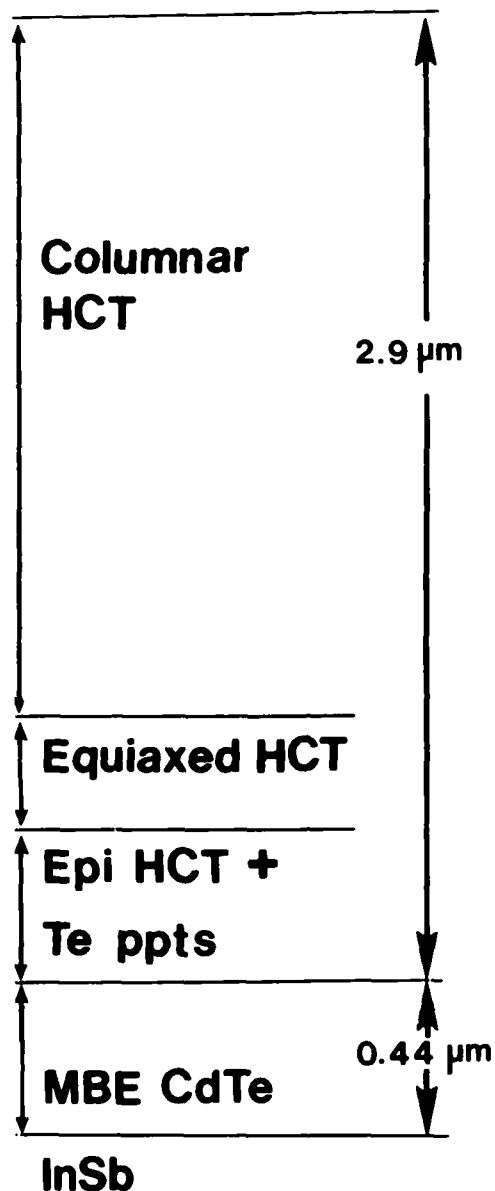
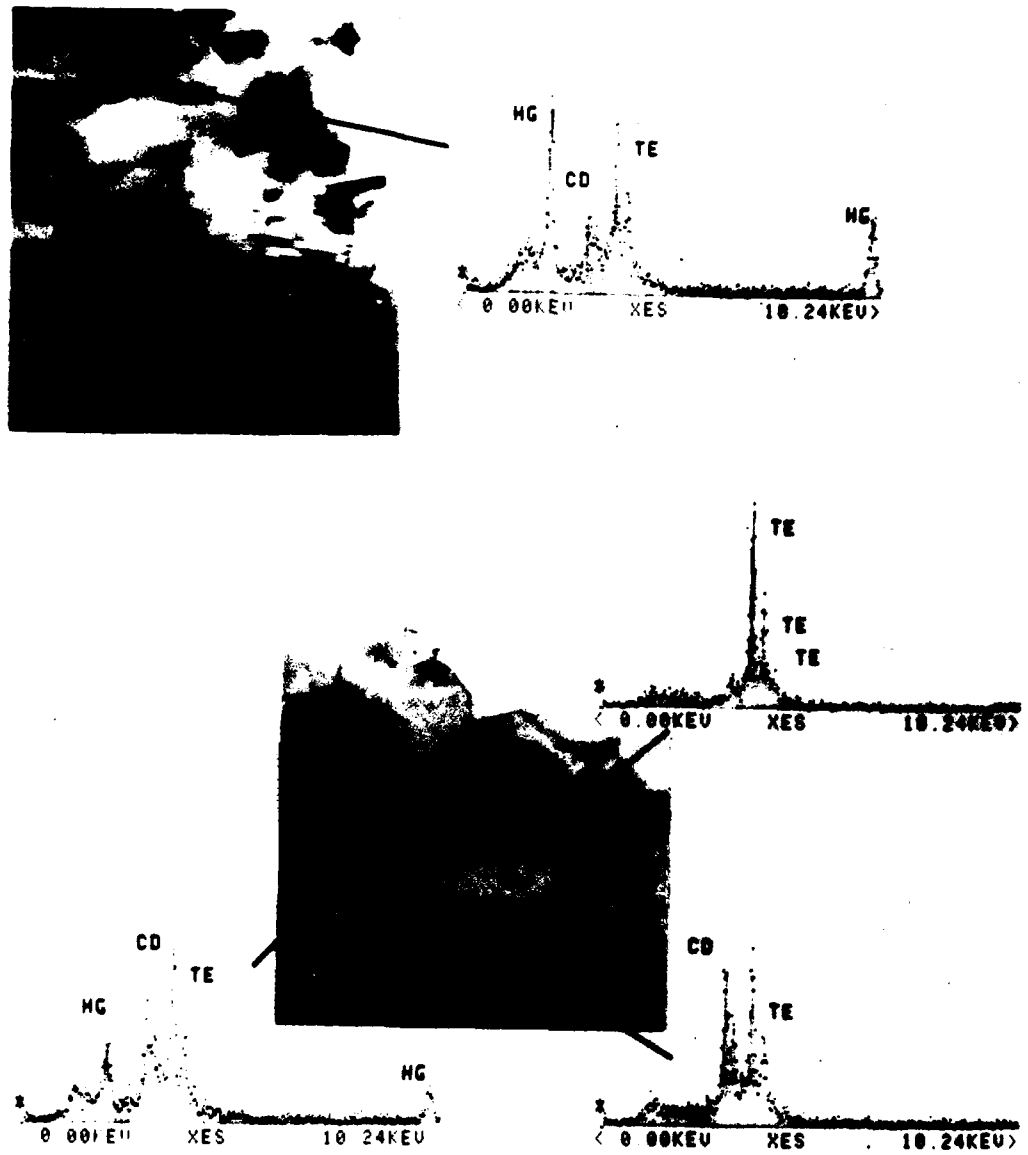


Figure 19. Cross-section transmission electron micrograph of MBE-grown  $\text{Hg}_{1-x}\text{Cd}_x\text{Te}/\text{CdTe}/\text{InSb}$  (001) substrate structure (see text for details); sample number MBV 88.



**Figure 20.** High spatial resolution compositional data from EDS of cross section of sample MBV 88. The regions probed by the electron beam are indicated in the micrographs. Note the positive identification of microprecipitates of elemental Te in the  $Hg_{1-x} Cd_x Te$  film.

apparent. The origin of the Te precipitates is believed to be incomplete reaction between Cd (or Hg) and  $\text{Te}_2$  due to kinetic limitations of the  $\text{Cd}$  (or  $\text{Hg}$ ) +  $1/2 \text{Te}_2$  reaction at the low growth temperature. The value of this XTEM analysis is that it indicates the required change in MBE growth conditions to improve film quality; namely, an increase in growth temperature.

Improved films have since been grown at higher temperatures. Double-crystal X-ray rocking curve analysis (see Figure 21) of one such film, grown on a CdTe substrate, confirms that the structural quality is excellent (DCRC FWHM 53 arc sec) for the alloy film and is limited by the quality of the CdTe substrate. Figure 22 shows an infrared transmission spectrum for a  $6.4 \mu\text{m}$  thick film of  $\text{Hg}_{1-x}\text{Cd}_x\text{Te}$  ( $x \approx 0.22$ ) grown on an (001) orientation CdTe substrate at  $190^\circ\text{C}$ . The transmission edge is well defined, and the presence of the interference ripples is indicative of a smooth interface.

Curve 749512-A

DCRC MBE HgCdTe/CdTe (001) #152

$2.1 \mu\text{m } T_g = 190^\circ\text{C}$

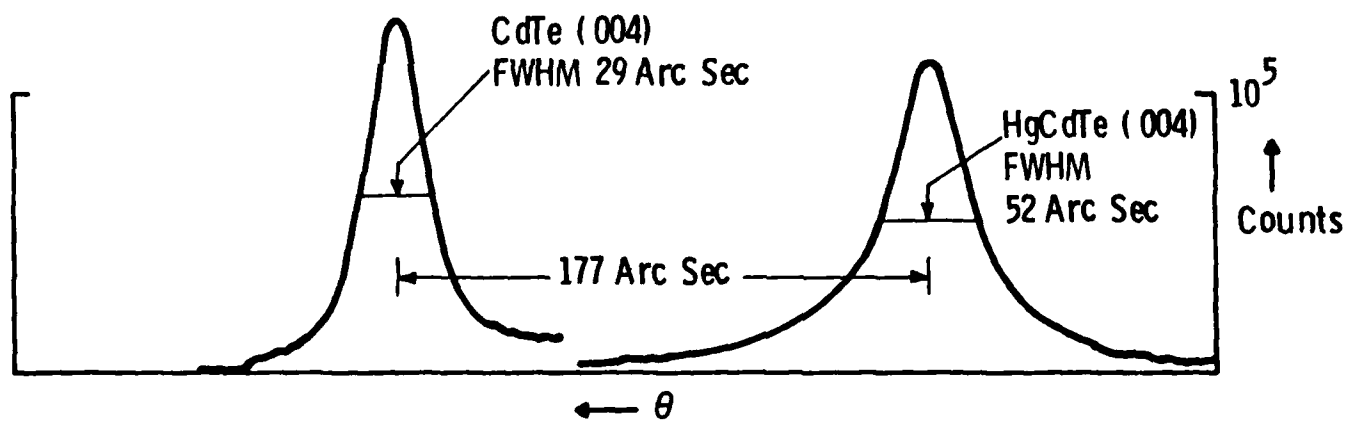


Figure 21. Double-crystal X-ray rocking curve of a  $2.1 \mu\text{m}$  thick  $\text{Hg}_{1-x}\text{Cd}_x\text{Te}$  ( $x \approx 0.4$ ) film grown on (001) orientation CdTe Substrate at  $190^\circ\text{C}$ . Growth of the  $\text{Hg}_{1-x}\text{Cd}_x\text{Te}$  film was preceded by a CdTe buffer layer  $0.1 \mu\text{m}$  thick, grown at  $T_g = 275^\circ\text{C}$ .

Curve 749612-A

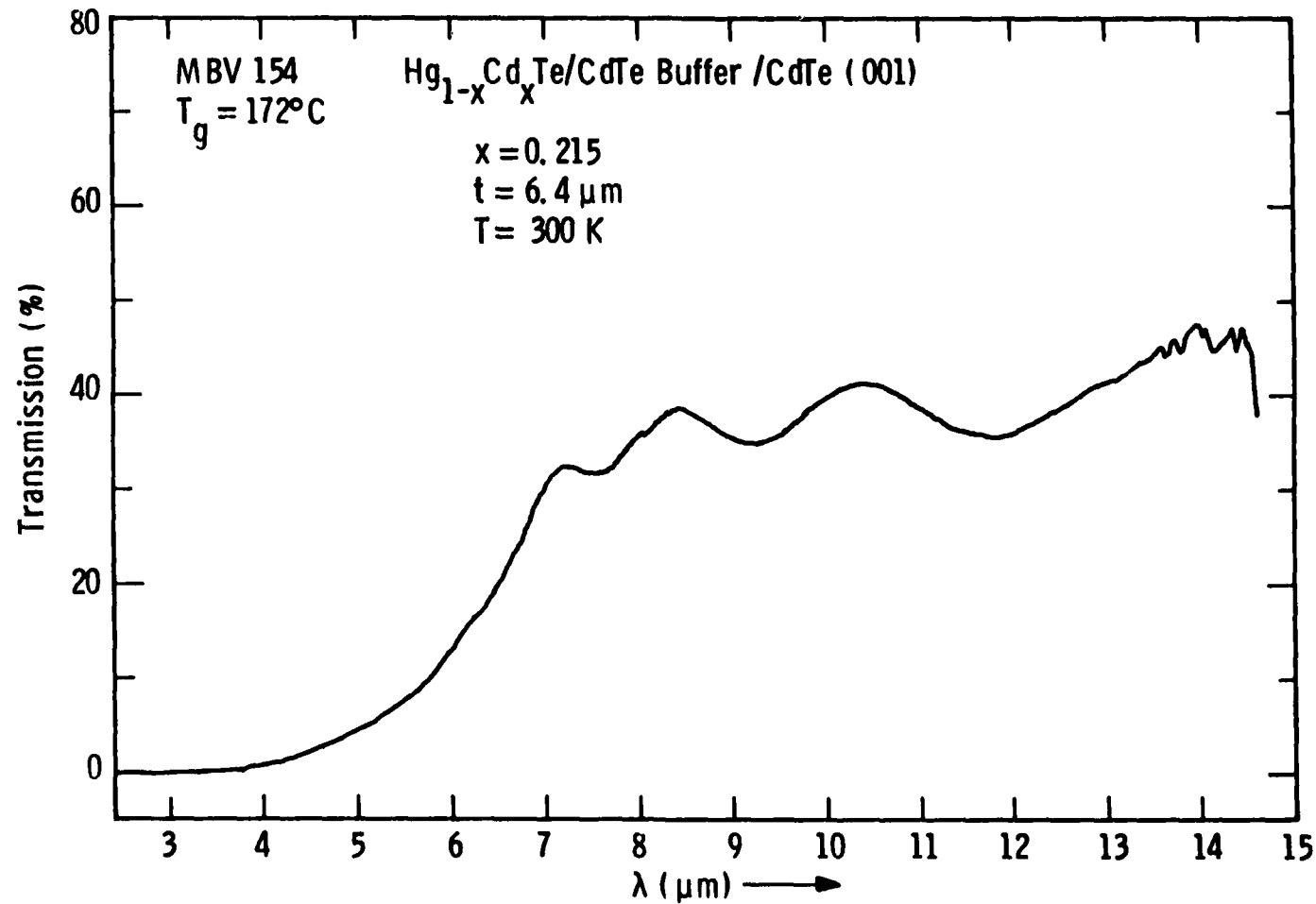


Figure 22. Infrared transmission spectrum for  $6.4 \mu\text{m}$  thick film of  $\text{Hg}_{1-x}\text{Cd}_x\text{Te}$  ( $x = 0.22$ ) grown on (001) orientation CdTe substrate at  $190^\circ\text{C}$ .

## 5. SUMMARY AND CONCLUSIONS

The main objectives of this contract have been achieved. The structural and optical quality of CdTe films grown on (001) orientation InSb substrates, at optimum (~185°C) growth temperatures, is excellent and represents the state of the art. The low ( $\leq 10^{15} \text{ cm}^{-3}$ ) carrier concentration in the film and the presence of the InSb/CdTe heterojunction leads to complete carrier depletion from films  $\leq 0.9 \mu\text{m}$  thick. The CdTe films are therefore ideal as substrates for  $\text{Hg}_{1-x}\text{Cd}_x\text{Te}$  film growth since they are free from extended defects and provide electrical isolation of the InSb substrate from the  $\text{Hg}_{1-x}\text{Cd}_x\text{Te}$  film. The growth of high-perfection CdTe films has been extended to large-area (~2 inch diameter) InSb substrates in the (second-generation) VG80HI machine.

The photoluminescence data clearly indicate the presence of an activated process (dependent on CdTe film growth temperature) for production of radiative (below band-gap) defect centers. This process is probably linked to the kinetics of film growth from the Cd and  $\text{Te}_2$  beams, but further studies are required to determine the nature of the defects and their formation. The presence of a doping limitation for In in MBE-grown CdTe films has been confirmed, but further studies are required to determine whether this limitation is general or confined to a particular set of growth conditions. These studies should include doping as a function of growth temperature and primary beam flux ratio ( $J_{\text{cd}}/J_{\text{Te}_2}$ ).

Magnetophotoconductivity data suggest the existence of an inversion layer in the InSb at the CdTe-InSb interface. Magnetotransport investigations of this inversion layer are in progress and will be supplemented by Hall mobility investigations to determine

whether electrons in the inversion layer have enhanced mobilities compared with electrons in bulk InSb.

The growth of  $Hg_{1-x}Cd_xTe$  films on CdTe films on InSb substrates and on CdTe substrates has been explored and a powerful tool (XTEM) for microstructural examination of these structures has been developed and applied for the first time.  $Hg_{1-x}Cd_xTe$  films of quality suitable for preliminary LWIR device fabrication have been grown.

## 6. REFERENCES

1. R. F. C. Farrow, Westinghouse Preliminary Program Description 82M1090: "Research Program to Investigate Molecular Beam Epitaxial Growth and Characterization of InSb/CdTe Heterostructures for Submicron Devices," submitted to ETADCOM, Ft. Monmouth, NJ (September 20, 1982).
2. R. G. van Welzenis and B. K. Ridley, Solid State Electronics 27(2), 113 (1984).
3. R. F. C. Farrow, G. R. Jones, G. M. Williams, and I. M. Young, Appl. Phys. Lett. 39, 954 (1981).
4. R. F. Brebrick and A. J. Strauss, J. Phys. Chem. Solids 25, 1441 (1964).
5. Y. Marfaing, Prog. Cryst. Growth Characterization 4, 317 (1981).
6. R. F. C. Farrow, S. Wood, J. C. Greggi, Jr., W. J. Takei, and F. A. Shirland, J. Vac. Sci. Technol. B3(2), 681 (1985).
7. S. Wood, J. Greggi, Jr., R. F. C. Farrow, W. J. Takei, F. A. Shirland, and A. J. Noreika, J. Appl. Phys. 55(12), 4225 (1984).
8. G. M. Williams, C. R. Whitehouse, N. G. Chew, G. W. Blackmore, and A. G. Cullis, J. Vac. Sci. Technol. B3(2), 704 (1985).
9. N. G. Chew, A. G. Cullis, and G. M. Williams, Appl. Phys. Lett. (Nov. 15, 1984).
10. P. J. Dean, G. M. Williams, G. Blackmore, J. Phys. D. Appl. Phys. 17, 2291 (1984).
11. G. R. Jones (RSRE, Malvern, UK) personal communication (1984).
12. J. P. Faurie, M. Boukerche, J. Reno, S. Sirananthan, C. Hsu, J. Vac. Sci. Technol. A3(1), 55 (1985).
13. A. W. Vere (RSRE, Malvern, UK) personal communication, 1984.
14. L. O. Bubulac, W. E. Tennant, D. D. Edwall, E. R. Uettner, and J. C. Robinson, J. Vac. Sci. Technol. A3(1), 163 (1985).

15. H. Holloway in The Use of Thin Films in Physical Investigations, Ed. J.C. Anderson, Academic Press (1966), p. 121.
16. Z. C. Feng, A. Mascarenhas, W. J. Choyke, R. F. C. Farrow, F. A. Shirland, and W. J. Takei, accepted for Appl. Phys. Lett. (1985).
17. J. P. Faurie, A. Million, and J. Piaguet, J. Cryst. Growth 59, 10 (1982).
18. K. Sugiyama, Japan J. Appl. Phys. 21, 665 (1982).
19. P. Migliorato, R. F. C. Farrow, A. Dean, and G. M. Williams, Infrared Physics 22, 331 (1982).
20. T. Takebe, J. Savaie, and T. Tanaka, Phys. Stat. 47, 123 (1978).
21. M. H. Patterson and R. H. Williams, J. Cryst. Growth 59, 281 (1982).
22. R. J. Wagner and B. D. McCombe, Phys. Stat. 64, 205 (1974).
23. B. D. McCombe, personal communication (1984).
24. R. Kaplan, Solid State Commun. 12(3), 191 (1973).
25. J. Hornstra and W. J. Bartels, J. Cryst. Growth 44, 513 (1978).
26. R. F. C. Farrow, J. Vac. Sci. Technol. A3(1), 60 (1985).
27. S. Wood, J. Gregg, Jr., and W. J. Takei, Appl. Phys. Lett. 46(4), 371 (1985).
28. J. P. Faurie, A. Million, and J. Piaguet, J. Cryst. Growth 59, 10 (1982).

# A study of the growth conditions necessary for reproducible preparation of high perfection CdTe films on InSb by MBE

R. F. C. Farrow, S. Wood, J. C. Gregg, Jr., W. J. Takei, and F.A. Shirland  
Westinghouse R & D Center, Pittsburgh, Pennsylvania 15235

J. Furneaux  
Naval Research Laboratory, Washington, D. C.

## APPENDIX 1

(Received 15 September 1984; accepted 15 October 1984)

The critical role of growth-related parameters including substrate preparation conditions, source conditioning, growth rate, and growth temperature has been identified in MBE growth of high-perfection CdTe films on InSb from a single CdTe effusion source.

## I. INTRODUCTION

The performance of a variety of device structures, based on the semiconductor CdTe, is known<sup>1</sup> to be limited by the defect structure and poor crystallographic quality of the material. The very close lattice match ( $\Delta a/a \approx 5.10^{-4}$ ) between InSb and CdTe is, therefore, particularly significant since it has for the first time allowed MBE growth<sup>2,3</sup> of CdTe films of structural perfection far superior to bulk CdTe wafers, and comparable to well-developed III-V compound semiconductors. The reproducible growth of such films, however, requires optimization of a number of growth-related parameters which include substrate surface preparation, source outgassing, film growth rate, and growth temperature. Here we discuss the critical role of these parameters.

## II. EXPERIMENTAL

The results described in this paper relate to growth of CdTe films from a single CdTe effusion source in a small Westinghouse-built machine equipped with a Varian 360-style vacuum load lock and sample manipulator, a Varian scanning ion gun (Type 981-2043), and a RHEED system. The system was ion-pumped (Varian triode pump, 400 l/s<sup>-1</sup>) and sublimation-pumped. A liquid nitrogen cooled cryo-shroud surrounded the source region, but not the deposition region. Base pressures were in the 10<sup>-10</sup> Torr range prior to growth, and in the 10<sup>-9</sup> Torr range during growth.

In this study the substrates were (100) orientation wafers polished on both sides supplied by the manufacturer (Metal Specialties, Inc., Fairfield, CT). They were free-etched before growth with a solution of 25:4:1, lactic acid: HNO<sub>3</sub>:HF.

The method of *in situ* cleaning was ion bombardment and subsequent annealing at ~200 °C. The details of this process, e.g., ion species, beam energy, and uniformity were found<sup>3</sup> to have a strong influence on film quality. Other parameters which influenced film quality were CdTe source outgassing and conditioning following loading of a new charge, orifice dimension, film growth rate, and growth temperature.

The techniques of double crystal x-ray rocking curve (DCRC) analysis and cross-section transmission electron microscopy (XTEM) were used to study the perfection of the film and interface region. These studies were supplemented by He<sup>+</sup> channeling, photoluminescence, and C-V profiling.

*In situ* RHEED examination provided a qualitative check on substrate surface ordering and film perfection, but it was totally insensitive to film quality when the DCRC linewidths of the films were below 40 arcsec.

## III. CRITICAL GROWTH-RELATED PARAMETERS

The basic assumption behind growth from a single CdTe effusion source is that of a steady state of Knudsen effusion in which the beam composition is locked<sup>2</sup> to the congruently subliming composition. Consideration of the self-diffusion coefficients of Cd and Te in crystalline CdTe shows that the approach to this steady state may take many hours at temperatures around 500 °C, but is very rapid at temperatures above 700 °C. We find that reproducible growth of CdTe films with DCRC linewidths below 25 arcsec is possible only if a new (crushed) CdTe charge is conditioned by heating to temperatures above 700 °C. Small orifices (<3 mm diam) enable this to be carried out without excessive loss of the charge.

A study of the influence of *in situ* substrate preparation conditions on film and interface structure has been reported by the authors elsewhere.<sup>3</sup> In brief, optimum quality was obtained for argon ion bombardment at 500 eV. Higher energies and heavier ion species, (e.g., Kr), caused extensive damage to the InSb surface and induced related defects in the film. A defocused and scanning ion beam was necessary to uniformly remove surface impurities prior to growth. Growth rates greater than 0.6 μm h<sup>-1</sup>, or changes in growth rate during growth, resulted in film defects such as dislocations and loops. This effect may be due to a kinetic limitation in the reaction between Cd and Te<sub>2</sub>, which results in inclusion of the nonvolatile species Te<sub>2</sub> in the film at high Cd and Te<sub>2</sub> arrival rates.

Substrate temperatures in the range 220–160 °C had little effect on the film quality, as judged by the DCRC, XTEM, or He<sup>+</sup> channeling data, except that the channeling minima ( $\chi$ ) for films grown at temperatures >220 °C were significantly higher (~0.08, compared with 0.06) than for films grown below this temperature. However, a systematic trend in native defect structure emerged from the photoluminescence study.

Figure 1 shows photoluminescence spectra recorded at 4 K from films grown at temperatures from 220 to 160 °C. The

CdTe/InSb &lt;100&gt;

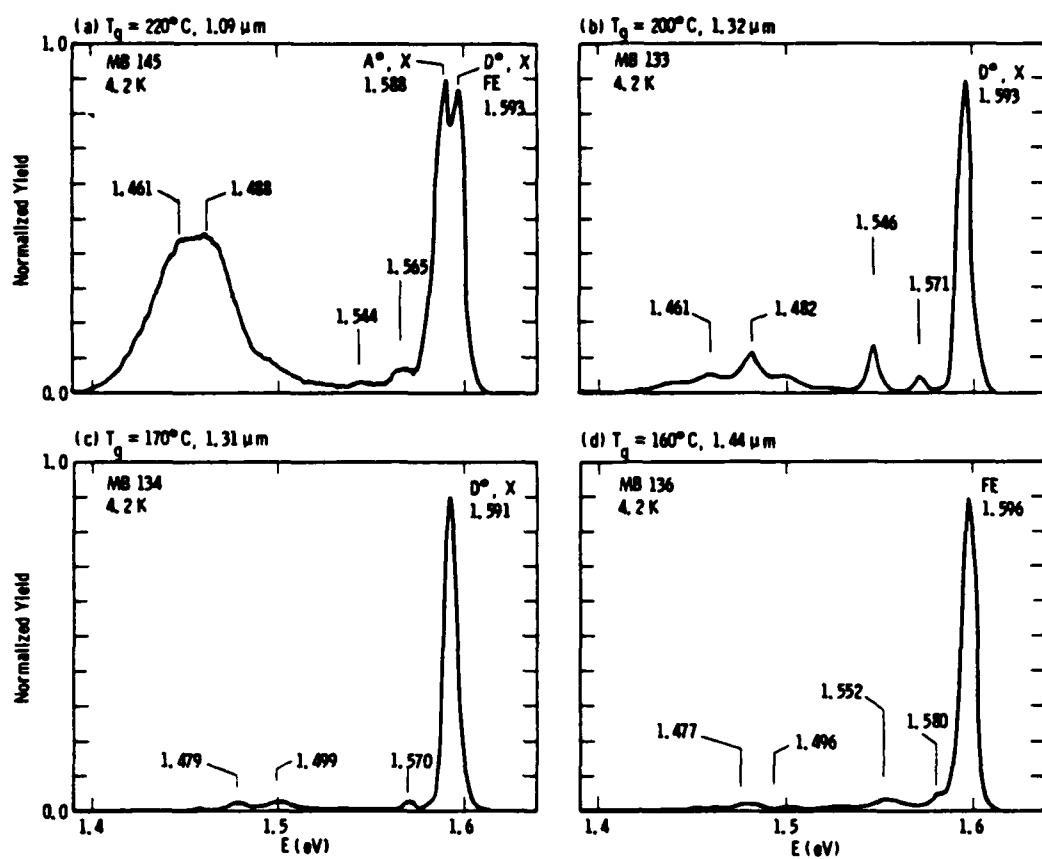


FIG. 1. 4.2 K photoluminescence spectra of MBE-grown films of CdTe on InSb(001). The excitation wavelength is 6471 Å. Note the progressive dominance, with decreasing growth temperature, of the near band edge peak over the broad donor-acceptor pair (DAP) and defect-related band centered around 1.45 eV.

near band edge peak becomes increasingly dominant with decreasing growth temperature, with a decreasing emission from the broad donor-acceptor pair region and defect related band around 1.45 eV. High energy resolution spectra have been recorded at 1.5 K and will be discussed<sup>4</sup> in a subsequent paper. These spectra suggest that the films contain fewer native defects at the lowest ground temperature.

#### IV. CONCLUSION

The critical role of growth-related parameters including substrate preparation conditions, source conditioning,

growth rate, and growth temperature has been identified in MBE growth of high-perfection CdTe films on InSb from a single CdTe effusion source.

<sup>1</sup>R. F. C. Farrow, J. Vac. Sci. Technol. (in press).

<sup>2</sup>R. F. C. Farrow, G. R. Jones, G. M. Williams, and J. M. Young, Appl. Phys. Lett. **39**, 956 (1981).

<sup>3</sup>S. Wood, J. C. Gregg, Jr., R. F. C. Farrow, W. J. Takei, F. A. Shirland, and A. J. Noreika, J. Appl. Phys. **55**, 4225 (1984).

<sup>4</sup>Z. C. Feng, A. Mascarenhas, W. J. Choyke, R. F. C. Farrow, F. A. Shirland, and W. J. Takei, Appl. Phys. Lett. (to be submitted).

# Microstructural studies of CdTe and InSb films grown by molecular beam epitaxy

APPENDIX 2

S. Wood, J. Greggi, Jr., R. F. C. Farrow, W. J. Takei, F. A. Shirland, and A. J. Noreika  
Westinghouse Electric Corporation, Research and Development Center, Pittsburgh, Pennsylvania 15235

(Received 27 January 1984; accepted for publication 2 March 1984)

Epitaxial thin films of CdTe ( $1\text{--}5 \mu\text{m}$ ) have been grown directly onto (001) InSb substrates or onto intermediate buffer layers of InSb ( $0.25\text{--}0.5 \mu\text{m}$ ) by molecular beam epitaxy. Cross-sectional transmission electron microscopy and high-resolution transmission electron microscopy have been used to characterize the film and interfacial microstructures. Inferences about film quality were also compared with single-crystal x-ray rocking curve data and agreed well. Resulting microstructural features were correlated with various experimental growth parameters and substrate cleaning procedures. Results show that near-perfect CdTe films can be grown on InSb substrates, but film quality is critically dependent upon substrate cleaning. Other factors observed to influence defect formation in the films include growth rate, total growth time, or a change in growth rate during film growth. Extended defects which form include twins, line dislocations, or looplike defects. Lattice imaging has demonstrated the lattice matching across the InSb film/InSb substrate interface, despite the formation of In precipitates during the heat cleaning procedure.

PACS numbers: 68.55. + b, 68.60. + q, 68.48. + f

## I. INTRODUCTION

The interest in producing large areas of high-quality, single-crystal CdTe is driven by the need for an adequate substrate for  $\text{Hg}_{1-x}\text{Cd}_x\text{Te}$  growth for infrared detectors. This application requires CdTe crystals which are essentially free of extended defects, precipitates, and low-angle boundaries; however, twins occur readily in Bridgman, solvent evaporation, and Czochralski grown material.<sup>1</sup> Molecular Beam Epitaxy (MBE) growth of CdTe on a lattice matched substrate offers one possible alternative for producing high perfection single-crystal material. MBE techniques permit the growth of epitaxial CdTe (Ref. 2) and  $\text{Hg}_{1-x}\text{Cd}_x\text{Te}$  (Ref. 3) films of device quality at temperatures well below those of other growth technologies. InSb is of particular interest as a CdTe film substrate for MBE growth because of the nearly perfect lattice match between the two zincblende structures ( $|\Delta a|/a \leq 5 \times 10^{-4}$  at  $25^\circ\text{C}$ ).<sup>2</sup> Thus it is expected that MBE growth of essentially defect-free films of CdTe on InSb should be possible.

In this work we have employed cross-sectional transmission electron microscopy (XTEM) and high-resolution transmission electron microscopy (HRTEM) to characterize the microstructures of thin films of CdTe ( $1\text{--}5 \mu\text{m}$ ) grown by MBE directly onto (001) InSb substrates or onto intermediate buffer layers of MBE grown InSb ( $0.25\text{--}0.5 \mu\text{m}$ ). XTEM provides information about the perfection of the MBE films throughout their entire thickness as well as allowing direct observation of the CdTe/substrate interface. Film quality and interface structure observed by XTEM have been correlated with experimental growth parameters and substrate cleaning procedures. Furthermore, it has been shown that film quality determined by single-crystal x-ray diffraction data correlates very well with the quality determined by XTEM characterization. This is the first comprehensive microstructural study of MBE grown CdTe films, although Chew, *et al.*<sup>4</sup> have presented some preliminary results of their work.

## II. EXPERIMENTAL PROCEDURE

Pertinent experimental parameters for the films grown by MBE and characterized by XTEM are listed in Table I. Most of the CdTe films were grown directly onto ion beam cleaned InSb substrates, but in two experiments (designated as samples 469 and 470) intermediate InSb buffer layers were grown on the substrate by MBE prior to CdTe growth in a continuous process. These latter films were grown in a Varian MBE 360 whereas those grown directly onto the substrate were grown in a Westinghouse built apparatus of similar design. All growth temperatures were  $<200^\circ\text{C}$ . For samples 469 and 470, the InSb substrate was cleaned by heat cleaning at  $\sim 400^\circ\text{C}$  in a beam of  $\text{Sb}_4$ , rather than by ion beam cleaning, as is shown in Table I. Additional experimental details are described in Ref. 2.

To prepare cross-sectional specimens for TEM observations, the InSb substrate-film composite was first cut into  $2 \times 2 \text{ mm}$  squares. Approximately 300 nm of  $\text{SiO}_2$  was then put onto the CdTe surface by uv-enhanced low-temperature pyrolysis as a protective measure. Specimens were sandwiched together and mounted end on in a low viscosity embedding medium (Ladd LX-112 resin), cured, and ground and polished to produce wafers  $\sim 0.1 \text{ mm}$  thick. After mounting on tungsten support rings, final thinning to obtain transparent regions was achieved by ion milling with  $\text{Ar}$  ions using the liquid nitrogen cooled stage of a Gatan dual ion miller. Initial milling conditions of 5 keV and  $15^\circ$  angle of incidence produced adequate thin regions throughout the InSb substrate/MBE layers but left small In-rich islands on the surface of the InSb. Later a final milling at 1.5–2 keV and  $10^\circ$  greatly minimized or even eliminated this surface In segregation. A Philips 400T electron microscope operating at 120 keV was used for all TEM evaluation. This instrument is equipped with a Kevex System 7000 x-ray energy dispersive spectrometer (EDS) for chemical analysis. In general, the TEM specimens were prepared such that the foil normals were [110].

TABLE I. Film parameters.

Sample no.	InSb film thickness ( $\mu\text{m}$ )	CdTe film thickness ( $\mu\text{m}$ )	CdTe growth time (h)	InSb cleaning	Anneal temp. ( $^{\circ}\text{C}$ )	Single-crystal x-ray rocking curve FWHM, arc min		
						InSb	CdTe	$R_{sc}^*$
053	None	1.35	3	Focussed Ar ion beam, 500 V	200	3.6	12	3.3
058	None	1.05	4.83	Defocussed Ar <sup>b</sup> ion beam, 500 V	200	3.6	6.8	1.9
086	None	1.0	3.0	Defocussed Ar ion beam 500 V	200	3.6	4.4	1.2
094	None	2.34	7.5	Defocussed Ar ion beam, 500 V	200	3.6	7.6	2.1
099	None	3.77	3.0	Defocussed Ar ion beam, 500 V	200	3.6	6.0	1.7
108	None	1.4	3.5	Defocussed Ar ion beam, 1 KV	200	3.6	4.7	1.3
469	0.21 <sup>c</sup>	0.66 <sup>d</sup>	2.0	400 °C in Sb <sub>4</sub>	None	3.6	4.0	1.1
470	0.6 <sup>c</sup>	0.61 <sup>d</sup>	1.5	400 °C in Sb <sub>4</sub>	None	3.6	5.0	1.4

\*  $R_{sc}$  = the ratio of the FWHM of the (008) Bragg diffraction for the CdTe film compared with the InSb substrate and is an inverse measure of film perfection. Subsequent analysis of the best films (086, 469) by double crystal rocking curve analysis has revealed line widths of  $\approx 25$  arc sec for the (004) Bragg diffraction ( $\text{Cu } K_{\alpha}$  radiation) from these films.

<sup>b</sup> With a beam current of  $\sim 0.1 \mu\text{A}/\text{cm}^2$  for typically 2 h.

<sup>c</sup> InSb buffer layer grown at 380 °C.

<sup>d</sup> CdTe layer grown at  $\sim 176$  °C.

Single-crystal rocking curve data were obtained using a Siemens Omega drive diffractometer on as-grown films prior to XTEM sample preparation. A single-crystal diffractometer has considerable instrumental broadening of the Bragg peak and double crystal diffractometry is necessary for an accurate quantitative assessment of film perfection when  $R_{sc}$  [the ratio of the FWHM of the (008) Bragg diffraction for the CdTe film compared with the InSb substrate, Table I] is close to unity (i.e.,  $< 1.4$ ).

### III. EXPERIMENTAL RESULTS

#### A. Growth of CdTe directly onto InSb substrates

Figures 1(a)–1(c) show BF XTEM micrographs of three CdTe films of progressively increasing crystallographic quality. Film thicknesses range between 1–1.35  $\mu\text{m}$ . Early experiments, of which sample 053 [Fig. 1(a)] is representative, used a scanned focussed, 500 V ion beam to clean the InSb substrate prior to growth. Bright field XTEM [Figs. 1(a) and 2] reveal a nonplanar, undulating interface between the InSb and CdTe and a very high twin density in the CdTe film. A high dislocation density (not clearly visible at these imaging conditions) is also present within the CdTe film. Twin reflections were utilized to obtain dark field (DF) images of the two sets of twins visible at this [110] orientation. One set of twins is shown in Fig. 2. The twins are highly faulted and nucleation appears to have primarily occurred at the "high" points of the InSb substrate. Note that, although many of the twins and dislocations have grown throughout the CdTe film, no extended defects propagate into or are generated within the InSb substrate. The spotty texture on the InSb are In-rich surface islands caused by ion milling.

In comparison to film 053, film 058, shown in Fig. 1(b) under two-beam ( $g = [311]$ ) dynamical conditions, has a much lower twin density and the twins are much narrower. For this experiment the substrate was cleaned using a defocused 500 V ion beam. Twin nucleation has again occurred at the InSb-CdTe interface, often in pairs, and the dislocations are often observed associated with the twins. The small ( $< 70$  nm) defects imaged under these diffracting conditions in the CdTe film are probably due to ion milling damage,<sup>4</sup> although somewhat larger looplike defects have been observed in other films as reported below.

Further improvements in CdTe film quality are evident in specimen 086 [Fig. 1(c)]. Substrate cleaning was again performed with a defocused 500 V ion beam. It is difficult in the better quality films such as 086 to determine extended defect concentrations from cross-sectional microscopy. However, a region in 086 extending  $> 150 \mu\text{m}$  in length was examined

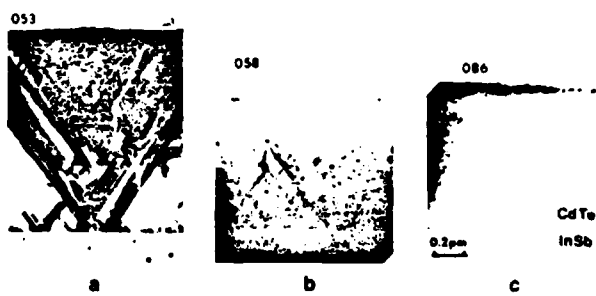


FIG. 1. BF XTEM micrographs of CdTe films on InSb substrates. Film quality improved with improved substrate cleaning from (a) a highly twinned and large dislocation density film to (c) a near perfect film with very few extended defects.

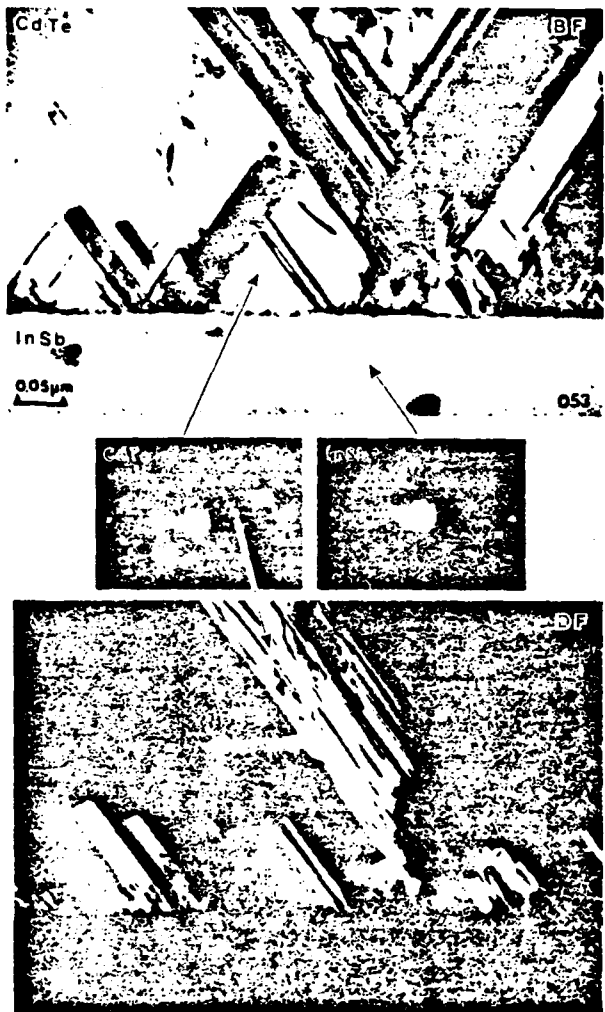


FIG. 2. XTEM micrographs of film 053 showing details of the CdTe/InSb interface structure and the twins.

in the TEM in which no defects were detected. Other areas contained an occasional dislocation, and no twins were observed in this film. In part, the clear delineation between the CdTe and InSb at the interface is thought to occur from the differential milling between the CdTe and InSb, although impurity decoration of the interface or interfacial strains have also been proffered as an explanation of the interfacial delineation.<sup>4</sup>

The conclusions concerning the CdTe film quality obtained from the electron microscopy observations correlate well with the single-crystal rocking curve data presented in Table I. The full width at half maximum (FWHM) of the (008) CdTe reflection decreases considerably from film 053 to 086 with 058 having an intermediate value. The correlation is more remarkable considering that the x-ray beam samples a larger area of film than generally observed by XTEM. TEM, however, has the further advantage in being able to delineate the specific microstructural feature responsible for film degradation.

Once it was established that high-quality films could be grown, subsequent experiments have concentrated on

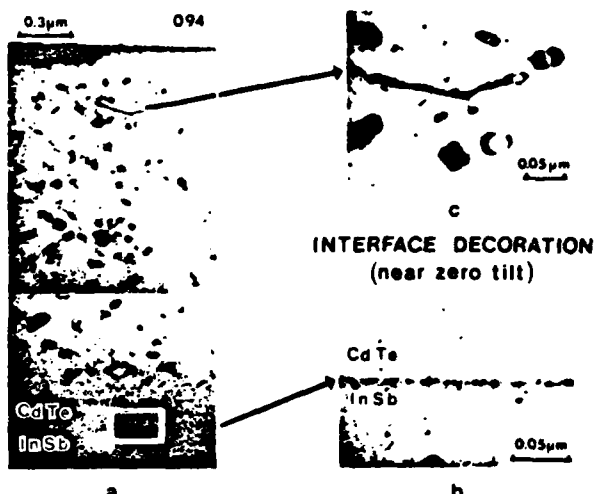


FIG. 3. BF XTEM micrographs of a relatively thick (2.34 μm) CdTe film showing (a) the defect distribution throughout the entire film thickness; (b) details of the interface structure; and (c) details of the bulk defects.

changing other variables such as growth time, growth rate, film thickness, and substrate cleaning procedures. Figures 3 and 4 show XTEM micrographs from, respectively, a thicker (2.34 μm) CdTe film (specimen 094) with a correspondingly larger growth time, and a film grown on an InSb substrate cleaned with a 1 kV ion beam instead of the more generally used 500 V beam (specimen 108). The thick film 094, contains no twins and very few dislocations, but it does have a high number density of looplike defects <50 nm in diameter. The density of these defects is low both near the InSb-CdTe interface and the CdTe surface, but for the remaining film thickness no gradation in number density is apparent. However, the size of these defects is a maximum in the center portion of the film. Further work is in progress to determine if they are dislocation loops or precipitates.

Specimen 108 (Fig. 4), grown on an InSb substrate cleaned with a 1 kV ion beam instead of the usual 500 V defocused ion beam, contains a relatively high dislocation density and very few twins. Most of these dislocations originate near interfacial precipitates, evident by the Moire fringe contrast. The small size of these precipitates and the relatively low number observed at the interface, especially in the cross-section configuration, makes their determination by either EDS or diffraction techniques difficult. However, they are probably indium rich, and their formation is due to the same ion beam induced instabilities which produce the indium-rich islands on the TEM specimens during thinning.

Specimen 094 (Fig. 3) also exhibits some sort of interfa-

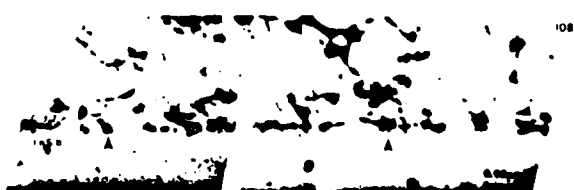


FIG. 4. BF XTEM montage of a CdTe/InSb film interface showing interfacial precipitation (arrowed) and dislocation generation.

cial decoration. These defects, however, were not easily resolved precipitates as in specimen 108 and did not generate dislocations in the CdTe layer. This observation would suggest that they occurred after growth had proceeded. One explanation is that this decoration is a finer version of the looplike structure observed near the center of the CdTe film and would explain the denuded region in the CdTe near the interface. Note again that specimens 094 and 108 show intermediate values for the single-crystal rocking curves.

Chew *et al.*<sup>4</sup> have observed that MBE growth of CdTe on InSb at lower temperatures than those utilized here results in highly faulted, columnar polycrystalline CdTe. In this study a very minimum amount of polycrystalline CdTe was observed in only one specimen (099) which was grown at 3–4 times the rate of the previous specimens. As shown in Fig. 5(a) these crystals were also highly faulted and columnar. These crystals did not originate at the CdTe-InSb interface but extended from a very complex defect as shown in Fig. 5(b). This defect, which did nucleate at the interface, is bounded at least on two opposing sides by a series of small microtwins. Figure 5(c) shows several examples of smaller defects of this nature originating at the interface. It is highly probable that the other two sides of these defects are composed of the remaining two sets of microtwins out of contrast in this orientation.

### B. Growth of CdTe with an InSb buffer layer

Two examples of XTEM micrographs from CdTe films grown on MBE InSb buffer layers of different thicknesses are presented in Figs. 6 and 7. Both substrates were heat cleaned at  $\sim 400^\circ\text{C}$  prior to InSb film growth at  $380^\circ\text{C}$ . Both specimens show precipitates at the InSb substrate-InSb

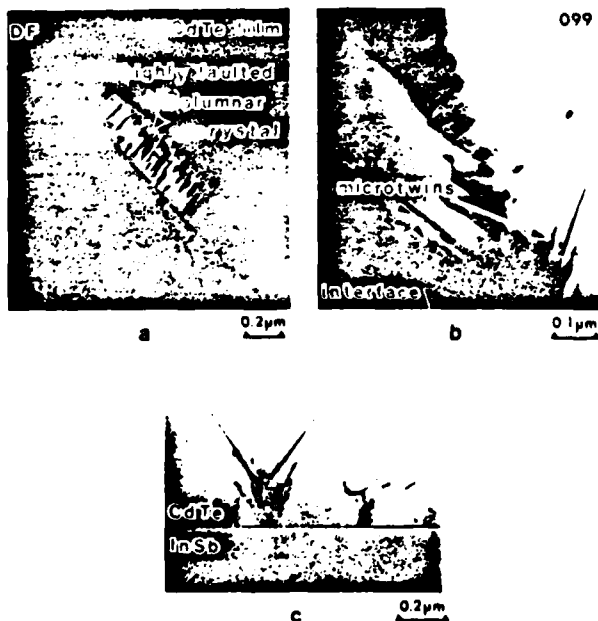


FIG. 5. XTEM micrographs of polycrystalline regions in a rapidly grown, thick ( $3.77 \mu\text{m}$ ) CdTe film. (a) DF of faulted polycrystals; (b) complex defect at base of polycrystal near interface; and (c) other examples of complex defect nucleated at interface.

film interface; and, in this situation, the size and number density are sufficient to determine that the precipitates are In rich by EDS techniques. Electron diffraction suggests that the precipitates are metallic indium by showing a precipitate reflection corresponding to the  $c$  axis of tetragonal indium normal to the interface. This orientation would then allow (100) and (010) planes of tetragonal In ( $a = b = 3.24 \text{ \AA}$ ) to be matched with the (200) and (020) planes of InSb ( $a_0/2 = 3.24 \text{ \AA}$ ). In some locations a thin residual layer of surface contamination which defines the actual interface shows these precipitates to be contained within the original substrate. Despite the presence of these precipitates the InSb buffer layers are mostly free of extended defects, and are lattice matched across the InSb/InSb interface as shown by Fig. 8.

For both specimens the InSb buffer-CdTe interface always appeared to be sharp and smooth. No decoration or precipitation on this interface was observed, and consequently, no defects were found to be nucleated at this interface. The few dislocations observed in the CdTe layer above the interface of specimen 470 (Fig. 6) were correlated with an experimental change of growth rate of the CdTe after  $\sim 0.25 \mu\text{m}$  of film growth. Problems, however, did arise in specimen 470 when the residual surface contamination at the InSb/InSb interface was more extensive in localized regions. Figure 9 shows the comparison between the two interface morphologies observed in specimen 470. The foils are tilted to observe the interface more closely. In Fig. 9(a) the interface shows only precipitates with a clean interface between them, whereas, in Fig. 9(b) the interface between the precipitates is covered with a thin coating. A small denuded region is observed around each precipitate. In this latter situation twins are observed to nucleate at the InSb/InSb interface, as shown in Fig. 10. Some of the twins are completely contained within the buffer layer, but many continue to grow throughout the entire thickness of both InSb and CdTe films. Twin-dislocation interactions similar to those seen in 058 are observed. Notice that for specimen 469, in which no extended defects are observed, the x-ray rocking curve data are as good as for 086. Also this specimen received the second-

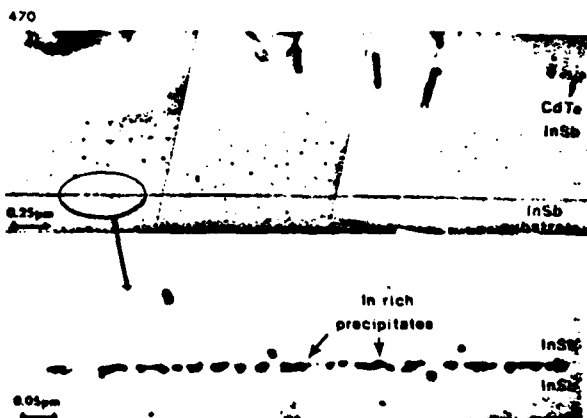


FIG. 6. BF XTEM montages of a CdTe film grown on an InSb buffer layer. Note the formation of In-rich precipitates in the heat cleaned InSb substrate surface. Dislocation generation in the CdTe film is due to a change in the growth rate.

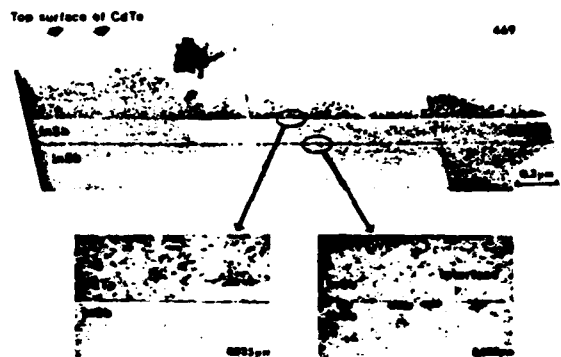


FIG. 7. BF XTEM micrographs of a good quality CdTe film grown on a thin ( $0.2 \mu\text{m}$ ) InSb buffer layer. The CdTe/InSb interface is clean whereas the InSb/InSb interface is defined by residual surface contamination and In-rich precipitates.

dary ion milling operation during preparation and shows no evidence of the In droplets on the InSb regions.

#### IV. DISCUSSION OF RESULTS

In this study cross-sectional electron microscopy has been employed to characterize films of CdTe grown by molecular beam epitaxy onto (001) InSb substrates. The film quality as determined by XTEM has been correlated with a number of experimental parameters such as growth rate, thickness, and InSb substrate surface preparation. A number of general comments can be made at this time concerning MBE growth of CdTe films.

One result of this work is that high-quality CdTe films, i.e., free of any extended defects, can be grown by MBE. This result in itself is significant since twin formation which occurs readily in bulk CdTe, as discussed by Vere *et al.*,<sup>1</sup> can be

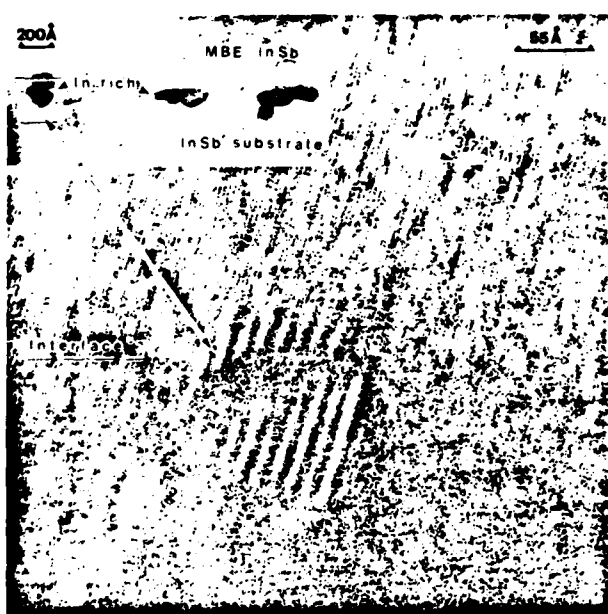


FIG. 8. High resolution TEM micrograph (lattice image) and XTEM micrograph (inset) of InSb film-InSb substrate interface with In-rich precipitates. Lattice matching occurs across the interface despite precipitate formation.

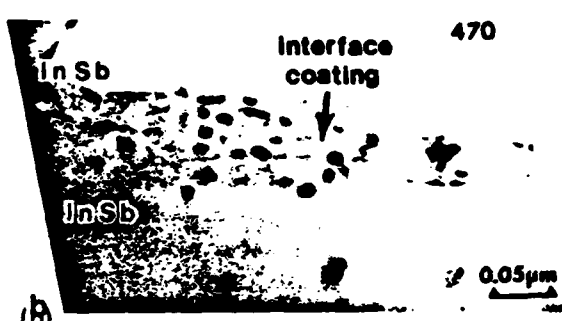
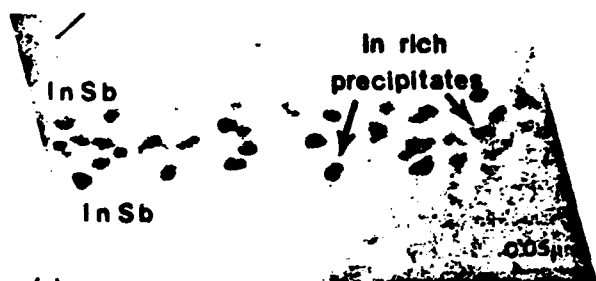


FIG. 9. BF XTEM micrographs comparing two InSb/InSb interface morphologies in specimen 470. Interface is tilted away from vertical.

eliminated in thin films grown by MBE. Twins, however, can occur in the MBE grown CdTe films. Although the tendency for twinning in bulk CdTe may be related to the reported low stacking fault energy of  $10.1 \pm 1.4 \text{ ergs/cm}^2$ ,<sup>5</sup> twins in the MBE films depend upon the availability of suitable nucleation sites. In the case of severe twinning these sites are related to surface irregularities on the InSb substrate surface. Also, any twins in the InSb substrate which intersect the surface are replicated in the CdTe by the MBE growth process. In general, dislocations are associated with the twins—the dislocation density being proportional to the twin density. However, situations do exist when dislocations can exist alone. Two cases observed here are the nucleation of dislocations on precipitates introduced at the InSb/CdTe

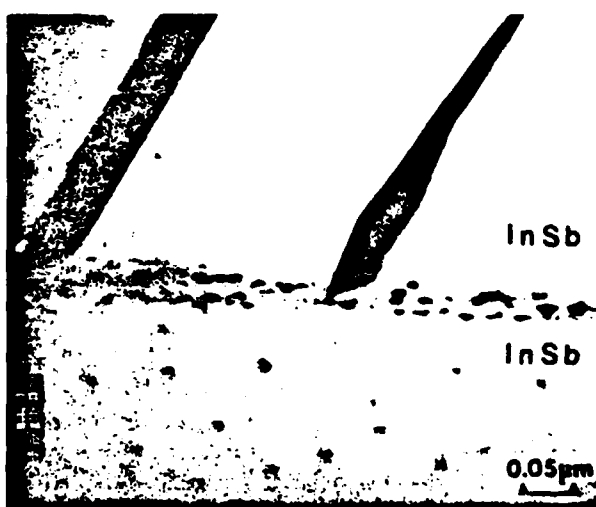


FIG. 10. Twin nucleation at the InSb/InSb interface in specimen 470 occurs only in those regions which have a surface coating between precipitates.

interface as a result of improper surface preparation and the generation of dislocations in the film incurred by a sudden change in the CdTe growth rate.

Substrate cleaning procedure and surface preparation are obviously of primary importance for growth of high-quality films. Similar conclusions have been reached by Chew *et al.*<sup>4</sup> Nucleation of twins at irregular interfaces and generation of dislocations on precipitates at the interface are two consequences of improper surface cleaning previously mentioned. The columnar polycrystals observed in specimen 099 appear to be a result of the rapid growth rate employed. However, we note that these polycrystals nucleated on complex faults composed of twins which, in turn, were nucleated only at localized areas on the InSb/CdTe interface. It is believed, therefore, that adequate substrate surface preparation could eliminate these faults and thereby allow growth of high-quality films over a wider range of growth rates than achieved here. The importance of the interface in determining film quality becomes more important when CdTe films grown on ion beam cleaned InSb substrates are compared with those grown on MBE InSb buffer layers. Although high quality films were grown on ion beam cleaned InSb, adequate surface preparation depends critically on ion energies, beam geometry, and cleaning time. In comparison the InSb buffer layer/CdTe interfaces always appear to be sharp and uniform, and, consequently, no defects were observed in the CdTe which had nucleated at the interface. (The exception, of course, are the replicated microtwins which nucleated at the InSb/MBE InSb interface.)

To date, no other microstructural data from MBE CdTe and InSb films has been published, but our microscopy analysis and general conclusions are in basic agreement with the data presented by Chew *et al.*<sup>4</sup> TEM analyses of the defect and precipitate structures observed in bulk CdTe have been performed<sup>6-8</sup> and compared with those in ZnSe.<sup>9</sup> Microtwins, extrinsic stacking faults,<sup>8</sup> and interstitial, or Frank, loops<sup>7</sup> have been observed by Ponce. Bean<sup>8</sup> in CdTe material obtained from II-VI Inc., recorded both Te and In<sub>2</sub>Te<sub>3</sub> precipitates, the former being associated with dense dislocation tangles. In<sub>2</sub>Te<sub>3</sub> particles were identified from Moire fringe spacings. In Bean's study<sup>8</sup> vacancy loops were only observed after ion implantation. Thus, the types of defects observed in the MBE films, when present, are consistent with those in bulk material.

Although, the precipitates associated with the heat cleaned InSb/InSb interface are either In or In-rich In-Sb compounds, those observed on the ion cleaned InSb/CdTe interface could be the In<sub>2</sub>Te<sub>3</sub> type observed by Bean. Their analysis in the present case is complicated by the low number density along the interface. Similarly, the looplike defects present in specimen 094 are most likely interstitial dislocation loops—possibly containing segregated Te. Further characterization will address this question. We note, however, that this film provides the single example in which the film quality was not determined predominantly by the nature of the InSb/CdTe interface.

It should be noted that the authors had some initial concern about the introduction of extended defects in the MBE film due to stresses generated by sample preparation

for XTEM. It is now apparent that XTEM samples with very low extended defect densities can be prepared by the techniques employed, as evidenced by the microstructures of films 086 and 460. Microstructural data also correlates well with single-crystal x-ray rocking curve broadening. Furthermore, as discussed by Vere *et al.*,<sup>1</sup> twins are not generally introduced by post-growth mechanical deformation, that is, they are not strain induced. Instead, they nucleate and propagate during growth. Some plastic deformation (dislocation motion) can occur, however, at room temperature, but in the samples evaluated in this work, this was prevented by maintaining adequate sample thickness prior to the final ion milling operation. Thus, we conclude the XTEM does yield a true representation of the microstructures of these films, but several specimens should be examined to identify any inhomogeneities across the original wafer. This was achieved in this work by mounting several specimens and evaluating in a comparative fashion. The variation in specimen 470 elucidates the misconception which might have arisen, had only one small portion of the wafer been examined.

A brief comparison with the ZnSe/GaAs system is also worthy of note since this is the only other example of growth of a II-VI compound on a III-V substrate for which XTEM data has been reported.<sup>9</sup> Ponce has examined the defect structures of highly doped ZnSe epitaxial layers grown by organometallic CVD on (100) GaAs substrates and observed Frank-type interstitial loops near the interface and in the bulk using HRTEM. In contrast, layers grown on (111) substrates exhibited a large twin density. Since this system has a much larger mismatch ( $\Delta a/a = 2.5 \times 10^{-3}$  at R.T.)<sup>10</sup> than the CdTe/InSb system, it is not clear how to interpret these comparative results at present. Furthermore, details of the substrate cleaning procedures, etc., are not known. It is of interest, however, that similar extended defects can be observed in the two systems.

## V. CONCLUSIONS

(1) Near-perfect epitaxial CdTe films can be grown by MBE on InSb substrates with or without an InSb buffer layer, but film quality is critically dependent upon substrate cleaning.

(2) Effective substrate cleaning can be obtained at an ion energy of 500 V; higher energies can produce precipitation and subsequent dislocation nucleation during MBE growth. Residual irregularities on the InSb substrate surface leads to microtwin nucleation at the InSb/CdTe interface. Dislocations are generally associated with these microtwins.

(3) Other factors which induce defect formation in the MBE CdTe films include high growth rates, long growth times, or a change in growth rate during film growth. Extended defects formed include twins, line dislocations, or looplike defects. Defects in the InSb which intersect the surface, such as microtwins, are replicated in the CdTe during MBE film growth.

(4) Heat cleaned InSb substrates can produce In precipitates in the surface layer which does not, however, induce defect formation in the InSb buffer layer. Twin nucleation does occur at this interface if the indium is more uniformly

distributed (i.e., coated) over the substrate prior to film growth.

(5) Lattice matching across the InSb MBE film/InSb substrate interface has been demonstrated.

(6) The defects delineated in the MBE CdTe films are consistent with other analyses in bulk CdTe.

(7) The film quality observed by XTEM is in excellent agreement with the single-crystal x-ray rocking curve data.

#### ACKNOWLEDGMENTS

The authors wish to thank C. W. Hughes for assistance with the XTEM sample preparation and Jack Dinan for his encouragement. This work was sponsored in part by the Army Research Office and Night Vision Laboratory under contract no. DAAG29-83-C-0008.

- <sup>1</sup>A. W. Vere, S. Cole, and D. J. Williams, *J. Electron. Mater.* **12**, 551 (1983).
- <sup>2</sup>R. F. C. Farrow, G. R. Jones, G. M. Williams, and I. M. Young, *Appl. Phys. Lett.* **39**, 954 (1981).
- <sup>3</sup>J. P. Faure, A. Million, and J. Piaguet, *J. Cryst. Growth* **59**, 10 (1982).
- <sup>4</sup>N. G. Chew, G. M. Williams, and A. G. Cullis, presented at the Electron Microscopy Analysis Group Conference, England, 1983.
- <sup>5</sup>E. L. Hall and J. B. VanderSande, *Philos. Mag. A* **37**, 137 (1978).
- <sup>6</sup>F. A. Ponce, T. Yamashita, R. H. Bube and R. Sinclair, in *MRS Proceedings, Vol. 2, Defects in Semiconductors*, edited by J. Narayan and T. Y. Tan (North Holland, New York, 1981), p. 503.
- <sup>7</sup>D. J. Smith, F. A. Ponce, T. Yamashita and R. Sinclair, *Proceedings of the International Conference on High Voltage Electron Microscopy* (University of California at Berkeley, California, 1983).
- <sup>8</sup>J. C. Bean, "Ion Implantation in Cadmium Telluride," Ph.D. Thesis, Stanford University (1976).
- <sup>9</sup>W. Stutius, J. G. Werthen and F. A. Ponce, presented at the Electronic Materials Conference, University of Vermont, Burlington, Vermont, 1983 (unpublished).
- <sup>10</sup>J. D. H. Donnay, editor, "*Crystal Data Determinative Tables*," Volume 4, Inorganic Compounds 1967-69, 3rd edition (U. S. Dept. of Commerce, National Bureau of Standards and the JCPDS International Centre for Diffraction Data, 1978).

A Photoluminescence Study of Molecular Beam Epitaxy-Grown CdTe Films  
on (001) InSb Substrates\*

Z.C. Feng and A. Mascarenhas

Department of Physics and Astronomy, University of Pittsburgh  
Pittsburgh, PA 15260

W.J. Choyke

Department of Physics and Astronomy, University of Pittsburgh  
Pittsburgh, PA 15260  
and  
Westinghouse R&D Center  
Pittsburgh, PA 15235

R.F.C. Farrow, F.A. Shirland, and W.J. Takei  
Westinghouse R&D Center  
Pittsburgh, PA 15235

Abstract

The radiative defect density,  $\rho$ , as determined by high resolution low temperature photoluminescence, was determined for eleven single crystal films of CdTe grown by molecular beam epitaxy on (001) InSb in the temperature interval  $170^{\circ}\text{C}$  to  $285^{\circ}\text{C}$ . A minimum of 0.6% is found for  $\rho$  near  $185^{\circ}\text{C}$  as compared to 2.5% for the best previously reported value, indicating a high degree of perfection for our films. X-ray double crystal rocking curves have also been obtained for these films and a minimum in the full width at half maximum is also found in the neighborhood of  $185^{\circ}\text{C}$ .

\*Supported in part by NSF Grant DMR-84-03596 and ARO/NVL/ERADCOM Contract 29-83-C-0008.

The considerable interest in the growth of high quality CdTe films is largely due to promising applications in optoelectronics, integrated optics and solarcells as well as its use as a buffer layer for the growth of  $Hg_{1-x} Cd_x Te$  for infrared detectors. To date, molecular beam epitaxy (MBE) has been applied to the growth of CdTe films on a variety of substrates such as InSb<sup>[1-5]</sup>, GaAs<sup>[6-8]</sup> and sapphire<sup>[9-11]</sup>. In the case of InSb (001) substrates, one has an almost perfect lattice matched substrate, and high structural perfection CdTe films have been grown at the Westinghouse R&D Center. These films were at first examined by cross-sectional transmission electron microscopy (XTEM), and high resolution transmission electron microscopy (HRTEM)<sup>[3]</sup>.

This letter reports photoluminescence (PL) and double-crystal rocking curve (DCRC) studies on our high structural quality MBE CdTe films grown on (001) InSb substrates. The PL spectra are recorded with high resolution, low temperature (<2K) spectroscopy and the DCRC spectra are obtained with a double crystal spectrometer of special design. Several groups have published PL results of MBE CdTe at 77K<sup>[4,6,7,10]</sup>, 94K<sup>[8]</sup>, 6.5K<sup>[4,7]</sup> and 4.2K<sup>[5]</sup>. The ratio,  $\rho$ , of the intensity of a band at 1.4eV, attributed to defects, to that of the principal bound exciton (PBE) peak ( $\sim$ 1.58eV at 77K,  $\sim$ 1.59eV below 6K) has been adopted as a figure of merit for the quality of the CdTe films<sup>[4,6,8,10]</sup>. Previous authors have not published evidence for the free exciton (FE) line or the phonon replicas of the FE and bound exciton (BE) lines. It is well known<sup>[12]</sup> that high quality CdTe crystals show a series of sharp FE and BE lines and their respective phonon replicas

as well as weak luminescence lines or a weak luminescence band. Indeed, our high resolution low temperature PL spectra (1.4K and 2.0K) show these features.

The quality of MBE CdTe films is affected by surface preparation<sup>[13]</sup>, substrate temperature,  $T_s$ , during growth and other growth related parameters<sup>[4,5,7,11]</sup>. Several groups have changed the substrate temperatures in order to optimize the quality of MBE CdTe films grown on GaAs<sup>[6,7]</sup> and on InSb<sup>[4,5,14]</sup>. The temperature intervals used were too gross for an accurate determination of an optimum  $T_s$ . To improve on the accuracy, we chose eleven values of  $T_s$  in the temperature range  $170^{\circ}\text{C}$  to  $285^{\circ}\text{C}$ . For  $T_s$  between  $170^{\circ}\text{C}$  and  $200^{\circ}\text{C}$ , we have measured six samples and we find an optimum  $T_s$  in the neighborhood of  $185^{\circ}\text{C}$ .

PL spectra are obtained at 1.4K using 514.5 nm excitation at a power level of 15mW incident on the sample. The spectral resolution is better than 0.1 meV. Fig. 1 shows the 1.4K near edge PL spectrum of sample 209 grown with a  $T_s$  of  $188^{\circ}\text{C}$  at a growth rate of  $0.61\mu\text{m/hr}$ . One can see sharp FE and BE lines. Greater details of this spectrum will be reported elsewhere.

Fig. 2 shows spectral features, some of which have been attributed to defects, for sample 209 under identical measurement conditions as in Fig. 1. For samples with a  $T_s$  between  $285^{\circ}\text{C}$  and  $250^{\circ}\text{C}$ , one observes only a broad defect band whereas between  $170^{\circ}\text{C}$  to  $225^{\circ}\text{C}$ , peaks are observed on top of a broad band. The major peak in this region, marked C, is at  $1.4754\text{eV}$ . In the high temperature range we define the parameter  $\rho$ , the radiative defect density, to be the ratio of the peak of the broad band at  $1.44\text{eV}$  to the PBE at about  $1.59\text{eV}$ . In the range  $170^{\circ}\text{C}$  to  $225^{\circ}\text{C}$ , we define  $\rho$  to be the ratio of the principal defect peak at  $\sim 1.47\text{eV}$  to the PBE at  $\sim 1.59\text{eV}$ .

Fig. 3 gives the relationship between radiative defect density ( $\rho$ ) and the substrate temperature  $T_s$  during MBE growth of the CdTe films. A minimum of about 0.6% is obtained near  $185^{\circ}\text{C}$ . The lowest value of  $\rho$  previously reported is about 2.5%<sup>[4,7,8,10]</sup>. The observed minimum is entirely consistent with our observation of the sharpness and magnitude of the FE lines in this growth temperature region.

We now compare  $\rho$  obtained from our low temperature PL measurements with the full width at half maximum ( $w_{\frac{1}{2}}$ ) determined from double crystal rocking curve (D.C.R.C.) x-ray studies. The CuK $\alpha$  (400) reflection in the parallel setting with a (100) InSb monochromator was used for these measurements. Table I gives values of substrate temperature during growth,  $T_s$ , film thickness, growth rate, full width at half maximum ( $w_{\frac{1}{2}}$ ), and  $\rho$  the radiative defect density for eleven CdTe films grown in the range  $170^{\circ}\text{C}$  to  $285^{\circ}\text{C}$ . The full width at half maximum for the substrate (InSb) peaks were in the 12 to 14 arc-second range. It can be seen in Table I that our minimum for  $\rho$  determined by PL coincides with the minimum in  $w_{\frac{1}{2}}$  as determined from the x-ray measurements. However, the observed values of  $w_{\frac{1}{2}}$  are a weak function of substrate temperature,  $T_s$ , and have a large scatter. It would have been difficult to assign an optimum  $T_s$  from the D.C.R.C. measurements alone. It appears that P.L. and D.C.R.C. measurements are sensitive to different physical parameters and consequently provide complementary information. We suggest that any MBE film growth program should characterize samples with low temperature PL, DCRC, as well as XTEM.

In summary, we have given evidence for the fact that CdTe films grown by MBE on <100> InSb substrates in the temperature range 285<sup>0</sup>C to 170<sup>0</sup>C. appear to have an optimum crystal perfection at a substrate temperature, T<sub>s</sub>, of about 185<sup>0</sup>C. More details of these experiments will appear in a future publication.

TABLE I. A comparison of DCRC x-ray studies and  $\rho$  as determined by PL  
on MBE grown CdTe films with substrate temperatures from  
 $170^{\circ}\text{C}$  to  $285^{\circ}\text{C}$ .

Sample No.	Substrate( $T_s$ ) Temperature	Film Thickness ( $\mu\text{m}$ )	Growth Rate ( $\mu\text{m}/\text{hr}$ )	D.C.R.C. $w_{\frac{1}{2}}$ (arc-sec)	$\rho$
205	170	1.27	0.54	20.4	0.09
203	173	1.17	0.52	24.2	0.067
208	183	1.23	0.70	19.5	0.016
228	185	1.34	0.76	18.3	0.006
209	188	1.21	0.70	18.9	0.012
258	200	1.41	0.70	27.6	0.020
249	225	1.32	0.66	24.6	0.019
250	250	1.27	0.64	25.9	0.10
218	265	1.40	0.70	20.6	0.27
219	275	1.30	0.52	25.3	0.46
220	285	0.88	0.70	23.7	0.80

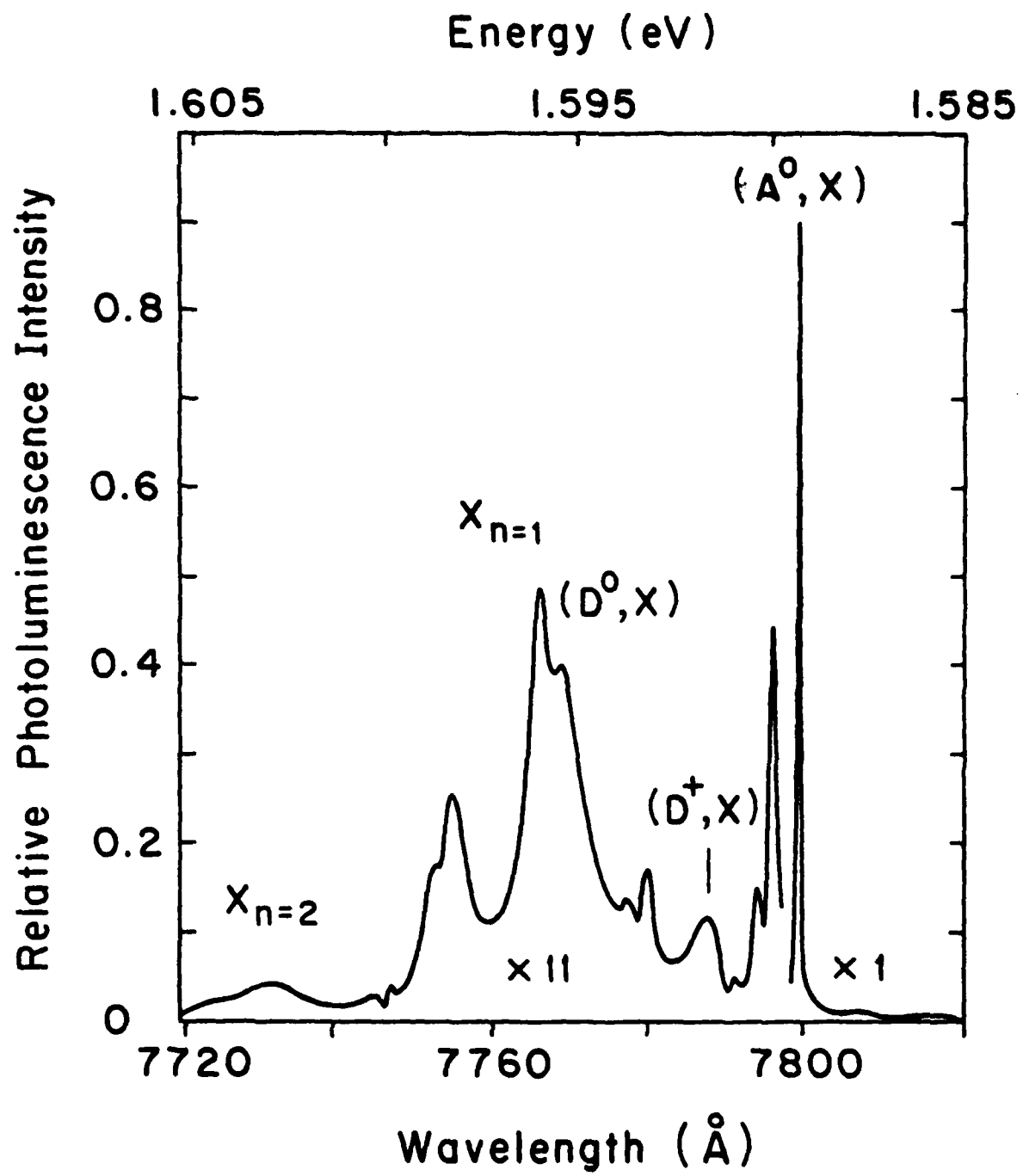
### References

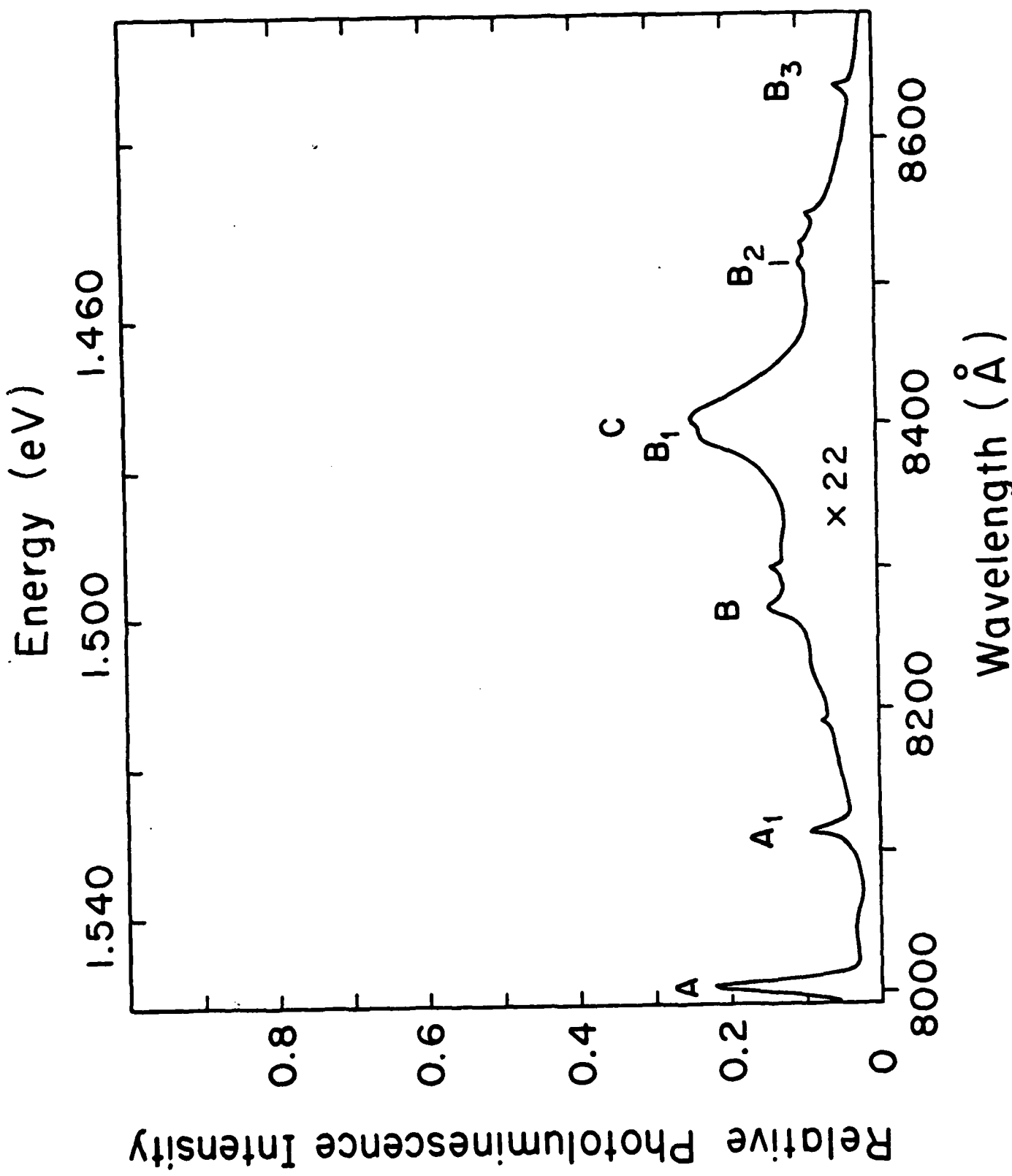
- [1] R.F.C. Farrow, G.R. Jones, G.M. Williams and I.M. Young, Appl. Phys. Lett., Vol. 39, 954 (1981).
- [2] T.H. Myers, Y. Lo and J.F. Schetzina, J. Appl. Phys., Vol 53, 9232 (1982).
- [3] S. Wood, J. Greggi, Jr., R.F. C. Farrow, W.J. Takei, F.A. Shirland, and A.J. Noreika, J. Appl. Phys., Vol. 55, 4225 (1984).
- [4] H.A. Mar and N. Salansky, J. Appl. Phys., Vol. 56, 2369 (1984).
- [5] R.F.C. Farrow, S. Wood, J.C. Greggi, Jr., W.J. Takei and F.A. Shirland, J. Vac. Sci. Technol. (1985) in press.
- [6] K. Nishitani, R. Ohkata and T. Murotani, J. Electron. Mater., Vol. 12, 619 (1983).
- [7] H.A. Mar, K.T. Chee, and N. Salansky, Appl. Phys. Lett., Vol. 44, 237 (1984).
- [8] R.N. Bicknell, N.C. Giles-Taylor, R.W. Yanka, and J.F. Schetzina, J. Vac. Sci. Technol., B2, 417 (1984).
- [9] T.H. Myers, Y. Lo, R.N. Bicknell, and J.F. Schetzina, Appl. Phys. Lett., Vol. 42, 247 (1983).
- [10] S.T. Edwards, A.F. Schreiner, T.M. Myers, and J.F. Schetzina, J. Appl. Phys., Vol. 54, 6785 (1983).
- [11] R.N. Bicknell, T.H. Myers, and J.F. Schetzina, J. Vac. Sci. Technol., A2, 423 (1984).
- [12] K. Zanio, Cadmium Telluride, in R.K. Willardson and A.C. Beer, ed., Semiconductors & Semimetals, Vol., 13, Academic Press, New York (1978).

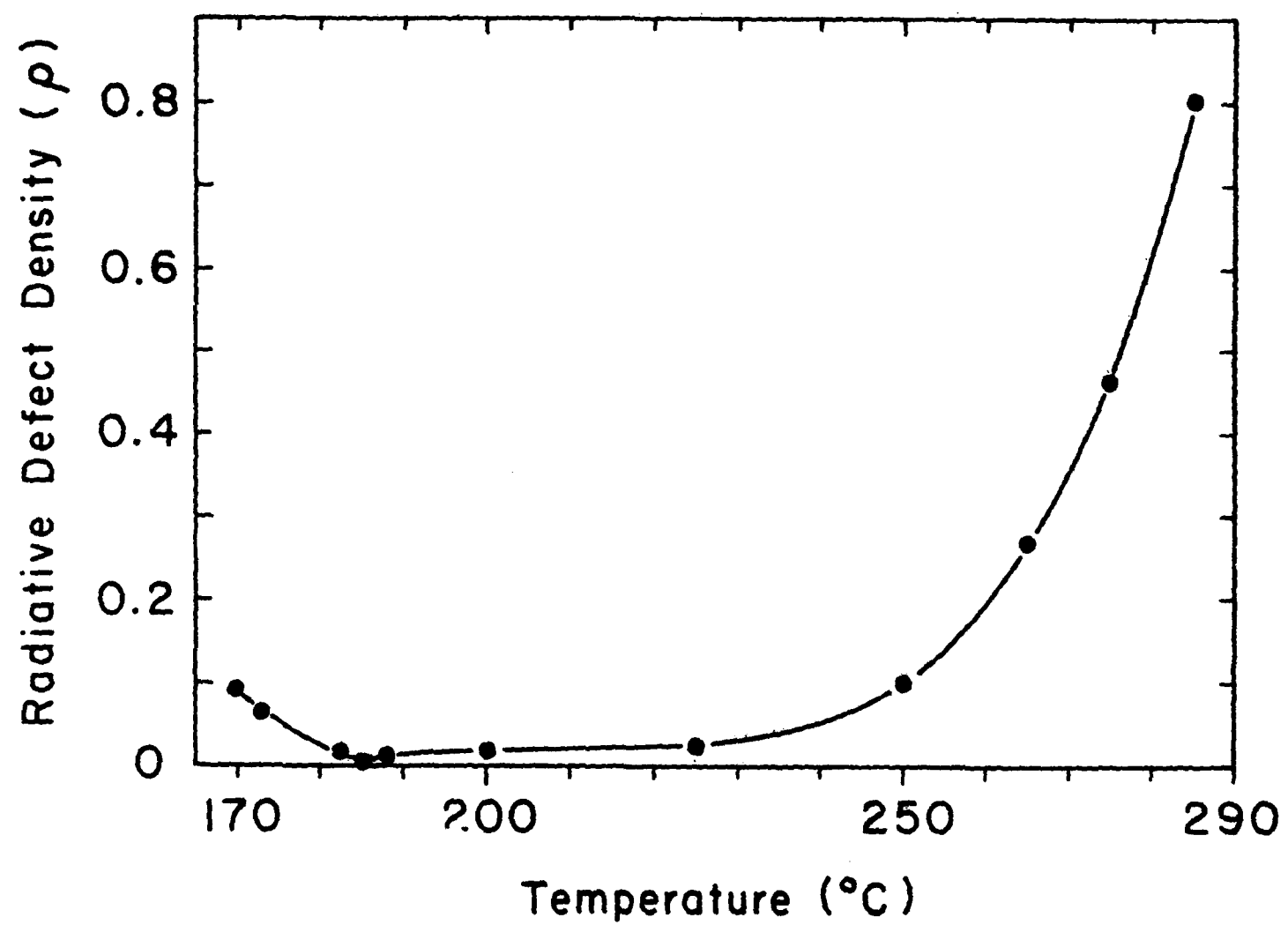
- [13] T.H. Myers, J.F. Schetzina, S.T. Edwards, and A.F. Schreiner, *J. Appl. Phys.*, Vol. 54, 4232 (1983).
- [14] N.G. Chew, A. G. Cullis, and G.M. Williams, *Appl. Phys. Lett.*, Vol. 45, 1090 (1984).

Figure Captions

- Fig. 1. Near edge 1.4K PL spectrum of MBE CdTe film 209 grown at a  $T_s$  of  $188^0\text{C}$  at a growth rate of  $0.61\mu\text{m/h}$ .  $x_{n=1}$  and  $x_{n=2}$  at  $1.5961\text{eV}$  and  $1.6043\text{eV}$  are the  $n=1$  and  $n=2$  states of the FE. The PBX ( $A^0, X$ ) at  $1.5892\text{eV}$  is assigned to a neutral acceptor.
- Fig. 2. Spectral features, some of which may be attributable to defects, for sample 209 under identical measurement conditions as in Fig. 1. The major peak marked C is found to be at  $1.4754\text{eV}$ .
- Fig. 3. Radiative defect density ( $\rho$ ) and the substrate temperature  $T_s$  during MBE growth of the CdTe films. A minimum of about 0.006 is observed near  $185^0\text{C}$ . Measurement conditions are identical to those used in obtaining the data in Figs. 1 and 2.







## Transmission electron microscopy of liquid phase epitaxial $Hg_{1-x}Cd_xTe$ layers on CdTe substrates

Susan Wood, J. Greggi, Jr., and W. J. Takei

*Westinghouse Electric Corporation, Research and Development Center, Pittsburgh, Pennsylvania 15235*

(Received 1 October 1984; accepted for publication 3 December 1984)

Epitaxial  $Hg_{1-x}Cd_xTe$  films were grown on (111)A CdTe substrates by the tellurium solvent, horizontal tube slider liquid phase epitaxy technique. Their microstructures were subsequently investigated by both planar and cross-sectional transmission electron microscopy (TEM). Planar TEM showed the top surface of the films to be precipitate free with a general dislocation density  $< 10^6/cm^2$  except for localized regions containing high dislocation densities associated with linear surface features on the  $Hg_{1-x}Cd_xTe$ . Cross-sectional TEM showed the interface region to be nonplanar due to meltback during epilayer growth. A three-dimensional dislocation structure was confined to a band in the interface region having a graded Hg composition.

$Hg_{1-x}Cd_xTe$  is currently a prime material candidate for multispectral infrared development, especially in the 8–12- $\mu m$  wavelength range. Liquid phase epitaxy (LPE) of  $Hg_{1-x}Cd_xTe$  on CdTe substrates, which are transparent at

these wavelengths, is one of the main growth techniques employed. This letter describes results from a cross-sectional transmission electron microscopy (XTEM) and planar TEM study of LPE  $Hg_{1-x}Cd_xTe$  grown on CdTe. Both interfa-

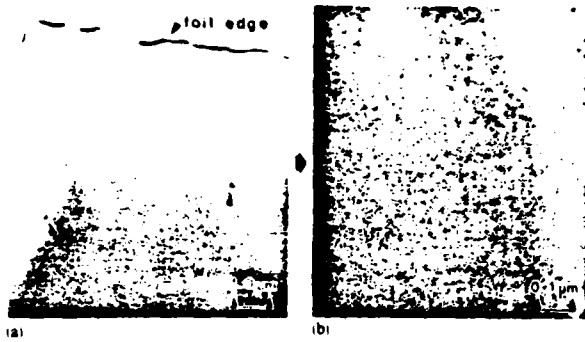


FIG. 1. (a) Typical planar TEM view of the front surface of LPE  $\text{Hg}_{1-x}\text{Cd}_{0.3}\text{Te}$  foil (prepared by ion milling); (b) Higher magnification micrograph illustrates the absence of ion-milling induced defects.

cial and near surface microstructures are described.

The LPE  $\text{Hg}_{1-x}\text{Cd}_x\text{Te}$  epitaxial films were grown by the tellurium solvent, horizontal tube slider technique originally developed by Harmon.<sup>1</sup> Growth temperatures were  $\sim 495^\circ\text{C}$  (5° supersaturation). (111)A CdTe substrates obtained from the Two-Six Corporation were pad polished with bromine-methanol and lightly free-etched immediately before insertion into the growth system. The epitaxial  $\text{Hg}_{1-x}\text{Cd}_x\text{Te}$  films, where  $x \approx 0.3$ , were  $\sim 16\ \mu\text{m}$  thick. Planar TEM specimens were prepared by careful grinding and polishing of the back surface to  $\approx 75\ \mu\text{m}$  thick followed by ion milling from the CdTe side with a liquid nitrogen cooled stage. The planar TEM specimens were prepared by ion milling to determine, in part, the potential success of the technique for preparing cross-sectional TEM specimens. Perforation of the planar specimens was achieved at the front surface of the epitaxial  $\text{Hg}_{0.7}\text{Cd}_{0.3}\text{Te}$  layer. XTEM specimens were subsequently prepared using a procedure similar to that described previously for CdTe/InSb specimens by Wood *et al.*<sup>2</sup> All microscopy was performed using a Philips 400T electron microscope operating at 120 kV. This instrument is equipped with a Kevex System 7000 x-ray energy dispersive spectrometer (EDS) for chemical analysis. The specimens were cooled to  $-185^\circ\text{C}$  with a LN stage.

The micrographs shown in Fig. 1 are representative of the front surface microstructure observed generally in the  $\text{Hg}_{0.7}\text{Cd}_{0.3}\text{Te}$  epitaxial layer. These near-surface layers have low dislocation densities (a maximum of  $\sim 10^6/\text{cm}^2$ ) as represented by the low magnification micrograph in Fig. 1(a),

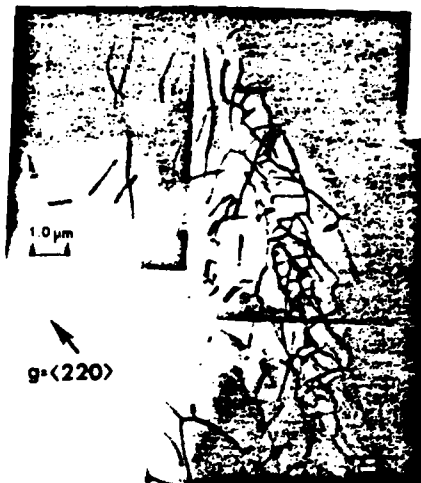


FIG. 2. Planar TEM montage of the dislocation microstructure associated with a linear macroscopic feature in the  $\text{Hg}_{1-x}\text{Cd}_{0.3}\text{Te}$  epilayer.

but large dislocation-free areas were also observed except in isolated regions addressed later. No precipitation of a second phase was observed. The overall quality of these films is much superior to that reported by Magee<sup>3</sup> for films on non-hydroplaned substrates. Note the excellent surface quality of these ion-milled foils as shown in the high magnification micrograph of Fig. 1(b).

Besides the general dislocation structure described above, isolated planar arrays of dislocations, or low angle boundaries, were observed as shown in Fig. 2. This boundary is comprised in part of the so-called 60° dislocations which predominate for the (111)⟨110⟩ slip system. This dislocation structure is similar to that observed by Magee<sup>3</sup> which he relates to residual polishing damage in the CdTe substrate prior to film growth. In our case this boundary was associated with the termination point of a raised linear feature observed on the surface of the film. The zone of high dislocation density is several micrometers wide and probably extends along the entire length of the feature which could be clearly seen with an optical microscope. These linear features were generally spaced several millimeters apart and were unidirectional.

A low magnification XTEM micrograph of a section of the same film in the vicinity of the interface is shown in Fig. 3. Several comments of the interfacial structure can immedi-

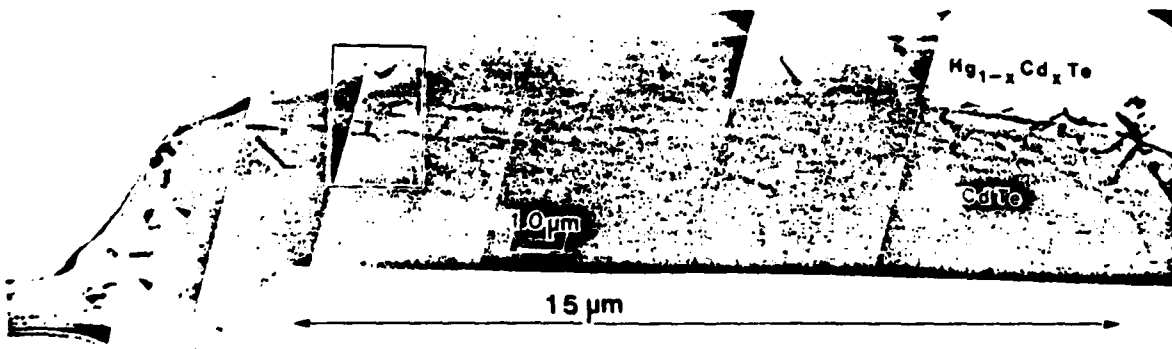


FIG. 3 XTEM montage of the transition region at the CdTe substrate/epitaxial  $\text{Hg}_{1-x}\text{Cd}_{0.3}\text{Te}$  interface.

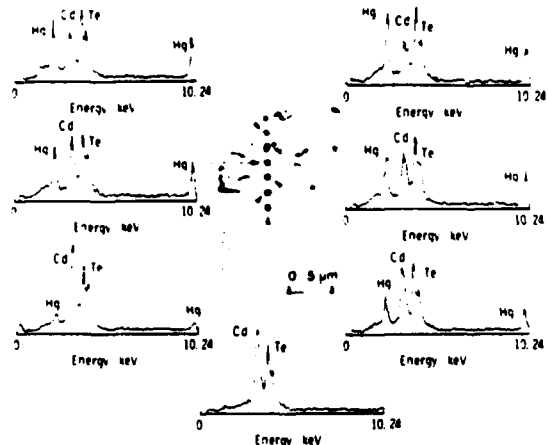


FIG. 4. EDS spectra showing variation in Hg concentration across the CdTe/Hg<sub>0.7</sub>Cd<sub>0.3</sub>Te interfacial region.

ately be made. Firstly, an abrupt interface, i.e., a sharp change of contrast, between the CdTe substrate and the Hg<sub>0.7</sub>Cd<sub>0.3</sub>Te epilayer is not observed. Instead, a three-dimensional array of misfit dislocations is present at a transition region at the interface in a zone approximately 1–2 μm wide. Secondly, this band of dislocations, which will be shown to define the interface, is nonplanar and can deviate locally up to 6 μm. Undulations may also be present on a larger scale which would not be apparent by TEM. This lack of planarity is probably due to nonuniform meltback of the substrate during epilayer growth. The absence of sharp interface contrast is due to a composition gradient shown qualitatively by the EDS spectra in Fig. 4 which were taken from the area outlined in Fig. 3. Qualitatively these spectra clearly show a progressive transition from the CdTe substrate (no Hg) to a high Hg concentration representative of the bulk Hg<sub>0.7</sub>Cd<sub>0.3</sub>Te over a depth of ~1.0 μm. The dislocations are confined to this transition zone. In fact, the first dislocation near the CdTe substrate coincides with the appearance of a small Hg peak in the spectra. Additional EDS data (not shown) taken in the arrowed regions of Fig. 3 show similar Hg concentration gradients verifying that the wavy dislocation array follows the interface. Higher magnification XTEM micrographs indicate the presence of small precipitates or loops associated with the dislocations. Except for small dislocation loops observed in general in the CdTe, only an occasional line dislocation was found either in the epitaxial Hg<sub>0.7</sub>Cd<sub>0.3</sub>Te layer or the CdTe beyond the transition zone.

Other authors have observed three-dimensional dislocation networks at LPE HgCdTe/CdTe interfaces<sup>3–5</sup> although not directly by the cross-sectional TEM technique. The thickness of this zone observed in our work is much less than that reported by Magee and Raccah<sup>6</sup> or Woolhouse *et al.*<sup>4</sup> for nonhydroplaned substrates. Direct comparison with the dislocation structures reported by James<sup>7</sup> is not possible because of the different perspectives given by planar and cross-sectional TEM. These dislocations are apparently a result of the lattice parameter misfit existing between epilayer and substrate (~0.21% for x = 0.3),<sup>8</sup> part of which is also accommodated by the gradation in Hg concentration. The association of a graded composition with the three-dimensional dislocation network has been suggested previously<sup>3,4</sup> and even indirectly correlated.<sup>3</sup> This work, however, is the first which unambiguously establishes this relationship using direct high spatial resolution imaging and chemical profiling techniques. While previous studies have theoretically calculated an expected planar dislocation spacing for abrupt interfaces,<sup>6,7</sup> the problem of anticipated dislocation arrays for graded interfaces has not been addressed. In fact, the kinetics of forming a combined graded composition/dislocation layer in this system is presently unclear. Although a variety of mechanisms has been proposed<sup>3,5,8</sup> further microscopy of thin epilayers might resolve this issue.

In summary, we have shown that the three-dimensional network of dislocations at the LPE HgCdTe/CdTe interface is associated with and generally confined to a zone with a graded Hg composition. The presence of such a dislocation structure may impact the electrical properties of IR devices fabricated from LPE material, but well beyond the interface region the epilayer had low line defect densities, except for localized subboundaries, and contained no observable second phases.

<sup>1</sup>T. C. Harmon, J. Electron. Mater. **8**, 191 (1979).

<sup>2</sup>Susan Wood, J. Gregg, Jr., R. F. C. Farrow, W. J. Takei, F. A. Shirland, and A. J. Noreika, J. Appl. Phys. **55**, 4225 (1984).

<sup>3</sup>T. J. Magee and P. M. Raccah, Proceedings of Infrared Information Services (IRIS), Detector No. 1, 127 (1982).

<sup>4</sup>G. R. Woolhouse, T. J. Magee, H. A. Kawayoshi, C. S. Leung, and R. D. Ormand, in Extended Abstracts of the 1984 U.S. Workshop on the Physics and Chemistry of Mercury and Cadmium Telluride, San Diego, CA, May 1984, p. 21.

<sup>5</sup>T. W. James and R. E. Stoller, Appl. Phys. Lett. **44**, 58 (1984).

<sup>6</sup>J. H. Basson and H. Booyens, Phys. Status Solidi A **80**, 663 (1983).

<sup>7</sup>R. B. Scholar, J. Vac. Sci. Technol. A **2**, 77 (1984).

<sup>8</sup>T. W. James, Electronic Materials Conference, Santa Barbara, CA, June 1984 (unpublished).

**END**

**FILMED**

**10-85**

**DTIC**